Identification of novel, non-invasive, early markers of *Oxyrrhis marina*-mediated *Dunaliella tertiolecta* grazing

Submitted in partial fulfilment of the requirements

of the degree of

Doctor of Philosophy

of the

Indian Institute of Technology Bombay, India

and

Monash University, Australia

by

Pranali Sharad Deore

Supervisors:

Prof. Santosh Noronha (IIT Bombay)

Prof. Sanjeeva Srivastava (IIT Bombay)

Prof. John Beardall (Monash University)

Dr. Santanu Dasgupta (Reliance Industries Limited)

The course of study for this award was developed jointly by
Monash University, Australia and the Indian Institute of Technology Bombay, India
and was given academic recognition by each of them.
The programme was administrated by The IITB-Monash Research Academy

(Feb 2020)

Declaration

I declare that this written submission represents my ideas in my own words and where others' ideas or words have been included, I have adequately cited and referenced the original sources.

I also declare that I have adhered to all principles of academic honesty and integrity and have not misrepresented or fabricated or falsified any idea/data/fact/source in my submission. I understand that any violation of the above will be cause for disciplinary action by the Institute and can also evoke penal action from the sources which have thus not been properly cited or from whom proper permission has not been taken when needed.

Notice 1

Under the Copyright Act 1968, this thesis must be used only under the normal conditions of scholarly fair dealing. In particular no results or conclusions should be extracted from it, nor should it be copied or closely paraphrased in whole or in part without the written consent of the author. Proper written acknowledgement should be made for any assistance obtained from this thesis.

Notice 2

I certify that I have made all reasonable efforts to secure copyright permissions for third-party content included in this thesis and have not knowingly added copyright content to my work without the owner's permission.

Student Name: Pranali Sharad Deore
IITB ID: 154024002
Monash ID: 27330753

Approval Sheet

The thesis entitled "**Identification of novel, non-invasive, early markers of *Oxyrrhis marina*-mediated *Dunaliella tertiolecta* grazing**" by Ms. Pranali Sharad Deore is approved for the degree of **Doctor of Philosophy.**

[redacted]

(Prof. G.K. Suraishkumar)
External Examiner

[redacted]

(Prof. Supreet Saini)
Internal Examiner

[redacted]

(Prof. Santosh Noronha)
IITB Supervisor

[redacted]

(Prof. Sanjeeva Srivastava)
IITB co-supervisor

[redacted]

(Prof. John Beardall)
Monash Supervisor

[redacted]

(Dr. Santanu Dasgupta)
Industry Supervisor

(Prof. Shireesh B. Kedare)
Chairperson

Date: 8th July 2020
Place: Online Viva-Voce

Dedicated to my late grandfather

List of Publications

List of publications included in this thesis: (published)

1. **Deore, P**, A Karthikaichamy, J Beardall, and S Noronha. 2020. Non-photochemical quenching, a non-invasive probe for monitoring microalgal grazing: an early indicator of predation by *Oxyrrhis marina* and *Euplotes* sp. *Applied Phycology*. 1(1), 20–31.
2. **Deore, P**, J Beardall, and S Noronha. 2020. Non-photochemical quenching: a non-invasive probe for monitoring microalgal grazing: influence of grazing-mediated total ammonia-nitrogen. *Applied Phycology*. 1(1), 32–43.

List of publications included in this thesis: (under review/ preparation)

1. **Deore, P**, J Beardall, and S Noronha. A perspective on current status of approaches for early detection of microalgal grazing. Review article. *Journal of Applied Phycology*.
2. **Deore, P**, J Beardall, Delgado, Y, Heraud, P and S Noronha. FTIR-based spectral signature in combination with chemometrics tools as an early marker of *Oxyrrhis marina* contamination in *Dunaliella tertiolecta* cultures.

List of publications not included in this thesis:

1. Delgado, Y, J Beardall, A Vonshak, **P Deore** and P Heraud. ATR-FTIR spectroscopy as a versatile tool for determining macromolecular composition and lipid productivity in *Nannochloropsis*. *Algal Research*. (under review).
2. Karthikaichamy, A, **P Deore,** S Srivastava, R Coppel, D Bulach, J Beardall and S Noronha. 2018. Temporal acclimation of *Microchloropsis gaditana* CCMP526 in response to hypersalinity. *Bioresource technology*. 254,23–30.
3. Karthikaichamy, A, **P Deore, V** Rai, D Bulach, J Beardall, S Noronha and S Srivastava. 2017. Time for multiple extraction methods in proteomics? A comparison of three protein extraction methods in the eustigmatophyte alga *Microchloropsis gaditana* CCMP526. *Omics: A Journal of Integrative Biology*. 21(11),678–683.

List of patents:

1. Method of contamination detection in algal culture (provisional Indian patent application no – E-2/692/2019/MUM).

Abstract

Microalgae-based food and fuel products are emerging as a sustainable solution to combat the global food and energy crisis. Year-round mass cultivation of microalgae for the development of commodity products is required to fulfil global demand. To date, open cultivation in raceway ponds is the only economically viable cultivation platform for the production of microalgal biomass at large-scale. Cultivation of single algal species with higher productivity, >25 g m^{-2} d^{-1}, is desirable. However, contamination by unwanted microbes is inevitable in open cultivation systems. Invasions by predators, consumers of microalgae, are one of the major hurdles in achieving biomass productivity at a minimum profitable selling price, 300–350 USD per ton. The initial signs of predator infestation often go unnoticed and proliferation of the predator quickly leads to clearance of microalgal prey cells. As a result, sudden microalgal culture collapse, 'pond crash', is inevitable. Currently used grazer monitoring technologies such as microscopy have a limited detection limit whereas oligonucleotide-based markers are offline and time consuming. For timely implementation of grazer mitigation strategies, early detection of predator infestation is required. The current work leverages intrinsic properties of the interaction between microalgal prey, here *Dunaliella tertiolecta*, and predator, here *Oxyrrhis marina*, to develop early signs of predator detection. This study reports perturbation in photosynthetic processes, particularly non-photochemical quenching, of the microalgal prey. Reduction in non-photochemical quenching level appears to be associated with a build-up of ammonia-nitrogen excreted by the predator. The crash-predictive potential of non-photochemical quenching and total ammonia-nitrogen levels indicates the presence of the predator within the first 48 h of infestation. Further, the nutrient-repackaging ability of predators probed using Fourier Transform Infrared spectroscopy combined with chemometrics methods revealed predator-specific signature spectra. Profiling of extracellular chemicals involved in early prey and predator interactions are yet another potential monitoring signal explored in this work. Overall, we report the crash-predicative potential of unique physiological process of microalgal prey and predator as means of early fault detection. An integrated, real-time and non-invasive algal pest detection approach is required for effective microalgal pond management.

List of Abbreviations

AL	actinic light
ATP	adenosine tri-phosphate
CAPS	*n*-cyclohexyl-3-aminopropanesulfonic acid
CHAPS	3-[(3-cholamidopropyl) dimethylammonio]-1-propanesulfonate
DCF-DH	2',7'-dichlorodihydrofluorescein diacetate
DMSO	dimethyl sulfoxide
FRET	fluorescence resonance energy transfer
FTIR	fourier transform infrared spectroscopy
GLY	glycine
HEPES	4-(2-hydroxyethyl)-1-piperazineethanesulfonic acid
ITS	internal transcribed spacer
LC-MS	liquid chromatography-mass spectroscopy
LHC	light harvesting complex
MBSP	minimum biomass selling price
Mid-IR	mid infrared radiation
ML	measuring light
NPQ	non-photochemical quenching
OEC	oxygen evolving complex
PAM	pulse amplitude-modulation
PAR	photosynthetically active radiation
PCR	polymerase chain reaction
Phe	pheophytin
PHE	phenylalanine
PIPES	piperazine-n,n′-bis (2-ethanesulfonic acid)
PQ	plastoquinone
PRO	proline
PSI	photosystem I
PSII	photosystem II
PUFA	polyunsaturated fatty acids
QA	quality assurance
QC	quality control
RC	reaction center

rETR	relative electron transport
RGB	red green blue
RLC	rapid light curve
ROS	reactive oxygen species
SP	saturation pulse
TRP	tryptophan
Tyr	tyrosine
VDE	violaxanthin de-epoxidase
VOC	volatile organic compounds

List of Symbols

$F_{m'}$	maximum fluorescence (light adapted)
F_0	minimal fluorescence
F_m	maximum fluorescence (dark adapted)
F_v	variable fluorescence
N_2	nitrogen
NH_3	ammonia
NH_3-N	ammonia-Nitrogen
NH_4^+	ammonium ion
NH_4^+-N	ammonium-Nitrogen

Table of Contents

List of Figures

List of Tables

Chapter 1

Introduction

1.1 Introduction

The world is currently at the brink of a major crisis that involves food, water, energy and climate change. The global population is increasing exponentially and expected to exceed 8.5 billion by 2030 (United Nations 2013). The global demand for food (Leng and Hall 2019) and energy (Dorian et al. 2006) is anticipated to increase by 50 % over this period. Moreover, freshwater requirements will rise by 30 % (Connor 2015). To-date 2.1 billion people live without any access to safe-water (United Nations 2019). In the year 2019 alone about 113 million people, across 53 countries, experienced acute hunger, the majority of these countries falling into a low-income group. The current rate of agricultural productivity in low-income countries is 0.96 % whereas an increase in the rate of productivity by 1.75 % is required mitigate the food shortage. To meet the projected food demand, 100 Mha additional agricultural land is required and, like non-renewable energy resources, land is a limited commodity (Pastor et al. 2019). Natural calamities like drought and flooding have often resulted in famine in the recent past. Total crop yield loss across the globe as an effect of global warming is reported to be ~13 % for major food crops such as wheat, maize, soybean and rice due to changes in the temperature landscape (which is estimated to increase by 2–4 °C in the near future). Further, meat and poultry food production adds to climate change due to release of anthropogenic greenhouse gases that account up to 14.5 % of total greenhouse gas emissions (Gerber et al. 2013).

Carbon dioxide is one of the main contributors to global warming and in recent years its concentration in the atmosphere has increased by 32 %, and has recently surpassed 400 ppm (Leung et al. 2014). The relentless increase in carbon dioxide levels are positively correlated with fossil fuel emissions due to the buildup of emission gases in the atmosphere. Fossil fuel reserves such as natural gas, oil and coal, are finite. With the current rate of energy production and utilization, the natural sources of gas and oil are estimated to last for about 50 (until ~2063) more years whereas coal reserves will last up to 112 (until ~2125) years (Stocker et al. 2013). Although fossil reserves are projected to be available for the next several decades, the burning of fossil fuel would cause the buildup of carbon dioxide to catastrophic levels leading to critical

levels of global warming in just few years. It is estimated that about 80 percent of current fossil reserves must be kept underground to avoid the net increase (< 2°C) in the global temperature, due to the emissions, as agreed by the Paris Agreement (Dudley 2015). It is evident that the solutions to address the increased demand for food, energy and water must be strategically planned such as to cause minimal impact on environment while adapting to the climate change.

One such global effort is a net-zero carbon emissions goal. The Paris Agreement (2016), signed by 194 states and the European Union have committed to mitigate carbon emissions by 2030. Under the agreement the targeted reduction in the emissions by Australia and India, the latter being the third largest carbon producer, are estimated to be 18-26 % (Australian Government 2015) and 22–35 % (Government of India 2015), respectively. Australia has set a target to produce 20 % of total energy requirements through renewable routes by 2020 whereas India aims to generate 40 % renewable energy by 2030. Both countries are actively implementing various energy-efficient approaches and harnessing the potential of non-renewable resources such as wind-, solar- and bio-energy to reduce carbon emissions.

In recent years various physical and chemical-based carbon capture technologies have been developed. However, the scale, volume, utilization and storage involved in such approaches makes the overall operation very time consuming and expensive. Moreover, these technologies can most effectively capture carbon from a point source where emissions levels are high as compared to diffused emission. In contrast, biological routes such as plant and microalgae-based capture can efficiently cascade the trapped carbon, from diffused and point emissions, into synthesis of biomolecules which completely alleviates carbon storage and utilization problems. The biological biomass used for the capture can be further valorized for food and energy production in a sustainable manner. Moreover, biomass combustion can reduce greenhouse gas emissions by 14–90 % as compared to burning fossil fuel, thereby reducing the overall carbon dioxide buildup (Smit et al. 2014).

The main sources of biomass are agro-, wood-residues, and energy crops such as corn, canola, switchgrass, jatropha. It is projected that an additional 3000 Mha of land must be cultivated with energy crops to continue to meet the current demand for energy. Corn is one of the major plants used for bioethanol production which is currently blended at 2–5 and 10 %, in India (Singh 2019) and Australia (Akbar et al. 2019), respectively, with traditional petroleum fuel. The major challenge in commercialization of such technologies is the intensive land requirement and choice of fuel over food that is unavailable for the large populations of at least 53 countries. Use of fuel wood or wood residues for bioenergy production is also expected to

increase by 6-fold by 2060, leading to ecologically stressed forests and disturbed climate balance (Raunikar et al. 2010). Therefore, an alternative source of biomass feedstock is needed for biofuel production, yet with effective carbon capture efficiency.

1.2 Microalgae as a clean feedstock

In recent years, microalgae have emerged as a potential renewable resource; that is, cultivated at large-scale for food and biofuel-based commodity products. Microalgae are autotrophs and the primary producers of pelagic food webs. Their ability to fix carbon dioxide would greatly help to reduce the overall carbon footprint. Commercial microalgae cultivation is estimated to fix 513 tonnes of carbon dioxide and produce up to 120 tons of dry biomass per hectare annually (Bilanovic et al. 2009). Moreover, microalgae can thrive in non-potable water and are theoretically estimated to require 84 % less water to produce 1 kg of biomass as compared to the other energy crops (Gouveia 2011, Hannon et al. 2010). The achievable productivity of bio-oil, an alternative to natural oil, of microalgae in mass culture is estimated to be 40–50 gallon per acre per year and significantly higher than that of oil energy crops such as jatropha and canola (Weyer et al. 2010). Micro- and macro-algae have been part of human diets in many ancient civilizations including Japan, China and Mexico. Currently microalgal proteins account for about 18 % of total non-animal-based protein market (Caporgno and Mathys 2018). The fatty acid profiles of many microalgal species are superior to that of traditional fish oil and microalgal fatty acids are recommended as great substitute as dietary supplements and aquaculture feed (Allen et al. 2019). In addition, microalgae can provide many high-value products such as pigments and bioactive compounds of medicinal and therapeutic properties. The market for the pigment carotene is projected to reach 1.53 billion USD by 2020 (Barreiro and Barredo 2018). The food vs. fuel debate can be put to the test in the case of microalgae as many biorefinery approaches suggest the possibility of sequential extraction of high-value compounds (Suganya et al. 2016), including proteins, prior to biomass gasification for fuel production. Overall, microalgal cultivation, especially marine species, is relatively less land- (Table 1.1) and water-intensive. For example, 60–454 and 1892 trillion L of input water is required for 227 billion L of biodiesel using marine microalgae and corn, respectively (Pereira da Silva and Ribeiro 2019). Therefore, marine microalgae are an ideal candidate to combat food, water and energy crises while at the same time drawing down CO_2 and contributing to the amelioration of the climate change. However, the limiting step in microalgal

mass-scale cultivation is commercial feasibility. The production cost of microalgal biomass is at least 5-fold higher than that of plant-based feedstock (Christiansen et al. 2018).

Table 1.1. Comparison of oil yield and land-use requirements of microalgae and other crop-based feedstocks for biodiesel production. Table is a reproduced version of the content published in Mata et al. (2010).

Feedstock type	Oil content (% oil by weight in biomass)	Oil yield (L oil hectare^{-1} year^{-1})	Land use (m^2 year kg^{-1} biodiesel)	Biodiesel productivity (kg biodiesel hectare^{-1} year^{-1})
Soybean	18	636	18	562
Cameline	42	915	12	809
Canola	41	974	12	862
Sunflower	40	1070	11	946
Microalgae (low oil)	30	58700	0.1	51927
Microalgae (medium oil)	50	97800	0.1	86515
Microalgae (high oil)	70	136900	0.1	121104

The desirable yield of dry microalgal biomass has been suggested to be 25 g $m^{-2}d^{-1}$ to be produced at the projected Minimum Biomass Selling Price (MBSP) 300–350 USD per ton for economically feasible cultivation (Davis et al. 2016). Both productivity and MBSP are mainly dependent on the type of cultivation setup. Closed photobioreactors and open raceway ponds are widely used for large-scale microalgal cultivation. Closed photobioreactor cultivation favors higher productivity albeit at the higher cost. However, open raceway pond cultivation is currently the only commercially viable way to produce microalgal biomass in the range of MBSP. The open pond cultivation conditions are highly uncontrolled, subject to harsh environmental conditions and prone to contamination by unwanted microbes (Lammers et al. 2017). The majority of reported contaminants to-date are the consumers of microalgae, i.e. predators, interchangeably referred to as grazers. The invasion and ingestion of microalgae, the prey, by predators leads to biomass loss and as a result a sudden ‘culture crash' is inevitable. Overall a microalgal biomass loss of 20–30 % due to predation is reported for open cultivation setups (Richardson et al. 2014). Although closed systems are less prone to culture crash, predator invasion is unavoidable as decontamination of large volumes of raw and recycled water is proven to be difficult and further adds to the cost. Many pilot- and commercial-scale

cultivation systems, mainly open ponds, are reported to be infested with fungi, virus, zooplankton such as amoebae, ciliates, copepods, rotifers, dinoflagellates, etc., and bacterial predators (Day et al. 2017).

Mass cultivation of microalgae as a food and energy crop is a relatively new practice, about 50 years old, compared to the traditional farming of plant species wherein the plant weedy species are studied in detail (Ferrell and Sarisky-Reed 2010). Consequently, practical knowledge of contaminating microbes that infest microalgal cultures is very limited. To date only a few predatory microalgal contaminants are well characterized and their life cycles remain largely unknown. The majority of the reported predators are heterotrophic zooplankton which lack chloroplasts and therefore must consume autotrophs, mixotrophs and bacteria to derive nutrients such as carbon (C), phosphorus (P) and nitrogen (N). Such nutrients, particularly N, are present in biologically unavailable forms for heterotrophs and thus can be only assimilated through feeding on autotrophs (Dagenais-Bellefeuille and Morse 2013). Once a suitable nutrient source in the form of microalgal prey is identified, the predator growth rate can exceed the prey doubling time (Hansen et al. 2000). An optimum ratio of C:N:P of 106:16:1, the Redfield ratio, is often assumed to be ideal for growth of microalgae (Geider and La Roche 2002), hence the medium composition for mass cultivation is designed to closely match the Redfield ratio. However, the nutrient quality of microalgae cultivated by adhering to the ratio makes it an ideal prey for the predator (Sterner and Elser 2002, Flynn et al. 2017). As a result, predator species can quickly dominate the microalgal culture, leading to the crash.

1.3 Occurrences of microalgal pond crash

Compared to traditional agriculture practices, commercial outdoor microalgal cultivation, particularly for biofuel production, is in its nascent phase. Currently many pilot-scale commercial trials, in open-raceway ponds, are underway as a collaborative effort between public and private partners. All of the open pond setups have reported occasions when they have experienced a sudden culture crash due to infestation by predatory bacteria and zooplankton. For instance, a pilot-scale commercial raceway pond setup, Algae Testbed Public-Private Partnership (ATP^3), attempted to cultivate different species of microalgae across six different geographical sites. During three years of cultivation trials at ATP^3 sites, 29 attempts out of 54 failed (~53 %) due to predator invasion leading to the pond crash (McGowen et al. 2017, Knoshaug et al. 2018). Another pilot-scale commercial cultivation trial conducted for six years across different locations of southwest of Gulf Coast USA as part of the National

Alliance for Advance Biofuels and Bioproducts (NAABB) reported repetitive pond crashes due to predators invasion, notably by ciliates and rotifers (Lammers et al. 2017). The Arizona Center for Technology and Innovation, (AzCATI) reported a raceway pond crash in *Chlorella* cultivation and characterized the different taxonomic range of invaders, the majority of which were fungi, virus, ciliates, flagellates and ciliates (Wang et al. 2018). Reliance Industries Limited (RIL) India reported invasion by ciliates and dinoflagellates, that collapsed *Chlorella vulgaris* cultures cultivated in open raceway ponds within 2 and 4 days, respectively, after the first microscopic signs of the infection (Karuppasamy et al. 2018). Columbus Algal Biomass (CAB) farms, in New Mexico and Las Cruces Test Sites jointly operated by Sapphire Energy, Inc and University of California reported infestation by *Cryptomycota*, a fungus-like parasite, in a *Scenedesmus dimorphous* culture. The pest, *Cryptomycota*, caused collapse of the culture two days after the initial symptoms of infection (McBride et al 2014). Ganuza et al. (2016) reported collapse of four pilot commercial-scale open pond (130,000 L) developed by Heliae Development, LLC reported a culture crash in less than two days after the first microscopic evidence of the presence of a pest which was later characterized as *Vampirovibrio chlorellavorus*, an obligate parasite. This underlines the severity of the contamination which quickly outnumbers the microalgal prey cell concentration and leaving a shorter timespan for decision making to implement any pest- deterrent treatments. Detailed information about occurrences of pond crash, type of microalgal prey and predator and timescale of culture crash is outlined in chapter 2 (Table 2.1)

The initial presence of the predators in the trials described above were reported to be minuscule in the seed cultures that are used for outdoor pond inoculation. Microscopy was the only means of predator tracking used by all cultivation setups except the CAB raceway ponds operated by Sapphire Energy. Microscopy is labor intensive, offline and requires a certain level of expertise to enumerate the predators (Day et al. 2017, Bartley et al. 2013). Moreover, the sample amount, 10–1000 μL, used for microscopy is very small compared to the scale of the outdoor culture. Therefore, microscopic estimation highly under-represents the actual concentration of the invading microbes. In addition to the microscopy, continuous flow cytometry monitoring can potentially indicate the presence of a predator at a critical threshold of 10^8 cells per ml (Day et al. 2012). However, this approach is difficult to scale up for large-scale cultivation. In contrast, oligonucleotide marker-based methods such as SpinDx™, RapTor™ (Lane et al. 2013) and 16s rRNA specific qPCR (Lammers et al. 2017) are proven to be very sensitive at low concentrations of predators. PCR based methods, however, tend to

be predator species specific and fail to detect uncharacterized predator infection. Such methods also require elaborate sample preparation to isolate nucleic acid material prior to the detection; hence, the methods are limited to the laboratory. Researchers at Sandia National Laboratory, USA recently reported Volatile Organic Compounds (VOC), degradation products of carotenoids, as an early marker of microalgal predation using gas chromatography (Reese et al. 2019), which is presently an offline mode of measurement. The currently used predator monitoring techniques are mainly offline and typically involve a time lag of 3–8 hours of sample processing. Meanwhile, the predator continues to feed on microalgal prey which leads to yet more biomass loss. Therefore, online or onsite monitoring tools, with minimum to no sample preparation time, set up in-line with the microalgal cultures are required.

Early signs of predator infestation can aid in timely implementation of prophylactic strategies, such as addition of grazer-deterrent chemicals (Van Ginkel et al. 2015), to increase overall success rate of mass scale cultivation (Karuppasamy et al. 2018). Ideally, early warning signs need to be online or on-site, non-invasive and real time measurements that can easily be scaled up to large volume cultures. In addition, warning measurements must be reliable, sensitive to minute predator concentrations and fairly universal across different prey-predator combinations.

The current research hypothesized that it would be possible to leverage the intrinsic properties (inherent process) of microalgal prey and predators to develop early warning signals of microalgal grazing. Photosynthesis is an inherent property of microalgae, unlike majority of heterotrophic predators reported to infest the cultures. Photosynthesis is reported to be negatively affected under various abiotic stress conditions. Knowledge of alterations in photosynthetic physiology under biotic stresses such as microalgal grazing is very limited. The prey and predator co-exist in nature and participate in nutrient recycling and repackaging, the bottom-to-top trophic transfer of nutrients. The recycled nutrients are exchanged between prey and predator (Deore et al. 2020a). Often such events are reported to perturb prey metabolism, particularly photosynthesis. Investigation of causal relationships between the recycled nutrients and photosynthesis could lead to identification of molecular markers which, further, can be used in tandem with photosynthetic measurements to monitor the presence of a predator.

Invasion of grazers in mass culture is likely to abide by the ecology of tropic transfer and as a result change the overall nutrient dynamics. The study identifies key nutrients, consequential to the prey and predator interaction, as markers of microalgal grazing using Fourier Transform Infrared spectroscopy (FTIR). The predator feeding process is quite intricate

and involves prey searching, recognition and detection using chemoattractants. Similarly, many microalgae are reported to release chemical cues as a response to predation. In addition to the identification of photosynthesis- and FTIR-based markers, the current study attempts to profile exo-metabolomic signals of microalgal prey and predator to identify early markers of grazing. The study uses *Dunaliella tertiolecta*, a high-pigment-accumulating species and one of the most widely exploited commercial microalgal strains, and *Oxyrrhis marina*, a model dinoflagellate as microalgal prey and predator strains, respectively.

1.4 Aims and Objectives

- Chapter 2 of the thesis systematically reviews the to date occurrences and conditions in outdoor cultivation that leads to culture collapse. Types of predators, currently practiced predator monitoring methods, associated cost and limitations are described in detail. In addition, chapter 2 describes indirect methods of grazer detection based on inherent features of microalgal prey and predators.
- An experimental validation of photosynthesis-based markers for detection of *Oxyrrhis marina* invasion using Pulse Amplitude Modulation (PAM) chlorophyll fluorescence is outlined in chapter 3.
- Chapter 4 investigates changes in photosynthetic parameters in relation to nutrient recycling-mediated by predator. Further, provides a detailed account on symptomatic potential of recycled nitrogen, ammonia, as a maker of *O. marina* invasion and its possible role in observed (chapter 3) photosynthesis perturbations.
- Chapter 5 leverages nutrient repackaging-mediated by *O. marina* as a means of fault, grazer detection using FTIR combined with chemometrics tools.
- Chapter 6 attempts to profile the exo-metabolomic cues of the prey-predator interactions in an untargeted manner using Liquid Chromatography-Mass Spectrometry (LC-MS). The thesis overall suggests an integrated pest, *O. marina*, detection approach in combination with traditional monitoring methods for effective management of microalgal mass cultures.

References

Akbar D, R Subedi, J Rolfe, N Ashwath, and A Rahman. 2019. "Reviewing commercial prospects of bioethanol as a renewable source of future energy—an Australian perspective." In *Advances in Eco-Fuels for a Sustainable Environment*, edited by K Azad, 441-458. Woodhead Publishing.

Allen KM, H Habte-Tsion, KR Thompson, K Filer, JH Tidwell, and V Kumar. 2019. "Freshwater microalgae (*Schizochytrium* sp.) as a substitute to fish oil for shrimp feed." *Scientific Reports* 9 (1):6178-6188. doi: 10.1038/s41598-019-41020-8.

Australian Government. 2015. Australia's 2030 climate change target.

Barreiro C, and J Barredo. 2018. "Carotenoids Production: A Healthy and Profitable Industry." In *Microbial Carotenoids*, edited by C Barreiro and J Barredo, 45-55. New York: Humana Press

Bartley ML, WJ Boeing, AA Corcoran, FO Holguin, and T Schaub. 2013. "Effects of salinity on growth and lipid accumulation of biofuel microalga *Nannochloropsis salina* and invading organisms." *Biomass and Bioenergy* 54:83-88. doi: https://doi.org/10.1016/j.biombioe.2013.03.026.

Bilanovic D, A Andargatchew, T Kroeger, and G Shelef. 2009. "Freshwater and marine microalgae sequestering of CO_2 at different C and N concentrations–response surface methodology analysis." *Energy Conversion and Management* 50 (2):262-267.

Caporgno MP, and A Mathys. 2018. "Trends in Microalgae Incorporation Into Innovative Food Products With Potential Health Benefits." *Frontiers in Nutrition* 5 (58):1-10. doi: 10.3389/fnut.2018.00058.

Christiansen K, DR Raman, G Hu, and R Anex. 2018. "First-order estimates of the costs, input-output energy analysis, and energy returns on investment of conventional and emerging biofuels feedstocks." *Biofuels Research Journal* 20:894-899.

Connor R. 2015. *The United Nations world water development report 2015: water for a sustainable world*. Vol. 1, *WWAP (United Nation World Water Assesment Programme)* Paris: UNESCO publishing.

Dagenais-Bellefeuille S, and D Morse. 2013. "Putting the N in dinoflagellates." *Frontiers in Microbiology* 4:369-683. doi: https://doi.org/10.3389/fmicb.2013.00369.

Davis R, J Markham, C Kinchin, N Grundl, EC Tan, and D Humbird. 2016. Process design and economics for the production of algal biomass: algal biomass production in open pond systems and processing through dewatering for downstream conversion. In *No. NREL/TP-5100-64772*. United States: National Renewable Energy Lab.

Day JG, Y Gong, and Q Hu. 2017. "Microzooplanktonic grazers – A potentially devastating threat to the commercial success of microalgal mass culture." *Algal Research* 27:356-365. doi: https://doi.org/10.1016/j.algal.2017.08.024.

Day JG, NJ Thomas, UE Achilles-Day, and RJ Leakey. 2012. "Early detection of protozoan grazers in algal biofuel cultures." *Bioresource Technology* 114:715-719.

Deore P, J Beardall, and S Noronha. 2020. "Non-photochemical quenching, a non-invasive probe for monitoring microalgal grazing: influence of grazing-mediated total ammonia-nitrogen." *Applied Phycology* 1 (1):32-43.

Dorian JP, HT Franssen, and DR Simbeck. 2006. "Global challenges in energy." *Energy Policy* 34 (15):1984-1991.

Dudley B. 2015. BP statistical review of world energy 2016. London, UK.

Ferrell J, and V Sarisky-Reed. 2010. National algal biofuels technology roadmap. United States EERE Publication and Product Library.

Flynn KJ, P Kenny, and A Mitra. 2017. "Minimising losses to predation during microalgae cultivation." *Journal of Applied Phycology* 29 (4):1829-1840.

Ganuza E, CE Sellers, BW Bennett, EM Lyons, and LT Carney. 2016. "A novel treatment protects *Chlorella* at commercial scale from the predatory bacterium *Vampirovibrio* chlorellavorus." *Frontiers in Microbiology* 7:848.

Geider R, and J La Roche. 2002. "Redfield revisited: variability of C:N:P in marine microalgae and its biochemical basis." *European Journal of Phycology* 37(1):1-17. doi: 10.1017/S0967026201003456.

Gerber PJ, H Steinfeld, B Henderson, A Mottet, C Opio, J Dijkman, A Falcucci, and G Tempio. 2013. *Tackling climate change through livestock: a global assessment of emissions and mitigation opportunities*: Food and Agriculture Organization of the United Nations (FAO).

Gouveia L. 2011. *Microalgae as a feedstock for biofuels Springer briefs in Microbiology*. New York: Springer.

Government of India. 2015. India's intended nationally determined contribution: Working towards climate justice. In *Vikaspedia*.

Hannon M, J Gimpel, M Tran, B Rasala, and S Mayfield. 2010. "Biofuels from algae: challenges and potential." *Biofuels* 1 (5):763-784.

Hansen PJ, PK BjØrnsen, and BW Hansen. 2000. "Zooplankton grazing and growth: scaling within the 2–2,000-µm body size range." *Limnology and Oceanography* 45 (8):1891-1891.

Karuppasamy S, AS Musale, B Soni, B Bhadra, N Gujarathi, M Sundaram, A Sapre, S Dasgupta, and C Kumar. 2018. "Integrated grazer management mediated by chemicals for sustainable cultivation of algae in open ponds." *Algal Research* 35:439-448.

Knoshaug EP, E Wolfrum, LM Laurens, VL Harmon, TA Dempster, and J McGowen. 2018. "Unified field studies of the algae testbed public-private partnership as the benchmark for algae agronomics." *Scientific Data* 5:180267-180277. doi: https://doi.org/10.1038/sdata.2018.267.

Lammers PJ, M Huesemann, W Boeing, DB Anderson, RG Arnold, X Bai, M Bhole, Y Brhanavan, L Brown, and J Brown. 2017. "Review of the cultivation program within the National Alliance for Advanced Biofuels and Bioproducts." *Algal Research* 22:166-186.

Lane TW, PD Lane, C Koh, LT Carney, and OD Solberg. 2013. Pond Crash Forensics: Microbiome Analysis and Field Diagnostics. Livermore, CA Heliae Development, USA.

Leng G, and J Hall. 2019. "Crop yield sensitivity of global major agricultural countries to droughts and the projected changes in the future." *Science of the Total Environment* 654:811-821.

Leung DYC, G Caramanna, and MM Maroto-Valer. 2014. "An overview of current status of carbon dioxide capture and storage technologies." *Renewable and Sustainable Energy Reviews* 39:426-443. doi: https://doi.org/10.1016/j.rser.2014.07.093.

McGowen J, EP Knoshaug, LM Laurens, TA Dempster, PT Pienkos, E Wolfrum, and VL Harmon. 2017. "The Algae Testbed Public-Private Partnership (ATP3) framework; establishment of a national network of testbed sites to support sustainable algae production." *Algal Research* 25:168-177. doi: https://doi.org/10.1016/j.algal.2017.05.017.

Pastor AV, A Palazzo, P Havlik, H Biemans, Y Wada, M Obersteiner, P Kabat, and F Ludwig. 2019. "The global nexus of food–trade–water sustaining environmental flows by 2050." *Nature Sustainability* 2 (6):499.

Pereira da Silva P, and LA Ribeiro. 2019. "Assessing Microalgae Sustainability as a Feedstock for Biofuels." In *Advanced Bioprocessing for Alternative Fuels, Biobased Chemicals, and Bioproducts*, edited by M Hosseini, 373-392. United States: Woodhead Publishing.

Raunikar R, J Buongiorno, JA Turner, and S Zhu. 2010. "Global outlook for wood and forests with the bioenergy demand implied by scenarios of the Intergovernmental Panel on Climate Change." *Forest Policy and Economics* 12 (1):48-56.

Reese KL, CL Fisher, PD Lane, JD Jaryenneh, MW Moorman, AD Jones, M Frank, and TW Lane. 2019. "Chemical profiling of volatile organic compounds in the headspace of algal cultures as early biomarkers of algal pond crashes." *Scientific Reports* 9 (1):1-10.

Richardson JW, MD Johnson, X Zhang, P Zemke, W Chen, and Q Hu. 2014. "A financial assessment of two alternative cultivation systems and their contributions to algae biofuel economic viability." *Algal Research* 4:96-104.

Singh K. 2019. "India's bioenergy policy." *Energy, Ecology and Environment* 4 (5):253-260.

Smit B, AA Park, and G Gadikota. 2014. "The grand challenges in carbon capture, utilization, and storage." *Frontiers in Energy Research* 2:55.

Sterner RW, and JJ Elser. 2002. *Ecological stoichiometry: the biology of elements from molecules to the biosphere*: Princeton University Press.

Stocker TF, G Qin, GK Plattner, SK Tignor, AJ Boschung, NY Xia, V Bex, and MP Midgley. 2013. *Climate Change 2013: The Physical Science Basis. Contribution of Working Group I to the Fifth Assessment Report of the Intergovernmental Panel on Climate Change*. Cambridge, United Kingdom and New York, NY, USA: Cambridge University Press.

Suganya T, M Varman, HH Masjuki, and S Renganathan. 2016. "Macroalgae and microalgae as a potential source for commercial applications along with biofuels production: A biorefinery approach." *Renewable and Sustainable Energy Reviews* 55:909-941. doi: https://doi.org/10.1016/j.rser.2015.11.026.

United Nations. 2013. UN Projects World Population to Reach 8.5 Billion by 2030, Driven by Growth in Developing Countries. In *United Nations Department of Economic and Social Affairs*. New York.

United Nations. 2019. World water development report.

Van Ginkel SW, T Igou, Z Hu, A Narode, S Cheruvu, S Doi, R Johnston, T Snell, and Y Chen. 2015. "Taking advantage of rotifer sensitivity to rotenone to prevent pond crashes for algal-biofuel production." *Algal Research* 10:100-103.

Wang Y, Y Gong, L Dai, M Sommerfeld, C Zhang, and Q Hu. 2018. "Identification of harmful protozoa in outdoor cultivation of *Chlorella* and the use of ultrasonication to control contamination." *Algal Research* 31:298-310.

Weyer KM, DR Bush, Al Darzins, and BD Willson. 2010. "Theoretical maximum algal oil production." *Bioenergy Research* 3 (2):204-213.

Chapter 2

Review of Literature

2.1 Introduction

The importance of marine microalgae cultivation in relation to current global framework and economic implications of grazer infestation on loss of biomass productivity are outlined in Chapter 1. Numerous occurrences of culture collapse in commercial scale microalgae cultivation operation due to predator infestation are outlined in Chapter 1 and Table 2.1. The present chapter reviews candidate microalgal strains prey, and types of microalgal predators that are reported to infest mass culture along with current predator monitoring tools. The chapter outlines the rationale of exploiting changes associated with prey and predator physiology, i.e. their intrinsic properties, to develop early warning signs of a potential culture crash. Furthermore, the chapter elaborates on the relevant background of technologies that can be deployed online to measure the intrinsic properties.

2.2 Microalgal prey

Many species of algae belonging to the Class Chlorophyta are of commercial interest and are important sources of pigments, polymers, novel bioactive compounds, protein and lipids. Marine green microalgal species such as *Nannochloropsis*, *Chlorella*, *Haematococcus*, *Dunaliella*, etc., are preferred strains due to their ability to accumulate high levels of protein, pigments and lipids, desirable for cost effective food- and fuel-based commodity products (Borowitzka 2018) . Performance robustness in relation to growth, biomass accumulation and high stress tolerance are other key factors in consideration of candidate algal strains for sustainable year-round commercial production (Spolaore et al. 2006). *Nannochloropsis* (Ma et al. 2016) and *Chlorella* sp. (Safi et al. 2014) are candidate strains for high lipid and protein, respectively. *Haematococcus* (Lorenz and Cysewski 2000) and *Dunaliella* sp. (Ben-Amotz et al. 1982) on the other hand are mainly cultivated for production of pigments such as astaxanthin and β-carotene, respectively. The current global market for β-carotene alone is estimated to be USD 532 million. Single cell protein, xanthophyll pigments and glycerol (Craigie and McLachlan 1964) are commodities produced using *Dunaliella* sp. biomass cultivated in outdoor open ponds.

D. tertiolecta and *D. salina* are the two most widely exploited commercial strains of *Dunaliella* sp. (Borowitzka et al. 1984). In recent years, *D. tertiolecta* has attracted tremendous commercial interest. A number of researchers have reported relatively higher lipid, >37 %, content compared to *D. salina* (Hosseini and Shariati 2009). Furthermore, chemical-inducible accumulation of lipid (20–40 %), desirable for biofuel production, in *D. tertiolecta* is reported by Liang et al. (2019). In addition, the strain is more amenable to genetic modification for trait enhancement as opposed to *Nannochloropsis* sp. which is reported to be difficult to transform due to the presence of a rigid cell wall (Scholz et al. 2014). *Dunaliella* is also reported to be ideal for single cell protein production, saline wastewater treatment and bioremediation applications (Hosseini and Shariati 2009). The overall commercial potential of *Dunaliella* sp. cultivation lies in co-production of biofuel along with sequential extraction of value-added products and pigments. Post extraction biomass can be processed into animal feed formulation (Ben-Amotz 2009). All of the above are required to effectively address the increasing need of food and fuel (Greenwell et al. 2010).

The commercial scale cultivation of *Dunaliella* sp. dates back to the 1980's and β-carotene was the first high-value ingredient produced from this alga (Ye et al. 2008). Large-scale cultivation of *Dunaliella* sp. is by far one of the most successful commercial setups (mostly in Australia, USA and Israel) as compared to the other microalgal species, *Nannochloropsis* and *Chlorella* (Parmar et al. 2011). *D. tertiolecta* is reported to withstand extreme environmental conditions; for example, hypo- and hypersaline conditions (0.05–2 M NaCl), high light (1000–2000 μmol photons m^{-1} s^{-1}), temperature (10–35^{o}C) tolerance (Goldman and Ryther 1976, Seepratoomrosh et al. 2016, Tol and White 2003). Environmental stress tolerance is a desirable trait of candidate microalgal strains for outdoor cultivation, where abiotic parameters can be uncontrolled and variable over the course of a day. The relative ease of cultivation, high (165 mg m^{-2} d^{-1}) productivity (García-González et al. 2003), and easy product extraction due to the presence of a less rigid cell wall (Ahmed et al. 2017) contributes to the commercial success of *Dunaliella* sp. cultivation. The resilient *D. tertiolecta* strain however shows a poor immunity against its consumers, predatory herbivorous.

2.3 Susceptibility of open cultures to microalgal grazing

The desirable biomass productivity at Minimum Biomass Selling Price (MBSP) (chapter 1) requires large volume cultivation. Rogers et al. (2014) reported a sea water requirement of 1463 million litres per day for a typical paddle wheel driven, 2-acre raceway

pond. Decontamination of large amounts of water on a daily basis is impractical and time consuming. Moreover, the step adds to increased biomass production cost. Although water filtration and hypochlorite treatments are cost effective ways to avoid contamination, the open and uncontrolled nature of the cultivation conditions makes raceway ponds more susceptible to contaminant infestation (Wang et al. 2013). Recycling of water post biomass harvesting, and an ensuing carry-over load of contaminants, is also a potential route of grazer transmission. Invaders are also likely to be present in the seed culture, used as inoculum for open ponds, albeit at low concentration. At this stage, predator numbers may be only < 0.005 % of total microalgal concentration and hence would remain undetected by routine microscopic inspection (Day et al. 2012, Flynn et al. 2017).

The seed cultures are generally cultivated under optimum and controlled conditions of parameters such as light, temperature, nutrients, etc. Therefore, an overall high growth rate of microalgae is favoured. Microalgae in the outdoor setup, depending on time of the day and depth in the culture, encounter different phases of high and low light. Duration of intense light, peak sunlight, lasts up to 4–5 hrs in a typical day, otherwise the culture is largely exposed to relatively low light (Richmond 2004). The availability of light is directly correlated to the amount of carbon fixation and the nutritional quality of microalga as prey. High light conditions combined with nutrient (P) limitation decouples carbon fixation from microalgal nutrient uptake. Reduced nutrient assimilation can thus lead to poor prey nutritional quality and thereby reduces grazing. In contrast, low light and low P/C conditions lead to increases in polyunsaturated fatty acids (PUFAs) content within microalgae (Tiselius et al. 2012, Urabe et al. 2002). High PUFA levels are one of the important markers of the nutritional quality of microalgal prey for zooplankton (Tiselius et al. 2012). Low light conditions, common to outdoor cultures, increase the nutritional value of the microalgal prey relative to its carbon content, thereby favouring grazing of microalgae (Urabe et al. 2002, Mitra and Flynn 2005). Some predator species are known to form cysts (Day et al. 2017) which germinate to produce viable predator progeny under suitable conditions such as nutrients availability (Montagnes et al. 2010). Shifts in environmental conditions post seed culture inoculation may trigger predator reproduction that can further increase active grazing on microalgal prey. As a result of increased grazing activity, the predatory microbes proliferate better in outdoor situations as opposed to in enclosed seed microalgal cultures. Closed cultivation platforms, photobioreactors, are also prone to contamination that is probably transmitted due to use of

large volumes of recycled water or inefficient sterilization of air through membrane filters (Wang et al. 2013).

2.3.1 Types of predators

Over the years, a variety of biological contaminants have been reported to infest microalgal cultures. Invaders often compete with the candidate microalgae for available nutrient resources and exist as cross-contaminant 'pest species' (Smith et al. 2005). A few parasites co-exist inside microalgae and negatively affect the growth of their microalgal host. Such associations can be detrimental as their association is reported to alter the physiological behaviour of microalgae. Parasite infection triggers cell clumping and further inhibits microalgal growth (Gutman et al. 2009, Schroeder et al. 2003). As opposed to the parasites, infestation with predator microbes is particularly devastating as predator species can quickly outcompete the microalgal prey (Day et al. 2012). Overall, 9 out of 10 contaminants are reported to be microalgal predators and pose a great threat to mass cultivation. Post et al. (1983) reported 14 different protozoa representatives of different genera that infested commercial-scale *D. salina* ponds. The list of microalgal pest and predator species is exhaustive (Day et al. 2017) and the current chapter describes contaminants that are particularly prevalent in the outdoor mass cultivation of microalgae.

2.3.1.1 Competitive and parasite microbes

Algae are known to co-exist with bacterial, fungal and virus communities in the phycosphere. Their association can be of a symbiotic or competitive nature. In addition, infestation by other photosynthetic organisms such as cyanobacteria, diatoms, etc, can result in competition for resources such as nutrients. Higher nutrient uptake by contaminating microbes can result in reduced growth rate of candidate microalgae and the culture then invariably becomes dominated by pest species. Although untypical of culture collapse, mediated by predators, pest species dominance is undesirable and raises biomass quality-control issues in steady state cultivation systems (Wang et al. 2013). For example, contamination with the toxin-producing cyanobacterium, *Microcystis aeruginosa*, renders algal biomass unsuitable for human and animal consumption (Roy-Lachapelle et al. 2017). Similarly, undesired *Scenedesmus* species are reported to displace *Chlorella* species in mass cultivation (Huo et al. 2017). This can lead to inefficient harvesting, extraction and conversion of biomass which can pose a great challenge to bio-process engineering. Viral and fungal microalgal pathogens mostly exist as parasites. Fungal pathogens produce motile life forms, zoospores, and can

become established as parasites in microalgal cultures. Chytrid species are reported to crash mass cultures of *Scenedesmus* (Carney et al. 2014, Fott 1967) and *Haematococcus* sp. (Gutman et al. 2009). The majority of the fungal parasites of microalgae are uncharacterised and little is known about their mode of infection. In addition, cyst formation makes the infection persistent as it is resistant to the majority of disinfection methods during the dormant phase (Fott 1967). In contrast, the occurrence of viral infections leading to culture collapse at a commercial scale are relatively few. However, phytoplankton mortality due to viral attack in the wild is reported (Brussaard 2004).

2.3.1.2 Predatory herbivorous microbes

Invasion of herbivores, consuming microalgae as a prey, is the major cause of culture crashes in commercial scale microalgae cultivation. To-date, a variety of zooplankton species are reported to infest microalgal mass cultures. However, grazing is observed to be prey species- and size-specific and, moreover, dependent on climatic conditions (Carney and Lane 2014, Day et al. 2017). Grazers of an average size <1 mm are reported to clear 1 % of total microalgal cells in one hour (Montagna 1995). At this rate, a non-dividing microalgal biomass can theoretically be completely cleared in just 4 days. In addition to the active prey ingestion grazer proliferation, increased abundance of predators (Flynn et al. 2017) can further reduce the time required for complete prey cell clearance. The most widely reported zooplankton predators in a commercial setting are ciliates, rotifers, copepods, amoebae and dinoflagellates.

There many reports of commercial and laboratory contamination with benthic ciliates that are algivorous. Such ciliates include for example, members of the Ciliophora - *C. steinii*, *Euplotes* sp., *Loxodes magnus* and *Lohmanniella* sp (Rothbard 1975, Karuppasamy et al. 2018). Ciliates are relatively smaller in size (20–90 µm), and are capable of consuming prey of roughly similar body size, compared to other predator species such as rotifers and copepods (Day 2013). *Brachionous calyciflorus*, *B. patulus* and *B. pilicatilis* are rotifers that are reported to graze on a variety of candidate microalgal prey species (Reese et al. 2019, Carney et al. 2016). Hence, they are predominantly observed in the majority of large scale microalgal culture setups. Copepods are crustaceans and are less documented in commercial cultivation setups. However, even at low copepod concentration, the highest microalgal prey clearance activity is reported (Day et al. 2017). *Poterioochromonas malhamensis*is a mixotrophic flagellate that is reported to be a persistent contamination of Chlorella sp. cultivation (Ma et al. 2018). Perhaps toxicity of the flagellate towards other pest species, cyanobacteria, and larger predator, rotifers,

(Boxhorn et al. 1998) may contribute to persistent infections. Flagellate predators are of particular concern in outdoor culture mainly due to their ability to ingest prey larger than own body volume. *Oxyrrhis marina*, a dinoflagellate, is one such example that can ingest prey cells larger, by several orders of its magnitude, than itself.

There is an ongoing effort to identify and characterise the invasive species found in large scale microalgae culture. Little is known about the majority of the invaders with respect to their mode of infection, life cycle, genetic information, feeding behaviour and prey selectivity. It is of paramount importance to understand the intricacies of predator behaviour to effectively formulate detection and mitigation measures. Therefore, in this study a well know dinoflagellate, *Oxyrrhis marina*, used as a predator of *Dunaliella tertiolecta*, the microalgal prey central to the research, was chosen as the model.

***Oxyrrhis marina* – a model predator species**

Oxyrrhis marina is a heterotrophic marine dinoflagellate. An elongate oval body with a posterior notch and two flagella, longitudinal and transverse, are the typical morphological features of *O. marina*. The reproduction and life cycle of the dinoflagellate are determined by environmental conditions. Cells divide vegetatively by binary fission under adequate nutrition conditions, whereas stress conditions trigger diploid zygote formation where vegetative cells acts as haploid gamete followed by cyst formation. Overall cell size ranges from 20–30 μm, though size can increase or shrink depending on the life cycle stage and food availability (Montagnes et al. 2010). *O. marina* ingests food, their prey, by engulfment and their feeding behaviour involves several stages – prey search, capture, processing, ingestion and digestion. Prey searching is assisted by environmental stimuli such as prey exudates, chemoattractants etc., and positive chemotaxis, movement towards prey, is observed. Prey capture is a function of flagellar movements which enable encircling of the prey prior to its capture and is commonly referred to as raptorial feeding. In addition, filament- and trichocyte-assisted prey capture by *O. marina* is also reported and is termed intercept feeding. Followed by the capture, the processing step determines the suitability of prey, based on size, biochemical profile, surface charge, etc., for ingestion. The prey and predator attachment mediated by receptors is a key prerequisite for prey ingestion to facilitate phagocytosis (Roberts et al. 2010). The initiation of phagocytosis involves microtubule rearrangement and engulfed prey cells appear under electron microscopy as electron-dense coagulated matter and a granular membranous mass during the digestion process inside vacuoles (Öpik and Flynn 1989). Versatile feeding behaviour and cyst formation abilities contribute to the overall robustness of *O. marina* as a

zooplankton predator (Montagnes et al. 2010). The dinoflagellate is also tolerant to high salinity, with a tolerance range 4–130 (Droop 1959), and hence an ideal predator of halotolerant *D. tertiolecta*.

2.4 Monitoring methods

Extensive research is underway to devise treatment regimens, that are mostly comprised of physical and chemical methods, to reduce the possibility of culture crash. For timely implementation of a treatment regime, early warning signals of predator presence are required to arrest its growth at the lowest concentration of predators. Currently practised grazer monitoring tools mostly rely on physical (direct) detection of predator presence either by observation, microscopy, or pattern matching of nucleic acid sequences from the invaders. Microscopy- and oligonucleotide-based markers are the most widely used grazer monitoring methods in commercial setups. This section systematically reviews currently used direct and indirect grazer monitoring methods, detection limits and challenges associated with each of them. Table 2.1 summarises occurrences, to-date, of commercial microalgal culture collapse, the causative agents responsible and implemented grazer monitoring methods.

2.4.1 Direct Methods

2.4.1.1 Microscopy

Microscope-assisted predator identification and enumeration is the most straightforward and cost-effective approach. Typically, microscopic enumeration is done using haemocytometer or Sedgwick Rafter chambers which require 10–20 µl and 1000 µl samples respectively. Such small sample volumes are not a good representation of the actual scale (1000–100,000 L) of the cultivation, and can lead to erroneous estimation, mostly under-representation, of predator load. As reported in a later chapter (chapter 3) microscopic screening is unable to detect algal predators, especially dinoflagellates and ciliates, at lower densities ($<10^3$ cells ml^{-1}). Further, dense phytoplankton cultures ($>10^6$ cells ml^{-1}) limit grazer enumeration and remedial dilution method can probably lead to false negative outcome. Moreover, predators of larger body size, such as rotifers and copepods, cannot be detected using the chambers. Predators at low concentration and of large size can be monitored using a sample fixed with Lugol's iodine in which cells are allowed to settle in sedimentation chambers. However, this requires 10–12 h of incubation prior to the screening on an inverted microscope.

In addition to the technical limitations, microscopic observations are highly dependent on observer's skill, experience and bias for accurate estimation. A staining-based microscopy approach for contaminant detection has been developed to overcome observers bias. For example, Calcofluor white dye, which stains chitin present in fungal cell wall, is used for chytrid identification (Rasconi et al. 2009). However, The stain is non-specific and can also stain cellulose rich cell walls of the microalga *H. pluvialis*, yielding false positive results (Damiani et al. 2006). SYTOX Green (Gerphagnon et al. 2013), Congo Red (Gachon et al. 2010), Nile Red (Gutman et al. 2009) and Methylene Blue (Karuppasamy et al. 2018) have also been used to detect contamination.

The outlined microscopic methods are offline, time consuming and subjected to manual error. High dependence on manual microscopic counts limits the intervals of sampling for screening efforts. In commercial setups, the frequency of microscopic screening is reported to be once a day or thrice a week. Such sampling regimes can fail to indicate early invasion and once spotted, significant biomass loss may have already occurred.

2.4.1.2 Continuous flow cytometer and *in situ* microscopy

In contrast to microscopic methods, continuous monitoring can be enabled by flow-through channels coupled with a camera recorder for particle (cells) analysis. Phytoplankton and zooplankton cells are classified and enumerated, typically involving a 50–100 ml sample volume, using cell shape, size and fluorescence as identification criteria (Poulton and Martin 2010). Further, optimisation of flow rate (0.1–1 ml min^{-1}) can enable screening of larger volumes of samples. Flow through designs can detect 1–10 grazers cells ml^{-1} (rotifers, ciliates and dinoflagellates) in dense phytoplankton cultures (10^7 cells ml^{-1}) of *Nannochloropsis oculata* (Day et al. 2012) and *Chlorella* sp. (Wang et al. 2017). Similarly, *in situ* microscopy (ISM) can be implemented as a means of online monitoring and enumeration of *Chlorella* and *Chlamydomonas* sp. growth (Havlik et al. 2013). ISM demonstrates online and real-time monitoring potential of camera-assisted flow- through designs to detect microalgal predators. The overall operating cost of flow cytometry systems (such as commercially available FlowCam and elzone counter) is estimated to be USD 1–5 per sample (Poulton and Martin 2010).

Table 2.1 List of occurrences of microalgal pond crash at commercial scale and currently practised grazer monitoring and mitigation methods.

Microalgal prey	Predator	Cultivation platform/ location	Detection methods	Collapse (d) after first sign of invasion	Treatment	References
Dunaliella salina	Amoebae, *Naegleria* sp. and *Cladotricha* sp.	120,000 L lagoon - Roche Algal Biotechnology, Australia.	Microscopy	-	-	(Post et al. 1983)
Dunaliella salina	Ciliates	400 and 2000 L outdoor ponds, Cadiz, Spain.	Microscopy	5–6	Quinine sulphate	(Moreno-Garrido and Cañavate 2001)
Chlorella sp.	Predatory bacteria, *Vampirovibrio chlorellavorus*	6000 and 130,000 L outdoor ponds, Heliae Development, USA.	Microscopy, oligonucleotide markers (16s rRNA)	2	pH shock treatment	(Ganuza et al. 2016)
Microchloropsis salina	Ciliates and rotifers	30 L, Open aquaria greenhouse, New Mexico, USA.	Microscopy	10–12	High salinity	(Bartley et al. 2013)
Chlorella sorokiniana	*Vampirobrio chlorellavorus*	5600 L ARID open cultivation pond, University of Arizona, AZ, USA.	Oligonucleotide marker 16s SSU rDNA	5–7	Benzalkonium chloride	(Steichen 2016, Lammers et al. 2017)
Chlorella vulgaris	Flagellate, *Poterioochromonas* sp.	792 L open pond, Arizona Center for Algae Technology and Innovation, Arizona, USA.	Microscopy, oligonucleotide markers (18s rRNA), Spetroradiometr-ic	~0.5	Ultrasonication, high CO_2 sparging	(Wang et al. 2018, Ma et al. 2018, Ma et al. 2017, Maes et al. 2018)

Microalgal prey	Predator	Cultivation platform/ location	Detection methods	Collapse (d) after first sign of invasion	Treatment	References
Chlorella vulgaris	Ciliate and Dinoflagellates, *Euplotes* sp. and *Oxyrrhis* sp.	Open raceway pond, Reliance Industries Limited, Mumbai, India.	Microscopy, continuous flow cytometer	3–5	Quaternary amines, organophosphates, Pendimethalin, Ethalfluralin, Rotenone, etc.	(Karuppasamy et al. 2018)
Scenedesmus dimorphus	Cryptomycota, *Amoeboaphelidium protococcarum*	350 L mini open ponds, Columbus Algal Biomass, Sapphire Energy Inc, New Mexico, USA.	Microscopy, oligonucleotide markers (qPCR)	2–3	Pyraclostrobin	(McBride et al. 2018)
Microchloropsis salina	Rotifer, *B. plicatilis*	20 L indoor lab cultivation, Sandia National Laboratory, CA, USA.	Microscopy, GC-MS based volatile organic compounds	2–3	-	(Reese et al. 2019)
Microchloropsis salina	*Rotifer, Brachionus sp.; Ciliate, Acineta sp.; Gastrotrich, Chaetonotus sp.*	550 L Open ponds, Texas A&M AgriLife Research Mariculture Laboratory, Texas, USA.	Microscopy, Microbiome analysis using Second generation sequencing	4–5	Sodium hypochlorite	(Carney et al. 2016)
Nannochloropsis oceanica, Chlorella vulgaris, Desmodesmus sp.	*Rotifer, ciliate, amoeba, etc.*	Algae Testbed Public-Private Partnership, USA and Hawaii.	Microscopy	-	-	(McGowen et al. 2017, Knoshaug et al. 2018)

The camera-based cell type classification and enumeration is based on pixel intensity (Deglint et al. 2018). Pixel processing is inherently limited in its computational ability to process overcrowded samples. Samples with higher cell concentrations and clumped cells tend to have heavy pixel load which contributes to poor identification of cell margins. Moreover, samples above 10^8 cells ml^{-1} tend to block the flow-through channel (Day et al. 2012). Furthermore, a requirement of laser assisted microscopic camera and risk of flow-through channel blockage limits the implementation of flow cytometry in outdoor setups.

2.4.1.3 Oligonucleotide markers

Advancement in areas of genomics have enabled the development of oligonucleotide-based markers, that are targeted towards nucleic acid signatures, as a means of early detection of contaminants. Polymerase chain reaction (PCR) using Internal Transcribed Spacer (ITS), or 18s and 16s rDNA as markers is the mostly commonly employed genomic approach for contaminant detection. (Carney et al. 2016). However, further sequencing (Steichen 2016) or allele-specific fragmentation pattern analysis (Fulbright et al. 2014) is required for definitive identification of invaders. PCR-based markers provide limited information about the estimation of predator load and hence fail to serve as early warning signals. A semi-quantitative tool, qPCR, that detects the presence of contaminants in real time using a signature probe tagged with a fluorophore is reported by (McBride et al. 2014) Designing of the qPCR probe requires prior knowledge of a contaminant-specific unique nucleotide sequence for targeted detection. Although multiplex qPCR reaction is an option to detect a variety of species at once its limited ability for estimation of uncharacterised and new invasive species, as might be expected in open ponds, is a major drawback of the technology. The techniques described above are also highly sophisticated and are limited to the laboratory use.

Researchers at Sandia National Laboratory have developed a portable proof-of-concept device for the targeted identification of invasive species. The laboratory implements a two-step approach for contamination detection. First, identification of unknown pathogens using the second-generation sequencing and bioinformatics pipeline, RapTOR™. Second, a FRET-based hybridization assay, SpinDx™, for capture and quantitation of predator load using signature molecular probes. The limit of contaminant detection by SpinDx™ is reported to be 1–10 cells for ciliates, chytrids and rotifer species. The operating cost is <2 USD for 20 samples and device cost is <USD 1000. The technological validation and implementation of this approach at the commercial raceway pond are ongoing (Lane et al. 2016). The overall success

of the oligonucleotide marker-based detection is highly dependent on prior knowledge of genomic information pertaining to the contaminants. A constant probe-designing effort is required to increase the coverage of the detection. In addition, a highly skilled technician is required for reliable execution of the analysis.

2.4.2. Indirect methods

2.4.2.1 Spectral markers

As opposed to direct methods, outlined above, a number of indirect contamination monitoring methods have emerged in last few years. One such method is hyperspectral reflectance-based monitoring of light backscatter combined with numerical models. The main source of light backscatter in case of microalgae ponds are the suspended cells. The method is based on differences in the reflectance pattern that arise due to variation in the reflective index, backscatter, of the different microalgal cell types (size and shape). Therefore, microalgal cells with different cell surface properties give rise to unique spectral features (Reichardt et al. 2014). Maes et al. (2018) reported variation in the spectral reflectance of *Chlorella vulgaris* culture infested with *Poterioochromonas* sp. and diatoms. Variation in the spectral feature at 708 nm is suggested to be associated with chlorophyll catabolism as a result of predation by *Poterioochromonas sp*. Similarly, changes in the photosynthetic pigments, specifically the chlorophyll-to-carotenoid ratio, of *S. dimorphus* infested with *A. protococcarum* is reported on the basis of hyperspectral confocal imaging by Collins et al. (2014). Multispectral imaging is also reported to serve as a non-invasive means of cyanobacteria monitoring in *Chlorella* sp. cultures. The red and green colour value contributed from cyanobacteria and *Chlorella*, respectively, acquired using RGB camera, is a relative indication of the respective species. The detection limit of pest invasion in terms of the concentration ratio of cyanobacteria-to-green algae is 0.08 (Murphy et al. 2014). However, the majority of the heterotrophic predators lack photosynthetic pigments so immediate applications of technologies relying on pigment colour discrimination is limited.

2.4.2.2 Metabolic markers

Microalgae and zooplankton interactions involve communication using metabolic cues as means of prey attraction, grazer deterrence and allelopathic signals. Reese et al. (2019) leveraged the elevated presence of Volatile Organic Carbon (VOC) as an indirect marker of *B.*

pilicatilis predation in *M. salina* cultures. Products of carotenoid oxidation contributed to elevated VOC and were identified as β-ionone and β-cyclocitral.

The indirect monitoring methods have a tremendous potential to be developed as an online monitoring tool. However, the spectral and metabolic features reported to-date are mainly due to the presence of the catabolic products of microalgal pigments. Chlorophyll degradation is prevalent under a variety of stress conditions and may not be an exclusive outcome of microalgal grazing. Moreover, the degradation products that arise after significant prey cell digestion by a predator are unlikely to be detected early on. As opposed to the degradation products, a metabolic prey cell response such as signals mounted against predator attack can serve as a better and early warning signal.

The culture collapses recorded in the literature have occurred within 3–5 days after the first sign of predator presence (Table 2.1) and, occasionally, a pond crashed in less than 2 days. Ideally an automated real-time monitoring system with a high interval rate of sample screening is required for early detection of the predator. A relatively quick, straightforward and easy to interpret measure of infestation is desirable so as to minimise detection time while maximising culture exposure to pest deterrent agents. Moreover, non-invasive monitoring tools implemented in-line with the cultivation setup can facilitate a quick corrective response. A universal screening method is preferable, which can be used to monitor cultures of a variety of microalgal prey and predator species. Leveraging unique and inherent properties of microalgal prey and predators can help to devise novel and fairly universal means of grazer detection. Section 2.5 reviews the background of technologies that are exploited to monitor changes associated with intrinsic properties for the development of early markers of *D. tertiolecta* grazing mediated by *O. marina*.

2.5 Unique properties and relevance of prey-predator interactions as a grazing marker

Photosynthetic pigments such as chlorophyll *a* and carotenoid composition are found to be altered under stress conditions, including grazing (section 2.4.2.1). Therefore, the underlying photosynthetic process that involves the pigments are also likely to be changed. Monitoring of photosynthesis reflects the true physiological state of cells as opposed to catabolic product detection which merely suggests underlying stress conditions. Moreover, photosynthesis is a unique property of all commercially important microalgal strains unlike their heterotrophic predators. Thus, controlled experiments for tracking the photosynthetic

process can provide valuable insights into grazing-mediated photosynthetic alteration that is exclusively contributed from microalgal prey. Temporally resolved unique photosynthetic responses (signatures) of *D. tertiolecta* as function of *O. marina* grazing can be further leveraged as a grazer-monitoring tool.

2.5.1 Photosynthesis

Autotrophic microalgae capture photon energy and convert this into chemical energy through the photosynthetic process to fuel the biological reactions within the cell. Photosynthesis is a multistep process that occurs within specialised membranes, the thylakoids, of the chloroplast (Figure 2.1). The chloroplasts of green algae are enclosed by two membranes which are referred to as the outer and inner chloroplast membranes, with the intermembrane space in-between. The thylakoids are often stacked into flat, disc-like sacs to form grana, which are interconnected through membranous extensions, lamellae, and are suspended within the stromal matrix. The membranes of the thylakoid sacs compartmentalise the space into the thylakoid lumen and stroma that is site of the light dependent and dark (light independent) reactions, respectively. The light reactions generate energy required by the dark reactions for carbon fixation to fuel the cells with essential biomolecules. The thylakoid membrane contains the photosynthetic pigments and proteins that are involved in the photosynthetic process (Lodish et al. 2000, Roig 2000).

Photosynthetic pigments, chlorophyll *a* and carotenoids, are the light absorbing units and form Light Harvesting Complexes (LHC). Chlorophyll *a* is the main photosynthetically active pigment in green algae and the primary site of light absorption. Proteins, D1 and D2, together with the LHC complexes forms the photosystem, PSII and PSI that operates in tandem with the help of electron acceptor and donor molecules for sequential electron transport. Reaction centres (RC) of PSII contain six chlorophyll *a*, two pheophytin molecules and two β-carotenes, acting as accessory pigments (Lodish et al. 2000, Roig 2000). A pair of specialised chlorophyll pigments, P680, absorbs light directly or via antenna chlorophyll within LHC to drive photochemistry. Accessory pigments also assist in dissipation of excess energy as heat (Emerson and Arnold 1932). Techniques that are relevant to photosynthesis and are used in this work are mainly associated with PSII photochemistry, hence PSI process are not covered here.

The light reactions of photosynthesis form a multistep process of electron transport reactions involving sequential oxidation and reduction mediated by electron carriers.

Photosynthesis is initiated on absorption of photons by LHC antenna in their ground energy state and the rapid transition of an electron in the pigment molecule into an excited energy state (10^{-15} s). The high energy, excited state, electron is passed on to the adjacent pigment molecules by resonance energy transfer and ultimately localised on P680 (Lakowicz 1999). Oxidised $P680^{+}$ returns to the ground state by accepting an electron from the Oxygen Evolving Complex (OEC) localised on the donor side of PSII. The OEC complex is composed of four oxo-bridged manganese atoms and one calcium atom ($Mn_4C_aO_5$) and is bound to the protein subunits of PSII (Joliot and Kok 1975). A complete oxidation cycle at the OEC, ultimately leading to water splitting, results in release of one oxygen, four electrons and four protons (50–1.5 ms) for 4 photons absorbed by PSII and its antenna.

The released electrons are further transferred from P_{680} to Phe^{-} (3–20 ps), then reduce PQ (200 ps) by linking with proton transfer across thylakoid membrane (Greenfield et al. 1997). Two molecules of PQ work in tandem to operate the electron transport chain between PSII and PSI. One molecule of PQ is permanently bound at Q_A and another detachable molecule bound at Q_B site. PQ has two electron pockets hence two reduction reactions must occur to fully reduce the PQ bound at Q_{B-} site in presence of two protons. In the first reduction reaction Q_{A-} reduces Q_B within 100–200 µs resulting in a Q_A/Q_{B-} state. The electron is passed on from another Q_{A-} resulting in a Q_A/Q_{2B-} state at the end of a second reduction reaction, within 400–600 µs. Fully reduced PQH_2 unbinds from the Q_B site and transfers electrons to the cytochrome b_6 complex and ultimately to PSI (Velthuys and Amesz 1974). Proton build up inside the thylakoid lumen occurs due to OCE oxidation and PQ movement and as a result a pH gradient (delta pH) is formed across the thylakoid membrane. Proton gradient fuels enzymatic process such as ATP synthase and violaxanthin de-epoxidase (VDE). The activity of the latter enzyme is crucial for a regulatory process, NPQ (Figure 2.1) , which directly affects photosynthetic efficiency (Govindjee 2014).

2.5.1.1 Chlorophyll *a* fluorescence

The photon energy absorbed by chlorophyll *a* can be utilised to perform photochemistry as explained in section 2.5.1. Light absorption triggers chlorophyll *a* excitation, Chla^{*}, and mostly returns to the ground state by transferring electron to adjacent chlorophyll *a* and eventually to the next electron carrier pheophytin (Phe) molecule present on the acceptor side of PSII. Alternatively, Chla^{*} can return to the ground state by releasing energy as fluorescence or dissipating excess energy as heat. Excess energy is dissipated to avoid the photodamage due

to triplet chlorophyll *a* (^{3}Chl *a*) and singlet oxygen ($^1O_2$) formation. Under steady state conditions the three processes - photochemistry, fluorescence and heat release is observed. Hence, monitoring one, fluorescence, can reveal important insights about photochemistry.

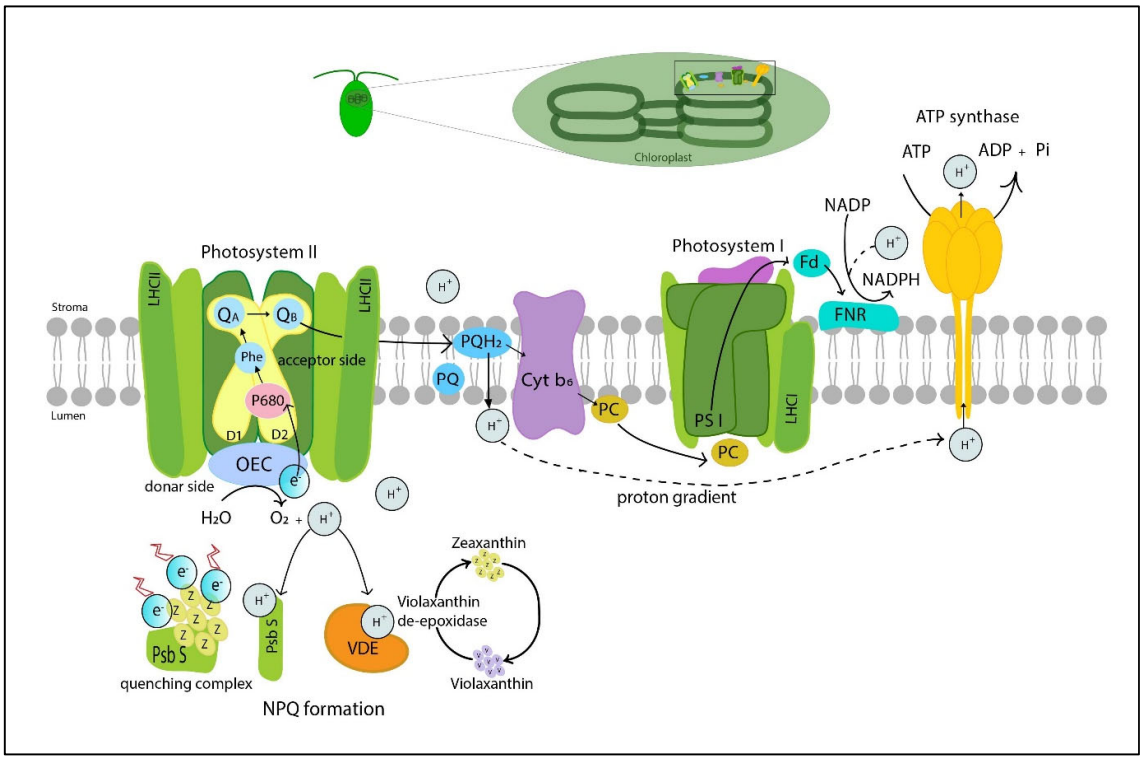

Figure 2.1 Schematic of electron transport and non-photochemical quenching formation within the chloroplast. OEC, Phe and PQ indicates oxygen evolving complex, pheophytin and plastoquinone, respectively. P680 is a specialised pair of reaction center chlorophyll *a* molecules, Q_A is a bound plastoquinone, Q_B is a plastoquinone that binds and unbinds from PSII pockets. Cyt b_6 is a cytochrome b_6 complex that mediates electron transfer from PQ to PC, plastocyanin and ultimately to PSI. Fd and FNR indicates ferrodoxin and ferrodoxin reductase complex, respectively. Dashed solid black line with arrow indicates accumulation of protons resulting in formation of proton gradient across thylakoid membrane.

Over the years, chlorophyll *a* fluorescence has proven to be a useful non-invasive technique for *in vivo* monitoring of PSII activity. The yield of fluorescence relies on the stable charge separation between the primary electron donor, P_{680}, of RC and the acceptor molecule, pheophytin. The resultant yield can be used to determine the rate kinetics and efficiency of process that occurs on acceptor, Q_A re-oxidation, and donor side, OEC oxidation, of PSII. A relatively low and high fluorescence yield is observed in two instances. First, oxidised Q_A allows RC to use absorbed energy to initiate the charge separation and a relatively low fraction of excitation energy is lost as fluorescence. Subsequent excitation event however encounters the inability of an already reduced Q_A to take up an electron from the PSII RC results in high

fluorescence (Govindjee et al. 2010). The initial rise in the fluorescence is observed to decline over time and the decline in fluorescence is termed 'quenching'. Quenching can be contributed from activation of processes involved in photosynthesis ('photochemical quenching') or due to an increased rate constant of heat dissipation through the process of non-photochemical quenching (NPQ). The activation of the latter is highly dependent on acidification of the intra-thylakoid space due to proton movement and induction of the xanthophyll cycle which leads to the production of a particular xanthophyll (zeaxanthin) that dissipates excess light energy as heat (Demmig-Adams 1990) .

NPQ primarily operates as a highly regulated photoprotective mechanism and its presence indicates stress conditions, especially super-optimal light, that generate excess strong oxidants at RCs with little scope for the utilization of excess absorbed energy. Depending on the relaxation (quenching) kinetics, NPQ is typically composed of three components; qE, an energy dependent component, qT, associated with state transitions and qI, which is associated with photoinhibition. Full NPQ expression requires rapid qE formation which is dependent on formation of a proton gradient across the thylakoid membrane and xanthophyll cycle activation (Niyogi et al. 1997b). Excess light absorption causes higher energy generation within photosytems than can be dissipated by processes such as carbon assimilation and as a result pH drops inside the lumen of the chloroplast. The decrease in the pH triggers the early onset of qE activation by protonation of a protein subunit, PsbS, of PSII and VDE an enzyme that converts the pigment xanthophyll to zeaxanthin. An altered PsbS protein, in association with zeaxanthin, forms a 'quenching complex' which assists in direct dissipation of excess energy (Figure 2.1), thereby completing NPQ activation (Müller et al. 2001). Any failure in NPQ expression triggers formation of reactive oxygen species (ROS) that can be extremely damaging to cell function. In addition to NPQ activation, lumen acidification also regulates Q^A oxidation kinetics(Nishio and Whitmarsh 1993). Both NPQ levels (Crofts 1967) and Q^A re-oxidation kinetics (Belatik et al. 2013, Bailey and Walker 1992) are altered in the presence of inhibitors that are known to disturb the formation of a proton gradient across thylakoid membrane.

All photosynthetic process are interconnected and alteration in one of them can have a profund effect on others which is manifested as altered chlorophyll *a* fluoresence yield. The non-invasive nature of fluoresence measurements have proven to be an excellent tool for *in vivo* monitoring of microalgal photosynthsis. However, the presence of ambient light interferes with the detection of the re-emitted fluorescence as red light from PSII activity. Such interference can be ruled out by operating measurements using modulated light of known

frequency. The Pulse Amplitude-Modulation (PAM) fluorescence technique is one such method that utilises repeated pulse application of modulated light for estimation of photosynthetic process.

2.5.1.2 Evaluation of photosynthetic processes using Pulse-Amplitude Modulated fluorescence (PAM)

The PAM technique described by Schreiber et al. (1996) for chlorophyll fluorescence measurements relies on the closed or open states of RCs. In the fully oxidised steady state of RCs, electron acceptors and the absence of the delta pH condition is referred as the 'open state'. The open steady state can be easily achieved by dark adaptation of samples. Exposure to light triggers ejection of electrons by P_{680} and reduction of the primary acceptor; at this stage the carriers are unable to accept additional electrons, which indicates a 'closed state' of RCs. Exposure of a dark-adapted sample to a very short (1 μs) modulated Measuring Light (ML) of low intensity allows only the charge separation to occur, and a low fluorescence is observed - termed 'minimal fluorescence' F_0. Exposure to a high intensity Saturation Pulse (SP) drives electron transfer from P_{680}* to PQ at the Q_A site, the RCs all become closed, and maximum fluorescence, F_m, is observed. (Figure 2.2). The difference between F_m and F_0 is referred to as variable fluorescence F_v which is used for estimation of maximal quantum efficiency of PSII, F_v/F_m. This is a measure of the maximum efficiency of PSII to drive photochemistry to fuel other physiologically important reactions such as ATP generation and carbon fixation within the cell (Genty et al. 1989, Schreiber 1986). Therefore, F_v/F_m is commonly used as an indicator of the physiological health of microalgae (Dijkman and Kromkamp 2006). The estimate of quantum efficiency is further used for a relative quantification of electron transport rate, rETR, under a given light intensity (PAR). rETR signifies the relative capacity of electron transport from the RC to the primary electron acceptor upon light irradiation. Exposure of samples to Actinic Light (AL) with repeated application of SP at equally spaced time intervals (~20 s) decreases the contribution to fluorescence from photochemical quenching due to successive closure of almost all RCs. The maximum fluorescence yield after light exposure is referred to as F_m'. At this stage there is an apparent successive decline due to increased competition between photochemical and non-photochemical quenching (F_m') values (Figure 2.3). The declining trend indicates the

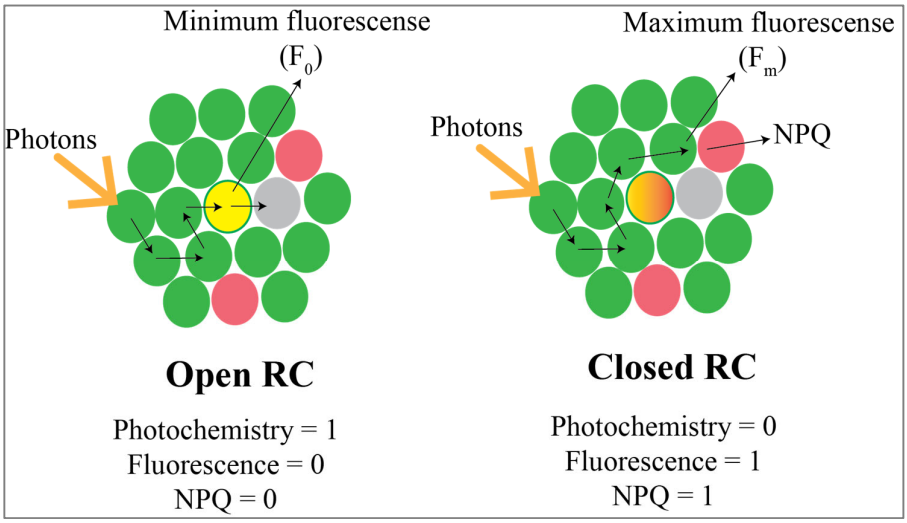

Figure 2.2 Schematic diagram of open and closed Reaction Centers (RC). Green circles indicate chlorophyll a and b, yellow and yellow-orange circles depicts open and close state of reaction center, respectively. The pheophytin molecule which takes part in charge separation, a primary step of photochemistry, is represented by the grey circle. The pink circles represent the accessory pigment, zeaxanthin, which mediates heat dissipation.

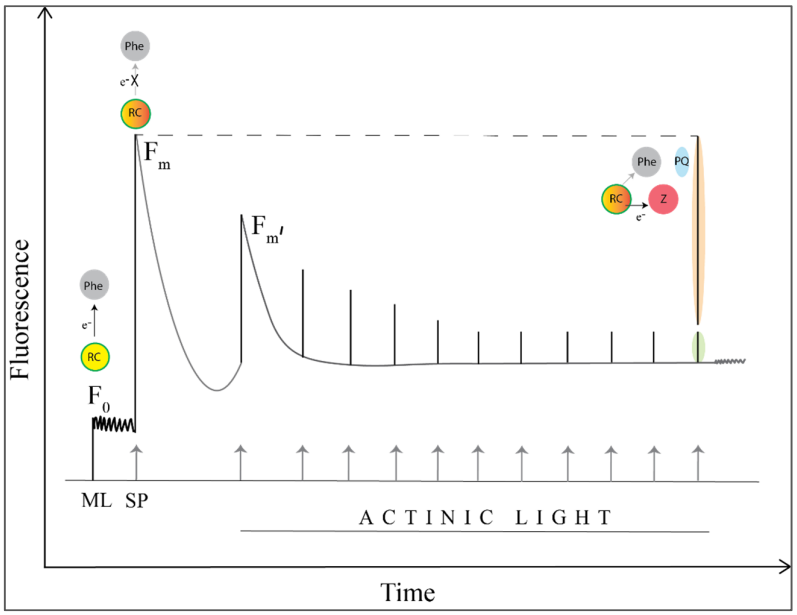

Figure 2.3 Schematic representation of Pulse-Amplitude Modulation chlorophyll fluorescence principle to deduce photosynthetic parameters. Yellow and yellow-orange circles represent open and closed reaction center, respectively. The pheophytin molecule is depicted by a solid grey circle. PQ, the blue eclipse shape, represents plastoquinol and the pink circle denotes zeaxanthin. The green and orange eclipse shape shaded areas indicate the signal contribution from photochemical and non-photochemical quenching process, respectively. ML is measuring light and SP is saturation pulse denoted by grey arrows in the presence of actinic light.

accumulation of proton gradient across thylakoid membrane and activation of CO_2 fixation in Calvin-Benson cycle. The decrease in the yield of fluorescence reflective of F_m' compared to F_m suggests the contribution of NPQ. The estimates of NPQ are obtained using the Stern-Volmer relationship (F_m-F_m')-1 (Ruban 2016). Elevated NPQ levels are associated with enhanced photoprotective ability whereas reduction is indicative of either lack of heat dissipating pigments in the LHC (Havaux et al. 2007) or dysfunctional quenching of the qE component (Jahns and Krause 1994).

The saturation pulse method can also be used to construct Rapid Light-Curves (RLCs) from rETR values under incremental light exposure. RLCs provides two important parameters – first, the maximum rate of relative electron transport ($rETR_{max}$) at saturating light intensity, and secondly, the light harvesting efficiency, alpha, which is an indication of energy harvesting capabilities by RCs and LHC-II (White and Critchley 1999).

In practice it is straightforward to have a single photosynthetic measurement as an early warning sign of microalgal grazing. Changes in the photosynthetic protein-pigment complex under abiotic stress conditions such as high light, temparature, nutrient limitation leads to reduced F_v/F_m and increased NPQ are reported by del Hoyo et al. (2011). Similar photosynthetic pigment alteration of microalgal prey is observed under grazing pressure (Fundel et al. 1998). Therefore, changes in F_v/F_m and NPQ are processes that could be be leveraged as a markers of microalgal grazing. It is vital to understand alterations in overall photosynthetic dynamics of the prey in order to further investigate the possible cause(s), contributed by predators, of the photosynthetic perturbation. In chapter 3 we present data suggesting that NPQ measurement is central to the ideal of investigating photosynthesis-based markers of grazing in cultures of *D. tertiolecta* infested with *O. marina*. Experimental validation and effectiveness of photosythetic-based markers are outlined in chapter 3.

2.5.2 Nutrient recycling

The biogeochemical (C, N, P, etc.) cycling of the ocean is fundamental to Earth's climatic conditions as it directly affects the extent of phytoplankton-mediated CO_2 fixation and release into the atmosphere. The overall microalgal productivity is mainly dependent on the amount of fixed nitrogen which is directly correlated with the rate of CO_2 fixation. In some situations availability of P, Fe and Zn can also affect the primary productivity of the ocean (Beardall et al. 2001). Some cyanobacterial species can fix nitrogen gas (N_2) into ammonia which further fuels the nitrogen cycle within pelagic food webs. Nitrogen is constantly

regenerated through a variety of biological processes such as direct release by phytoplankton (Mann 1982), bacteria, coral , viral infection and lysis of cells (Brussaard 2004), faecal pellet dissolution, and zooplankton-mediated excretion (Bronk and Steinberg 2008). The grazer-mediated excreted nitrogen occurs mainly in the form of ammonia-nitrogen (NH_3-N) and accounts up to 40–91 % (Klawonn et al. 2019) total regenerated nitrogen (Caron and Goldman 1990, Goldman et al. 1989). On average, microzooplankton such as ciliates and flagellates contribute 10^{-8}–10^{-5} µmol of recycled nitrogen, in the form of ammonia, per grazer per hour (Steinberg and Saba 2008). Up to 43 % of the total nitrogen requirement of microalgae is reported to be fulfilled by uptake of excreted ammonia as the main nitrogen source (Alcaraz et al. 1994). In addition, zooplankton feeding, which leads to digestion of autotrophic microalgae, can also contribute to the ammonia release, however at a lesser extent compared to metabolic activity of grazers, excretion (Bronk and Steinberg 2008). The grazing- and lysis-mediated NH_3-N regeneration is relevant to the microalgal pond conditions and possibly be the only source of ammonia nitrogen unless supplied as a medium component. Therefore, the recycled ammonia nitrogen can serve as a proxy for the presence of zooplankton predators.

The uptake of ammonia excreted by animals can have multiple effects on microalgal physiology. Perturbation in the photosynthetic process such as NPQ is of particular interest in the current study as ammonia at high concentration is a known uncoupler of photosynthesis. Detection of grazing-mediated ammonia, its correlation with NPQ levels and predator concentration are likely to serve a dual purpose. First, ammonia as a causal agent of NPQ alteration and second, symptomatic of predator invasion.

2.5.2.1 Ammonia and its effect on photosynthesis

Ammonia-nitrogen in aqueous solution exists as free ammonia, NH_3-N, or ammonium ion, NH_4^+-N and is cumulatively referred to here as Total Ammonia-Nitrogen (TAN). The relative levels of NH_3-N and NH_4^+-N are dependent on the pH of the medium with the latter form more prevalent at alkaline pH. Ammonium ions (NH_4^+) are actively taken up by the microalgal cells whereas free ammonia (NH_3) can freely diffuse across the cell membrane and also permeate through the thylakoid membrane of the chloroplast. Ammonia inside the thylakoid lumen reacts with protons, resulting in the formation of ammonium ions and as a result this distorts the proton gradient (section 2.5.1.2) present across the thylakoid membrane (Crofts 1967). NH_3 and H_2O are isoelectronic, i.e. possess similar same electronic structures, hence NH_3 can compete with the binding of water molecules at the OCE during the water

oxidation process (section 2.5.1) which can be manifested as an altered rate of electron transport (Velthuys 1980).

2.5.3 Nutrient repackaging

Microalgal biomass that is produced as an outcome of photosynthesis is transferred to higher trophic levels via ingestion of microalgal prey by the predators. The ingested nutrients for the predator are reallocated or repackaged into slightly more complex biomolecules through predator-specific metabolic pathways. For example, phytosterol obtained from microalgal prey such as *D. tertiolecta* (Wright 1979) acts as a precursor molecule for synthesis of cholesterol molecules by many zooplankton species (Mansour et al. 1999). Consequently, any cyanobacterial species that are devoid of essential fatty acids and the precursor sterol are deemed unsuitable as a diet by cladocerans predators (Martin-Creuzburg et al. 2008). A strong correlation between biomolecular composition of predators and nutrient quality of microalgal prey is observed. Often poor prey nutrient quality such as those found under nitrogen-depleted conditions results in lipid accumulation within microalgae that further affects the predator feeding pattern and reproduction (Brett and Muller-Navarra 1997). In addition, different zooplankton species assimilate prey nutrients at different rates along with variation in repackaged biomolecule composition (Persson and Vrede 2006). The differential sterol (Taipale et al. 2016), pigment (Serive et al. 2017) and fatty acid (Dalsgaard et al. 2003) composition of phytoplankton and zooplankton have been leveraged as a chemotaxonomic biomarker for taxonomic assessment of community structure and species composition (Mackey et al. 1996, Strandberg et al. 2015). Fatty acids such as omega-3 and omega-6 fatty acids, along with sterol molecules, are reported as an efficient chemotaxonomic biomarker for the classification of phytoplankton and zooplankton abundance as compared to traditional microscopic taxonomic identification. Sterol biomarkers are of particular interest due to differences in their molecular composition across phytoplankton and zooplankton species. Most microalgae primarily synthesise phytosterols, ergosterol and corbisterol, whereas zooplankton, and dinoflagellate species, exclusively accumulate 4-alpha-methyl sterols such as cholesterol (Volkman 2003). The phytosterols and cholesterols are structurally similar. Phytosterols of *D. tertiolecta* are usually characterised by the presence of an alkyl group (methyl or ethyl) at position C-24 and a double bond on the side chain at C-22 or 24 (Moreau et al. 2002). Cholesterol synthesized by dinoflagellates is characterised by an unique position of a methyl group at C-4 or C-23 positions (Withers et al. 1978).

Zooplankton predators such as *O. marina* accumulate cholesterol either by using precursor sterols as a building block or through a de novo synthesis pathway (Chu et al. 2008). Such scenarios are particularly relevant in the outdoor microalgal culture wherein shifts in the predator invasion quickly alter the taxonomic abundance. Probing biomacromolecule dynamics of grazing cultures can provide insights into differential accumulation of lipids, carbohydrates, proteins and sterols which can be further leveraged as a biomarker of microalgal predation. The changing biomacromolecule dynamics as a function of nutrient trophic 'bottom-up' transfer has been extensively studied in natural assemblages such as lakes, oceans and rivers (Hiltunen et al. 2015). However, the knowledge of bottom-up nutrient repacking in commercial scale microalgal cultures is limited. It is essential to screen all major class of molecules in order to develop a reproducible marker of *O. marina* grazing. Vibrational spectroscopy such as Fourier Transform Infrared Spectroscopy (FTIR) is a quick method to understand the relative content of all major classes of biomolecules using spectral features. The association of spectral features with a particular class of biomolecules and the basis of this classification approach is described in section 2.5.3.1

2.5.3.1 Evaluation of biomacromolecule dynamics using vibrational spectroscopy

Fourier Transform Infrared (FTIR) Spectroscopy is a non-invasive method to probe the biomacromolecules present in microalgal biomass from a spectral snapshot. The identification and relative quantitation of the biomolecules is based on the absorption principle, the Beer-Lambert law, to generate a spectral signature from the amount of absorbed and transmitted IR light measured by a detector. Mid Infrared Radiation (Mid-IR) spanning wavenumbers 4000–400 cm^{-1} of the electromagnetic spectrum is primarily used to promote transition of molecules between rotational and vibrational energy levels of the atom within the ground, low energy, state, unlike photon absorption which induces the atomic transition by excitation of an electron from a ground energy to a high energy, excited, state. The vibration pattern, nature of the bond, atomic mass, dipole moment and attached functional group determine the unique molecular absorption characteristics, as a spectral feature (Griffiths and De Haseth 2007).

A molecule in a 3D coordinate (x, y and z) system typically has 3 possible translational degrees of freedom that can possibly have 6 vibrational modes – symmetric, anti-symmetric, rocking, scissoring, wagging and twisting (Figure 2.4) The vibrational frequency of the bond increases with the increased strength of the bond (triple > double > single bond) and/or reduced atomic mass. Therefore, each chemical entity of different molecular composition (C–C, C=C,

C≡C, N–H, C=O, etc.,) has a characteristic IR absorption. Biomolecules are predominantly composed of a certain type of molecular bond such as amide (N–H) in proteins and carbonyl esters (C=O) in lipids, etc. Accordingly, characteristic wavenumbers can be assigned to the biomolecules (Vongsvivut et al. 2013). Table 2.2 summarises the biomolecule assignment based on the prevalent chemical nature and vibration pattern of the bond.

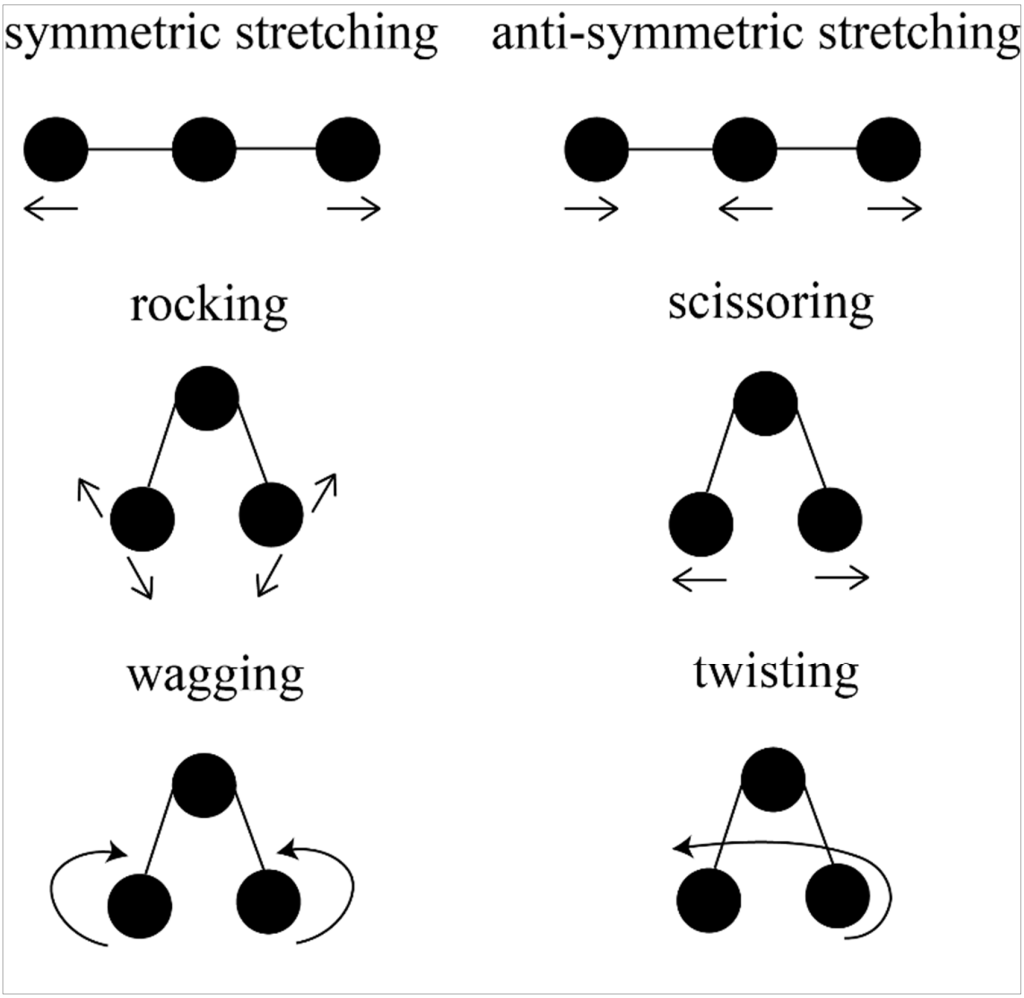

Figure 2.4 Types of stretching and bending molecular vibrational mode. Diagram reproduced from Ismail et al. (1997).

IR spectrophotometers deploy an interferometer, an optical device, that acts as a beam-splitter to divide IR radiation in to two optical beams. One of the two beams is reflected by a mirror placed at a fixed position while another beam reflects off from a moving mirror. The displacement of the mirror at a distance from the beam-splitter varies the wave interference, as a function of time or space. This, thereby, allows generation of multiple wavelengths from a single light source that greatly reduces the time required for each measurement. Both beams

reflected from the fixed and moving mirror converge together and are selectively absorbed by the sample. The amount of transmitted light is then recorded by the detector in the form of an

Table 2.2 FTIR wavenumber assignment as per the chemical nature, vibration pattern of the bonds and functional group present in major biomacromolecules of microalgae. Adapted from Ismail et al. (1997) and Vongsvivut et al. (2013).

Chemical bond	**Biomolecules**	**Vibration pattern**	**Wavenumber (cm^{-1})**
O-H	water, alcohol	stretching	3200-3600
C-H	proteins, primarily lipids and fatty acids	symmetric;	2872, 2852;
		anti-symmetric;	2960, 2925;
		scissoring;	1475, 1465;
		rocking;	1418
C=O (carbonyl ester)	lipids	stretching	1745, 1717, 1695
C=C	phenol rings of aromatic amino acids and cis-olefins	stretching	1496, 1638
N–H (amide)	proteins	stretching	1670, 1654, 1310
CH_2	polymethylene chains	wagging	1365
P=O	phosphodiester of nucleic acids and phospholipids	anti-symmetric	1232
C-O, C-C and C-O-C	carbohydrates	symmetric	1122, 1045 and1172

interferogram. Thus, the interferogram contains information in either time or space dimensions. A mathematical, Fourier transformation, processing is required for conversion of interferogram into readable frequency spectrum – percent of absorbed or transmitted light for each wavenumber. Further, measurements for every wavenumber or interferogram is repeated and co-added together to increase signal-to-noise ratio. Secondary derivatization of the frequency spectra is required for resolution of overlapping spectral peaks that are otherwise obscure (Ismail et al. 1997, Savitzky and Golay 1964).

The quantitative aspect of FTIR spectroscopy requires calibration using a set of standards of known composition determined using traditional wet chemistry methods. A correlation of IR intensities and measurements performed using wet chemistry methods are essential for the determination of relative quantities of the variable in an unknown sample. Availability of set of calibration standards that are a true representation of a mix of different analytes is limited. The Beer-Lambert's law essentially works well for a single variable, wavenumber, and analyte. However, FTIR inherently deals with multiple variables and multiple types of analytes in a single sample at a given point of time. A multivariate approach is required for the determination of contributions from additional components and model development to understand the interactions between the variables (Gautam et al. 2015).

Partial Least Square Regression (PLSR) is a multivariate factor analysis used for identification of important variables, using wavenumbers assigned to biomolecules, to explain the observed differences across samples e.g. control vs. grazing cultures. A training-based approach is used in PLSR for calibration model development for the factor or 'loading spectra' determination using a calibration standard concentration. The spectrum of the training set is further decomposed into a weighted sum, scores, of the loading spectra. The resultant scores are further regressed against the concentration of the standards into a model that is used for the inspecting unknown spectra, or samples, as a validation set (Wold et al. 2001).

The experimental methodology of FTIR combined with PLSR analysis for the identification of important variables and its relevance to the grazing-mediated nutrient repackaging is outlined in chapter 5.

2.5.4 Extracellular signalling

Interactions between two members of same, intra-, or different, inter-, species is mediated by chemical signals. Inter-species signalling is reported to involve secondary metabolites in microalgal prey and predator interactions. Detection of predators using extracellular chemical cues by prey species has evolved as an alarm signalling system to evade the predator attack (Xu and Kiørboe 2018) and are commonly referred to as kairomones or allelochemicals. Both microalgal prey and predators have evolved to detect allelochemicals emitted by each other and hence these can act in an antagonistic manner (Roy et al. 2013). The extracellular alarm cues can be broadly classified into two classes, allelochemicals emitted 'before' and 'after' the prey capture by predator. The former is received as a disturbance signal, release by the predator, and can evoke a defence response by the prey. Such responses are

occasionally manifested into release of a grazer deterrent chemical in a conspecific manner. Signals that are emitted after the prey capture are 'damage-release' alarm signals and indicate immediate risk of predation. The prey perceives a risk of grazing by detection of a 'predator recognition' signal prior to mounting a defence or escape response. The antagonistic predator species are also evolved to detect the prey-specific diffused extracellular cues for efficient prey search which is refereed as 'prey recognition' signals. The waterborne chemical ecology of disturbance, damage-release and prey-recognition signals can act as a reliable indicator of predation risk (Chivers and Smith 1998).

2.5.4.1 Allelopathic signals

The signalling exo-metabolome is mainly composed of short-peptides, free amino acids, lipids, fatty acids, alkaloids, aldehydes and phenolic compounds that mediate the allelopathic microalgal prey predator interactions (Mendes and Vermelho 2013). The free form of fatty acids ($RCOO^-$) are derivatives of forms of fatty acids present in the aqueous medium and are reported to serve as disturbance or damage-release signals in many microalgal species. Free fatty acids emitted by *Botryococcus braunni* can turn toxic under basic pH conditions (pH 8.0–9.0) and act as an inhibitory compound against the antagonistic species (Chiang et al. 2004). In addition, elevated production of extracellular polysaccharide by *B. braunni* is hypothesised to serve as a shield against its predators (Weiss et al. 2012). Growth retardation was observed in *D. salina* cells upon treatment with cell-free extract of *I. galbana* and the inhibitory activity was attributed to the extracellular fatty acid fractions (Sun et al. 2012). Fatty acids such as oleic acid, α-linoleic acid and chlorellin (DellaGreca et al. 2010) are reported for their allelochemical activity against green algae and diatoms. In contrast to the action of free fatty acids as the disturbance signal, polyunsaturated aldehydes (PUAs) mostly act as a damage-release signals with an exceptional release by cells of late stationary phase. PUAs such as oxylipins arise from enzymatic degradation of polyunsaturated fatty acids which mediates a grazer deterrence response emitted by diatoms against dinoflagellate (Ribalet et al. 2007) and copepod (Ianora et al. 2011) species. Several lipids classed such as glycolipids, sulfolipids, chlorolipids and phospholipids are reported in the exo-metabolome of *Chlorella* species (Kind et al. 2012b). Similarly, salinity stress is observed to elevate extracellular lipid secretion in *Scenedesmus* sp. (Petkov et al. 2010). Other classes of lipids such as sterols, polar lipids and esters of sterols are detected in extracellular secretions of *Psychotria viridis* and *N. salina*. Polar lipids, copepodamides, acts as the predator recognition signal and triggers toxin production by prey *Alexandrium minitum* as a defence response (Selander et al. 2015). Extracellular lipids are

hypothesised to act as a messenger molecule in microalgae. However, their exact role especially in grazing conditions is not clearly defined. Indole derivatives and nitrogen-rich alkaloids secretions of microalgae are reported to be detrimental to variety of bacterial and fungal species. Calothrixin A, hapalindoles, and bromoanaindolone are the most widely documented allelopathic indole derivatives emitted by cyanobacterial species (Doan et al. 2000, Volk et al. 2009). Nitrogen- and sulphur-rich compounds like alkaloids are also hypothesised to be elevated in algal ponds that are likely to undergo anerobic conditions due the failure of microalgal crop cultivation (Achyuthan et al. 2017). Microcystin, a cyclic heptapeptide, and saxitoxin, an alkaloid, are produced by cyanobacteria and dinoflagellates, respectively, and exert a neurotoxic response against their predators. An allelopathic peptide with a putative primary sequence TYR-PRO-PHE-PRO-GLY was found in the exometabolome of a diatom, *Pheodactylum tricornutum*, under grazing pressure from *Heterosigma akashiwo* (Brown et al. 2019). In contrast, free amino acids emitted by microalgae acts as the prey recognition signal and stimulates the chemosensory response of the predator. Gill and Poulet (1988) reported modulation of copepod feeding behaviour in presence of free amino acids that was a proxy for extracellular amino acid pool of microalgae. The trend of exo-metabolic dynamics can be translated into biotechnological applications such as the signature biomarkers of grazing. The extracellular cues observed in ecological interactions of prey-predator can be profiled using mass spectrophotometry (MS).

In addition to the presence of antagonistic species, extracellular metabolite secretions are also associated with the internal metabolite pool size, growth rate and biomass of microalgae (Jones and Cannon 1986). Therefore, metabolic footprinting of grazing cultures requires time-resolved mapping of the metabolome in correlation to the prey-ingestion rate for biomarker identification using MS approach. Chapter 6 attempts to profile the exo-metabolome in order to identify unique metabolic features of *D. tertiolecta* grazing by *O. marina*.

2.6 Conclusions

Chapter 2 outlines inherent features such as the photosynthetic processes of microalgal prey, *Dunaliella tertiolecta* and nutrient recycling and repackaging abilities of a predator, *Oxyrrhis marina*. Technological advancements such as PAM, FTIR and basic biochemical estimation methods can allow systematic probing of grazing cultures to enable monitoring the intrinsic processes. We hypothesised that underlying changes in these processes can serve as an indirect signal for the presence *O. marina*. Such indirect markers can be further implemented

to developed on-site grazer monitoring tools. Chapters 3, 4, 5 and 6 demonstrate the effectiveness of the mentioned technologies as an early warning sign of culture collapse.

References

Achyuthan KE, JC Harper, RP Manginell, and MW Moorman. 2017. "Volatile metabolites emission by in vivo microalgae—an overlooked opportunity?" *Metabolites* 7 (3):39-85.

Ahmed RA, M He, RA Aftab, S Zheng, M Nagi, R Bakri, and C Wang. 2017. "Bioenergy application of *Dunaliella salina* SA 134 grown at various salinity levels for lipid production." *Scientific Reports* 7 (1):8118.

Alcaraz M, E Saiz, and M Estrada. 1994. "Excretion of ammonia by zooplankton and its potential contribution to nitrogen requirements for primary production in the Catalan Sea (NW Mediterranean)." *Marine Biology* 119 (1):69-76.

Bailey KJ, and DA Walker. 1992. "Changes in fluorescence quenching brought about by feeding dithiothreitol to illuminated leaves." *Plant Physiology* 99 (1):124-129.

Bartley ML, WJ Boeing, AA Corcoran, FO Holguin, and T Schaub. 2013. "Effects of salinity on growth and lipid accumulation of biofuel microalga *Nannochloropsis salina* and invading organisms." *Biomass and Bioenergy* 54:83-88. doi: https://doi.org/10.1016/j.biombioe.2013.03.026.

Beardall J, E Young, and S Roberts. 2001. "Approaches for determining phytoplankton nutrient limitation." *Aquatic Sciences* 63 (1):44-69.

Belatik A, S Hotchandani, and R Carpentier. 2013. "Inhibition of the Water Oxidizing Complex of Photosystem II and the Reoxidation of the Quinone Acceptor QA− by Pb2+." *PLoS One* 8 (7):e68142. doi: 10.1371/journal.pone.0068142.

Ben-Amotz A. 2009. *The alga Dunaliella*. Boca Raton, FL: CRC Press.

Ben-Amotz A, A Katz, and M Avron. 1982. "Accumulation of β-carotene in halotolerant alge: purification and characterization of β-carotene-rich globules from *Dunaliella bardawil* (Chlorophyceae)." *Journal of Phycology* 18 (4):529-537.

Borowitzka LJ, TP Moulton, and MA Borowitzka. 1984. "The mass culture of *Dunaliella salina* for fine chemicals: from laboratory to pilot plant." Eleventh International Seaweed Symposium.

Borowitzka MA. 2018. "Commercial-Scale Production of Microalgae for Bioproducts. ." In *Blue biotechnology: production and use of marine molecules*, edited by SL Barre and SS Bates. Weinheim, Germany: Wiley-VCH Verlag GmbH & Co. KGaA.

Boxhorn JE, DA Holen, and ME Boraas. 1998. "Toxicity of the Chrysophyte flagellate *Poterioochromonas malhamensis* to the rotifer *Brachionus angularis*." *Hydrobiologia* 387:283-287.

Brett M, and D Muller-Navarra. 1997. "The role of highly unsaturated fatty acids in aquatic foodweb processes." *Freshwater Biology* 38 (3):483-499.

Bronk DA, and DK Steinberg. 2008. "Nitrogen Regeneration." In *Nitrogen in the Marine Environment*, edited by DG Capone, DA Bronk, MR Mulholland and EJ Carpenter, 385-467. San Diego, USA: Academic Press.

Brown ER, MR Cepeda, SJ Mascuch, KL Poulson-Ellestad, and J Kubanek. 2019. "Chemical ecology of the marine plankton." *Natural Product Reports*.

Brussaard CP. 2004. "Viral Control of Phytoplankton Populations—a Review." *Journal of Eukaryotic Microbiology* 51 (2):125-138.

Carney LT, and TW Lane. 2014. "Parasites in algae mass culture." *Frontiers in Microbiology* 5:278-286. doi: 10.3389/fmicb.2014.00278.

Carney LT, SS Reinsch, PD Lane, OD Solberg, LS Jansen, KP Williams, JD Trent, and TW Lane. 2014. "Microbiome analysis of a microalgal mass culture growing in municipal wastewater in a prototype OMEGA photobioreactor." *Algal Research* 4:52-61.

Carney LT, JS Wilkenfeld, PD Lane, OD Solberg, ZB Fuqua, NG Cornelius, S Gillespie, KP Williams, TM Samocha, and TW Lane. 2016. "Pond Crash Forensics: Presumptive identification of pond crash agents by next generation sequencing in replicate raceway mass cultures of *Nannochloropsis salina*." *Algal Research* 17:341-347. doi: https://doi.org/10.1016/j.algal.2016.05.011.

Caron DA, and JC Goldman. 1990. *Protozoan nutrient regeneration*. Edited by GM Carpriulo, *Ecology of Marine Protozoa*. New York, USA: Oxford University Press.

Chiang I, W Huang, and J Wu. 2004. "Allelochemicals of *Botryococcus braunii* (chlorophyceae) 1." *Journal of Phycology* 40 (3):474-480.

Chivers DP, and R Smith. 1998. "Chemical alarm signalling in aquatic predator-prey systems: a review and prospectus." *Ecoscience* 5 (3):338-352.

Chu FE, ED Lund, PR Littreal, KE Ruck, E Harvey, J Le Coz, Y Marty, J Moal, and P Soudant. 2008. "Sterol production and phytosterol bioconversion in two species of heterotrophic protists, *Oxyrrhis marina* and *Gyrodinium dominans*." *Marine biology* 156 (2):155-169.

Collins AM, HD Jones, RC McBride, C Behnke, and JA Timlin. 2014. "Host cell pigmentation in *Scenedesmus dimorphus* as a beacon for nascent parasite infection." *Biotechnology and Bioengineering* 111 (9):1748-1757.

Craigie JS, and J McLachlan. 1964. "Glycerol as a photosynthetic product in *Dunaliella tertiolecta* Butcher." *Journal of Botony* 42:777--778.

Crofts AR. 1967. "Amine uncoupling of energy transfer in chloroplasts I. Relation to ammonium ion uptake." *Journal of Biological Chemistry* 242 (14):3352-3359.

Dalsgaard J, MS John, G Kattner, D Müller-Navarra, and W Hagen. 2003. "Fatty acid trophic markers in the pelagic marine environment." *Adavnces in Marine Biology* 46:255-340. doi: https://doi.org/10.1016/S0065-2881(03)46005-7.

Damiani MC, PI Leonardi, OI Pieroni, and EJ Cáceres. 2006. "Ultrastructure of the cyst wall of *Haematococcus pluvialis* (Chlorophyceae): wall development and behaviour during cyst germination." *Phycologia* 45 (6):616-623.

Day JG. 2013. "Grazers: the overlooked threat to the sustained production of future algal biofuels." *Biofuels* 4:459-461.

Day JG, Y Gong, and Q Hu. 2017. "Microzooplanktonic grazers – A potentially devastating threat to the commercial success of microalgal mass culture." *Algal Research* 27:356-365. doi: https://doi.org/10.1016/j.algal.2017.08.024.

Day JG, NJ Thomas, UE Achilles-Day, and RJ Leakey. 2012. "Early detection of protozoan grazers in algal biofuel cultures." *Bioresource Technology* 114:715-719.

Deglint JL, C Jin, and A Wong. 2018. "Investigating the Automatic Classification of Algae Using Fusion of Spectral and Morphological Characteristics of Algae via Deep Residual Learning." *arXiv preprint arXiv:1810.10889*.

del Hoyo A, R Alvarez, EM del Campo, F Gasulla, E Barreno, and LM Casano. 2011. "Oxidative stress induces distinct physiological responses in the two Trebouxia phycobionts of the lichen *Ramalina farinacea*." *Annals of Botany* 107 (1):109-118. doi: 10.1093/aob/mcq206.

DellaGreca M, A Zarrelli, P Fergola, M Cerasuolo, A Pollio, and G Pinto. 2010. "Fatty acids released by Chlorella vulgaris and their role in interference with *Pseudokirchneriella subcapitata*: experiments and modelling." *Journal of Chemical Ecology* 36 (3):339-349.

Demmig-Adams B. 1990. "Carotenoids and photoprotection in plants: a role for the xanthophyll zeaxanthin." *Biochimica et Biophysica Acta (BBA)-Bioenergetics* 1020 (1):1-24.
Dijkman NA, and JC Kromkamp. 2006. "Photosynthetic characteristics of the phytoplankton in the Scheldt estuary: community and single-cell fluorescence measurements." *European Journal of Phycology* 41 (4):425-434.
Doan NT, RW Rickards, JM Rothschild, and GD Smith. 2000. "Allelopathic actions of the alkaloid 12-epi-hapalindole E isonitrile and calothrixin A from cyanobacteria of the genera Fischerella and Calothrix." *Journal of Applied Phycology* 12 (3-5):409-416.
Droop MR. 1959. "Water-soluble factors in the nutrition of *Oxyrrhis marina*." *Journal of the Marine Biological Association of the United Kingdom* 38 (3):605-620.
Emerson R, and W Arnold. 1932. "The photochemical reaction in photosynthesis." *The Journal of General Physiology* 16 (2):191-205.
Flynn KJ, P Kenny, and A Mitra. 2017. "Minimising losses to predation during microalgae cultivation." *Journal of Applied Phycology* 29 (4):1829-1840.
Fott B. 1967. "*Phlyctidium scenedesmi* spec. nova, a new chytrid destroying mass cultures of algae." *Zeitschrift für Allgemeine Mikrobiologie* 7 (2):97-102.
Fulbright SP, MK Dean, G Wardle, PJ Lammers, and S Chisholm. 2014. "Molecular diagnostics for monitoring contaminants in algal cultivation." *Algal Research* 4:41-51. doi: https://doi.org/10.1016/j.algal.2013.11.008.
Fundel B, H Stich, H Schmid, and G Maier. 1998. "Can phaeopigments be used as markers for Daphnia grazing in Lake Constance?" *Journal of Plankton Research* 20 (8):1449-1462.
Gachon CM, T Sime-Ngando, M Strittmatter, A Chambouvet, and GH Kim. 2010. "Algal diseases: spotlight on a black box." *Trends in Plant Science* 15 (11):633-640.
Ganuza E, CE Sellers, BW Bennett, EM Lyons, and LT Carney. 2016. "A novel treatment protects *Chlorella* at commercial scale from the predatory bacterium *Vampirovibrio* chlorellavorus." *Frontiers in Microbiology* 7:848.
García-González M, J Moreno, JP Cañavate, V Anguis, A Prieto, C Manzano, FJ Florencio, and MG Guerrero. 2003. "Conditions for open-air outdoor culture of *Dunaliella salina* in southern Spain." *Journal of Applied Phycology* 15 (2):177-184. doi: 10.1023/a:1023892520443.
Gautam R, S Vanga, F Ariese, and S Umapathy. 2015. "Review of multidimensional data processing approaches for Raman and infrared spectroscopy." *EPJ Techniques and Instrumentation* 2 (1):2-8.
Genty B, JM Briantais, and NR Baker. 1989. "The relationship between the quantum yield of photosynthetic electron transport and quenching of chlorophyll fluorescence." *Biochimica et Biophysica Acta (BBA)-General Subjects* 990 (1):87-92.
Gerphagnon M, D Latour, J Colombet, and T Sime-Ngando. 2013. "A double staining method using SYTOX green and calcofluor white for studying fungal parasites of phytoplankton." *Applied Environmental Microbiology* 79 (13):3943-3951.
Gill CW, and SA Poulet. 1988. "Responses of copepods to dissolved free amino acids." *Marine Ecology Progress Series. Oldendorf* 43 (3):269-276.
Goldman JC, MR Dennett, and H Gordin. 1989. "Dynamics of herbivorous grazing by the heterotrophic dinoflagellate *Oxyrrhis marina*." *Journal of Plankton Research* 11 (2):391-407.
Goldman JC, and JH Ryther. 1976. "Temperature-influenced species competition in mass cultures of marine phytoplankton." *Biotechnology and Bioengineering* 18 (8):1125-1144.

Govindjee KJ, J Messinger, and J Whitmarsh. 2010. *Photosystem II*. Edited by Kern JF Govindjee, J Messinger and J Whitmarsh. Vol. 10, *Encyclopedia of life sciences (ELS).* Chichester, USA: Wiley.

Govindjee U. 2014. *Non-photochemical quenching and energy dissipation in plants, algae and cyanobacteria*. Edited by B Demmig-Adams, G Garab and W Adams III. Vol. 40. Dordrecht, The Netherlands: Springer.

Greenfield SR, M Seibert, G Govindjee, and MR Wasielewski. 1997. "Direct measurement of the effective rate constant for primary charge separation in isolated photosystem II reaction centers." *The Journal of Physical Chemistry B* 101 (13):2251-2255.

Greenwell HC, LML Laurens, RJ Shields, RW Lovitt, and KJ Flynn. 2010. "Placing microalgae on the biofuels priority list: a review of the technological challenges." *Journal of The Royal Society Interface* 7 (46):703-726.

Griffiths PR, and JA De Haseth. 2007. *Fourier transform infrared spectrometry*. Vol. 171. New Jersey, USA: John Wiley & Sons.

Gutman J, A Zarka, and S Boussiba. 2009. "The host-range of *Paraphysoderma sedebokerensis*, a chytrid that infects *Haematococcus Pluvialis*." *European Journal of Phycology* 44 (4):509-514.

Havaux M, L Dall'Osto, and R Bassi. 2007. "Zeaxanthin has enhanced antioxidant capacity with respect to all other xanthophylls in Arabidopsis leaves and functions independent of binding to PSII antennae." *Plant Physiology* 145 (4):1506-1520.

Havlik I, KF Reardon, M Ünal, P Lindner, A Prediger, A Babitzky, S Beutel, and T Scheper. 2013. "Monitoring of microalgal cultivations with on-line, flow-through microscopy." *Algal Research* 2 (3):253-257.

Hiltunen M, U Strandberg, SJ Taipale, and P Kankaala. 2015. "Taxonomic identity and phytoplankton diet affect fatty acid composition of zooplankton in large lakes with differing dissolved organic carbon concentration." *Limnology and Oceanography* 60 (1):303-317.

Hosseini A, and M Shariati. 2009. "*Dunaliella* biotechnology: methods and applications." *Journal of Applied Microbiology* 107 (1):14-35.

Huo S, C Shang, Z Wang, W Zhou, F Cui, F Zhu, Z Yuan, and R Dong. 2017. "Outdoor growth characterization of an unknown microalga screened from contaminated *Chlorella* culture." *BioMed Research International* 2017.

Ianora A, MG Bentley, GS Caldwell, R Casotti, AD Cembella, J Engström-Öst, C Halsband, E Sonnenschein, C Legrand, and CA Llewellyn. 2011. "The relevance of marine chemical ecology to plankton and ecosystem function: an emerging field." *Marine Drugs* 9 (9):1625-1648.

Ismail AA, FR van de Voort, and J Sedman. 1997. "Fourier transform infrared spectroscopy: Principles and applications." In *Techniques and Instrumentation in Analytical Chemistry*, edited by J. R. J. Paré and J. M. R. Bélanger, 93-139. Elsevier.

Jahns P, and GH Krause. 1994. "Xanthophyll cycle and energy-dependent fluorescence quenching in leaves from pea plants grown under intermittent light." *Planta* 192 (2):176-182.

Joliot P, and B Kok. 1975. "Oxygen evolution in photosynthesis." In *Energetics of Photosynthesis*, edited by Govindjee, 387-412. New York, USA: Academic Press.

Jones AK, and RC Cannon. 1986. "The release of micro-algal photosynthate and associated bacterial uptake and heterotrophic growth." *British Phycological Journal* 21 (4):341-358.

Karuppasamy S, AS Musale, B Soni, B Bhadra, N Gujarathi, M Sundaram, A Sapre, S Dasgupta, and C Kumar. 2018. "Integrated grazer management mediated by chemicals for sustainable cultivation of algae in open ponds." *Algal Research* 35:439-448.

Kind Tobias, John K Meissen, Dawei Yang, Fernando Nocito, Arpana Vaniya, Yu-Shen Cheng, Jean S VanderGheynst, and Oliver Fiehn. 2012. "Qualitative analysis of algal secretions with multiple mass spectrometric platforms." *Journal of Chromatography A* 1244:139-147.

Klawonn I, S Bonaglia, MJ Whitehouse, S Littmann, D Tienken, Marcel MM Kuypers, V Brüchert, and H Ploug. 2019. "Untangling hidden nutrient dynamics: rapid ammonium cycling and single-cell ammonium assimilation in marine plankton communities." *The ISME journal* (13):1960-1974.

Knoshaug EP, E Wolfrum, LM Laurens, VL Harmon, TA Dempster, and J McGowen. 2018. "Unified field studies of the algae testbed public-private partnership as the benchmark for algae agronomics." *Scientific Data* 5:180267-180277. doi: https://doi.org/10.1038/sdata.2018.267.

Lakowicz JR. 1999. *Principles of fluorescence spectroscopy*. Second ed. New York: Kluwer Academic-Plenum

Lammers PJ, M Huesemann, W Boeing, DB Anderson, RG Arnold, X Bai, M Bhole, Y Brhanavan, L Brown, and J Brown. 2017. "Review of the cultivation program within the National Alliance for Advanced Biofuels and Bioproducts." *Algal Research* 22:166-186.

Lane T, K Poorey, H Geng, DJ Curtis, and LT Carney. 2016. Algal crop protection strategies and technologies. No- SAND2016-8236C. Livermore, United States: Sandia National Laboratory

Liang M, L Xue, and J Jiang. 2019. "Two-stage cultivation of *Dunaliella tertiolecta* with glycerol and triethylamine for lipid accumulation: A viable way to alleviate the inhibitory effect of triethylamine on biomass." *Applied Environmental Microbiology* 85 (4):2614-2618.

Lodish H, A Berk, SL Zipursky, P Matsudaira, D Baltimore, and J Darnell. 2000. "Photosynthetic stages and light-absorbing pigments." In *Molecular Cell Biology*. New York: WH Freeman.

Lorenz RT, and GR Cysewski. 2000. "Commercial potential for *Haematococcus* microalgae as a natural source of astaxanthin." *Trends in Biotechnology* 18 (4):160-167.

Ma M, Y Gong, and Q Hu. 2018. "Identification and feeding characteristics of the mixotrophic flagellate *Poterioochromonas malhamensis*, a microalgal predator isolated from outdoor massive *Chlorella* culture." *Algal Research* 29:142-153.

Ma M, D Yuan, Y He, M Park, Y Gong, and Q Hu. 2017. "Effective control of *Poterioochromonas malhamensis* in pilot-scale culture of *Chlorella sorokiniana* GT-1 by maintaining CO2-mediated low culture pH." *Algal Research* 26:436-444. doi: https://doi.org/10.1016/j.algal.2017.06.023.

Ma X, T Chen, B Yang, J Liu, and F Chen. 2016. "Lipid production from *Nannochloropsis*." *Marine Drugs* 14 (4):61.

Mackey MD, DJ Mackey, HW Higgins, and SW Wright. 1996. "CHEMTAX-a program for estimating class abundances from chemical markers: application to HPLC measurements of phytoplankton." *Marine Ecology Progress Series* 144:265-283.

Maes D, TA Reichardt, TJ Jensen, TA Dempster, JA McGowen, K Poorey, T Hipple, T Lane, and JA Timlin. 2018. Spectroradiometric Detection of Competitors and Predators in Algal Ponds. United States: Sandia National Lab.(SNL-NM), Albuquerque, NM (United States); Sandia.

Mann KH. 1982. *Ecology of coastal waters: a systems approach*. Vol. 8. Berkeley and Los Angeles: University of California Press.

Mansour MP, JK Volkman, AE Jackson, and SI Blackburn. 1999. "The fatty acid and sterol composition of five marine dinoflagellates." *Journal of Phycology* 35 (4):710-720.

Martin-Creuzburg D, E von Elert, and KH Hoffmann. 2008. "Nutritional constraints at the cyanobacteria—*Daphnia magna* interface: the role of sterols." *Limnology and Oceanography* 53 (2):456-468.

McGowen J, EP Knoshaug, LM Laurens, TA Dempster, PT Pienkos, E Wolfrum, and VL Harmon. 2017. "The Algae Testbed Public-Private Partnership (ATP3) framework; establishment of a national network of testbed sites to support sustainable algae production." *Algal Research* 25:168-177. doi: https://doi.org/10.1016/j.algal.2017.05.017.

Mendes LB, and AB Vermelho. 2013. "Allelopathy as a potential strategy to improve microalgae cultivation." *Biotechnology for Biofuels* 6 (1):152.

Mitra A, and KJ Flynn. 2005. "Predator–prey interactions: is 'ecological stoichiometry'sufficient when good food goes bad?" *Journal of Plankton Research* 27 (5):393-399.

Montagna PA. 1995. "Rates of metazoan meiofaunal microbivory: a review." *Vie et Milieu* 45 (1):1-10.

Montagnes DJ, CD Lowe, L Martin, PC Watts, N Downes-Tettmar, Z Yang, EC Roberts, and K Davidson. 2010. "*Oxyrrhis marina* growth, sex and reproduction." *Journal of Plankton Research* 33 (4):615-627.

Moreau RA, BD Whitaker, and KB Hicks. 2002. "Phytosterols, phytostanols, and their conjugates in foods: structural diversity, quantitative analysis, and health-promoting uses." *Progress in Lipid Research* 41 (6):457-500.

Moreno-Garrido I., and J. P. Cañavate. 2001. "Assessing chemical compounds for controlling predator ciliates in outdoor mass cultures of the green algae *Dunaliella salina*." *Aquacultural Engineering* 24 (2):107-114. doi: https://doi.org/10.1016/S0144-8609(00)00067-4.

Müller P, X Li, and KK Niyogi. 2001. "Non-photochemical quenching. A response to excess light energy." *Plant Physiology* 125 (4):1558-1566.

Murphy TE, K Macon, and H Berberoglu. 2014. "Rapid algal culture diagnostics for open ponds using multispectral image analysis." *Biotechnology Progress* 30 (1):233-240.

Nishio JN, and J Whitmarsh. 1993. "Dissipation of the proton electrochemical potential in intact chloroplasts (II. The pH gradient monitored by cytochrome *f* reduction kinetics)." *Plant Physiology* 101 (1):89-96.

Niyogi Krishna K, Olle Björkman, and Arthur R Grossman. 1997. "The roles of specific xanthophylls in photoprotection." *Proceedings of the National Academy of Sciences* 94 (25):14162-14167.

Öpik H, and KJ Flynn. 1989. "The digestive process of the dinoflagellate, *Oxyrrhis marina* Dujardin, feeding on the chlorophyte, *Dunaliella primolecta* Butcher: a combined study of ultrastructure and free amino acids." *New Phytologist* 113 (2):143-151.

Parmar A, Niraj K Singh, A Pandey, E Gnansounou, and D Madamwar. 2011. "Cyanobacteria and microalgae: A positive prospect for biofuels." *Bioresource Technology* 102 (22):10163-10172. doi: https://doi.org/10.1016/j.biortech.2011.08.030.

Persson Jonas, and Tobias Vrede. 2006. "Polyunsaturated fatty acids in zooplankton: variation due to taxonomy and trophic position." *Freshwater Biology* 51 (5):887-900.

Petkov G, R Kambourova, and V Bankova. 2010. "Extracellular substances of total bacterial flora from cultures of the green alga *Scenedesmus*." *Comptes rendus de l'Académie bulgare des Sciences* 63 (2):235-240.

Post FJ, LJ Borowitzka, MA Borowitzka, B Mackay, and T Moulton. 1983. "The protozoa of a Western Australian hypersaline lagoon." *Hydrobiologia* 105 (1):95-113. doi: 10.1007/bf00025180.

Poulton NJ, and JL Martin. 2010. *Imaging flow cytometry for quantitative phytoplankton analysis-FlowCAM*. Edited by B Karlson, C Cusack and E Bresnan, *Microscopic and Molecular Methods for Quantitative Phytoplankton Analysis, IOC Manuals and Guides*.

Rasconi S, M Jobard, L Jouve, and T Sime-Ngando. 2009. "Use of calcofluor white for detection, identification, and quantification of phytoplanktonic fungal parasites." *Applied Environmental Microbiology* 75 (8):2545-2553.

Reese KL, CL Fisher, PD Lane, JD Jaryenneh, MW Moorman, AD Jones, M Frank, and TW Lane. 2019. "Chemical profiling of volatile organic compounds in the headspace of algal cultures as early biomarkers of algal pond crashes." *Scientific Reports* 9 (1):1-10.

Reichardt TA, AM Collins, RC McBride, CA Behnke, and JA Timlin. 2014. "Spectroradiometric monitoring for open outdoor culturing of algae and cyanobacteria." *Applied optics* 53 (24):F31-F45.

Ribalet F, JA Berges, A Ianora, and R Casotti. 2007. "Growth inhibition of cultured marine phytoplankton by toxic algal-derived polyunsaturated aldehydes." *Aquatic Toxicology* 85 (3):219-227.

Richmond A. 2004. *Handbook of microalgal culture: biotechnology and applied phycology*. Vol. Part-I. Oxford: Blackwell Science Ltd.

Roberts EC, EC Wootton, K Davidson, HJ Jeong, CD. Lowe, and DJ Montagnes. 2010. "Feeding in the dinoflagellate *Oxyrrhis marina*: linking behaviour with mechanisms." *Journal of Plankton Research* 33 (4):603-614. doi: 10.1093/plankt/fbq118.

Rogers JN, JN Rosenberg, BJ Guzman, VH Oh, LE Mimbela, A Ghassemi, MJ Betenbaugh, GA Oyler, and MD Donohue. 2014. "A critical analysis of paddlewheel-driven raceway ponds for algal biofuel production at commercial scales." *Algal Research* 4:76-88. doi: https://doi.org/10.1016/j.algal.2013.11.007.

Roig X. 2000. *The Molecular Structure of the Photosynthetic Apparatus*. Edited by PG Falkowski and JA Raven. 2 ed. Vol. 3, *Aquatic Photosynthesis*. Princeton, Oxford: Princeton University Press.

Rothbard S. 1975. "Control of *Euplotes* sp. by formalin in growth tanks of *Chlorella* sp. used as growth medium for the rotifer *Brachionus plicatilis* which serves as feed for hatchlings." *Bamidgeh* 27 (4):100-109.

Roy-Lachapelle A, M Solliec, M Bouchard, and S Sauvé. 2017. "Detection of cyanotoxins in algae dietary supplements." *Toxins* 9 (3):76.

Roy JS, KL Poulson-Ellestad, RD Sieg, RX Poulin, and J Kubanek. 2013. "Chemical ecology of the marine plankton." *Natural Product Reports* 30 (11):1364-1379.

Ruban AV. 2016. "Nonphotochemical chlorophyll fluorescence quenching: mechanism and effectiveness in protecting plants from photodamage." *Plant Physiology* 170 (4):1903-1916.

Safi C, B Zebib, O Merah, P Pontalier, and C Vaca-Garcia. 2014. "Morphology, composition, production, processing and applications of *Chlorella vulgaris*: A review." *Renewable and Sustainable Energy Reviews* 35:265-278.

Savitzky A, and MJ Golay. 1964. "Smoothing and differentiation of data by simplified least squares procedures." *Analytical Chemistry* 36 (8):1627-1639.

Scholz MJ, TL Weiss, RE Jinkerson, J Jing, R Roth, U Goodenough, MC Posewitz, and HG Gerken. 2014. "Ultrastructure and composition of the *Nannochloropsis gaditana* cell wall." *Eukaryotic Cell* 13 (11):1450-1464.

Schreiber U. 1986. "Detection of rapid induction kinetics with a new type of high-frequency modulated chlorophyll fluorometer." In *Current Topics in Photosynthesis*, edited by J Amesz, AJ HoffH and JV Gorkum, 259-270. Dordrecht: Springer.

Schreiber U, M Kühl, I Klimant, and H Reising. 1996. "Measurement of chlorophyll fluorescence within leaves using a modified PAM fluorometer with a fiber-optic microprobe." *Photosynthesis Research* 47 (1):103-109.

Schroeder DC, J Oke, M Hall, G Malin, and WH Wilson. 2003. "Virus succession observed during an *Emiliania huxleyi* bloom." *Appllied Environmental Microbiology* 69 (5):2484-2490.

Seepratoomrosh J, P Pokethitiyook, M Meetam, K Yokthongwattana, W Yuan, W Pugkaew, and K Kangvansaichol. 2016. "The effect of light stress and other culture conditions on photoinhibition and growth of *Dunaliella tertiolecta*." *Applied Biochemistry and Biotechnology* 178 (2):396-407.

Selander E, J Kubanek, M Hamberg, MX Andersson, G Cervin, and H Pavia. 2015. "Predator lipids induce paralytic shellfish toxins in bloom-forming algae." *Proceedings of the National Academy of Sciences* 112 (20):6395-6400.

Serive B, E Nicolau, J Bérard, R Kaas, V Pasquet, L Picot, and J Cadoret. 2017. "Community analysis of pigment patterns from 37 microalgae strains reveals new carotenoids and porphyrins characteristic of distinct strains and taxonomic groups." *PLoS One* 12 (2):e0171872.

Smith VH, BL Foster, JP Grover, RD Holt, MA Leibold, and F deNoyelles. 2005. "Phytoplankton species richness scales consistently from laboratory microcosms to the world's oceans." *Proceedings of the National Academy of Sciences* 102 (12):4393-4396.

Spolaore P, C Joannis-Cassan, E Duran, and A Isambert. 2006. "Commercial applications of microalgae." *Journal of Bioscience and Bioengineering* 101 (2):87-96.

Steichen S. 2016. "Tracking an algal predator: monitoring the dynamics of *Vampirovibrio chlorellavorus* in outdoor culture." Master of Science, School of Plant Sciences, The University of Arizona.

Steinberg DK, and GK Saba. 2008. "Nitrogen Consumption and Metabolism in Marine Zooplankton." In *Nitrogen in the Marine Environment* edited by DG Capone, DA Bronk, MR Mulholland and EJ Carpenter, 1135-1196. San Diego: Academic Press.

Strandberg U, SJ Taipale, M Hiltunen, AW Galloway, MT Brett, and P Kankaala. 2015. "Inferring phytoplankton community composition with a fatty acid mixing model." *Ecosphere* 6 (1):1-18.

Sun Y, S Xu, W Li, J Zhang, and C Wang. 2012. *Antialgal substances from Isochrysis galbana and its effects on the growth of Isochrysis galbana and six species of feed microalgae*. Edited by E Zhu and S Sambath. Vol. 134, *Information Technology and Agricultural Engineering*. Berlin, Heidelberg: Springer.

Taipale SJ, M Hiltunen, K Vuorio, and E Peltomaa. 2016. "Suitability of phytosterols alongside fatty acids as chemotaxonomic biomarkers for phytoplankton." *Frontiers in Plant Science* 7:212--228.

Tiselius P, BW Hansen, and D Calliari. 2012. "Fatty acid transformation in zooplankton: From seston to benthos." *Marine Ecology Progress Series* 446:131-144. doi: 10.3354/meps09479.

Tol LS, and AL White. 2003. "Long-term hyposaline and hypersaline stresses produce distinct antioxidant responses in the marine alga *Dunaliella tertiolecta*." *Journal of Plant Physiology* 160 (10):1193-1202.

Urabe J, M Kyle, W Makino, T Yoshida, T Andersen, and JJ Elser. 2002. "Reduced light increases herbivore production due to stoichiometric effects of light/nutrient balance." *Ecology* 83 (3):619-627.

Velthuys BR. 1980. "Mechanisms of electron flow in photosystem II and toward photosystem I." *Annual Review of Plant Physiology* 31 (1):545-567.

Velthuys BR, and J Amesz. 1974. "Charge accumulation at the reducing side of system 2 of photosynthesis." *Biochimica et Biophysica Acta (BBA)-Bioenergetics* 333 (1):85-94.
Volk RB, U Girreser, M Al-Refai, and H Laatsch. 2009. "Bromoanaindolone, a novel antimicrobial exometabolite from the cyanobacterium *Anabaena constricta*." *Natural Product Research* 23 (7):607-612.
Volkman J. 2003. "Sterols in microorganisms." *Applied Microbiology and Biotechnology* 60 (5):495-506.
Vongsvivut J, P Heraud, A Gupta, M Puri, D McNaughton, and C Barrow. 2013. "FTIR microspectroscopy for rapid screening and monitoring of polyunsaturated fatty acid production in commercially valuable marine yeasts and protists." *Analyst* 138 (20):6016-6031.
Wang H, W Zhang, L Chen, J Wang, and T Liu. 2013. "The contamination and control of biological pollutants in mass cultivation of microalgae." *Bioresource Technology* 128:745-750. doi: https://doi.org/10.1016/j.biortech.2012.10.158.
Wang Y, M Castillo-Keller, E Eustance, and M Sommerfeld. 2017. "Early detection and quantification of zooplankton grazers in algal cultures by FlowCAM." *Algal Research* 21:98-102. doi: https://doi.org/10.1016/j.algal.2016.11.012.
Wang Y, Y Gong, L Dai, M Sommerfeld, C Zhang, and Q Hu. 2018. "Identification of harmful protozoa in outdoor cultivation of *Chlorella* and the use of ultrasonication to control contamination." *Algal Research* 31:298-310.
Weiss TL, R Roth, C Goodson, S Vitha, I Black, P Azadi, J Rusch, A Holzenburg, TP Devarenne, and U Goodenough. 2012. "Colony organization in the green alga *Botryococcus braunii* (Race B) is specified by a complex extracellular matrix." *Eukaryotic Cell* 11 (12):1424-1440.
White AJ, and C Critchley. 1999. "Rapid light curves: a new fluorescence method to assess the state of the photosynthetic apparatus." *Photosynthesis Research* 59 (1):63-72.
Withers NW, RC Tuttle, GG Holz, DH Beach, LJ Goad, and TW Goodwin. 1978. "Dehydrodinosterol, dinosterone and related sterols of a non-photosynthetic dinoflagellate, *Crypthecodinium cohnii*." *Phytochemistry* 17 (11):1987-1989.
Wold Svante, Michael Sjöström, and Lennart Eriksson. 2001. "PLS-regression: a basic tool of chemometrics." *Chemometrics and Intelligent Laboratory Systems* 58 (2):109-130. doi: https://doi.org/10.1016/S0169-7439(01)00155-1.
Wright JL. 1979. "The occurrence of ergosterol and (22 E, 24 R)-24-ethylcholesta-5, 7, 22-trien-3β-ol in the unicellular chlorophyte *Dunaliella tertiolecta*." *Canadian Journal of Chemistry* 57 (19):2569-2571.
Xu J, and T Kiørboe. 2018. "Toxic dinoflagellates produce true grazer deterrents." *Ecology* 99 (10):2240-2249.
Ye Z, J Jiang, and G Wu. 2008. "Biosynthesis and regulation of carotenoids in *Dunaliella*: progresses and prospects." *Biotechnology Advances* 26 (4):352-360.

Chapter 3

Grazing-mediated photosynthetic alterations and non-photochemical quenching as an early indicator of predation by *Oxyrrhis marina* and *Euplotes* sp.

A reformatted version of this chapter is currently accepted in the journal *Applied Phycology* as: Deore, P, Kathikaichamy A, Beardall J and Noronha S. 2020. "Non-photochemical quenching, a non-invasive probe for monitoring microalgal grazing: an early indicator of predation by *Oxyrrhis marina* and *Euplotes* sp." 1(1)20–31.

3.1 Introduction

Detection of early warning signs of grazer infestation is a crucial determinant of the effectiveness of predator mitigation methods such as chemical or physical treatments (Table 2.1). Currently used monitoring methods are offline and often have poor detection limits. Therefore, these methods fail to provide accurate estimates of the predator load. Microscopy and oligonucleotide-based markers are widely employed grazer monitoring methods which are based on direct detection of predators (Day et al. 2017). Thus, only an increase in the predator cell concentration or amplified sequences of targeted nucleic acid can reveal the extent of the contamination. Challenges associated with each of these approaches are outlined in detail in chapter 2 (Section 2.4). In contrast, indirect effects of grazing on physiological aspects of microalgal prey, other than growth, is poorly understood at the large-scale. In an ecological sense, prey ought to respond against the predator attack prior to the initiation of grazer ingestion process (Section 2.5.4). In-depth understanding of the changes within prey cells can help devise indirect measures of predator infestation early on. Photophysiological responses of microalgal prey cells represent one such indirect measure that is reported to be modulated under a range of environmental cues including grazing. Fundel et al. (1998) and Ratti et al. (2013) reported a grazing-mediated modulation of photosynthetic pigments and process, respectively. In this chapter, we hypothesized that it would be possible to leverage the changes associated with the photosynthetic process of microalgal prey, here *Dunaliella tertiolecta*, as a marker of grazing mediated by *Oxyrrhis marina* and *Euplotes* sp.

Microalgal cells are exposed to different intensities of light in outdoor culture depending on cell density, rate of turbulence, light fluctuations and nutrient status. Thus, the

reaction center (RC) of photosynthetic units respond differently such that antenna complexes in some cells absorb excess energy while others are shadowed (Demory et al. 2018). Non-photochemical quenching (NPQ) acts as a safeguard mechanism in algal cells that assists in dissipation of excess energy through specialised pigments, carotenoids, associated with LHC complex of PSII. NPQ measurements have largely been used to understand the mechanism and quantitate the protective process within the microalgae cell. Failure of NPQ activation can lead to transfer of excess energy to oxygen and as result reactive oxygen species (ROS) are generated which can potentially damage various cellular process (Müller et al. 2001). PAM-based photosynthetic measurements, including NPQ, have been reported to change under abiotic stress conditions such as high temperature (Eggert et al. 2007), light (Kok 1956), salinity (Karthikaichamy et al. 2018) and nutrient stress (Shelly et al. 2010). According to a recent report, NPQ levels were negatively affected in green algae, cyanobacteria, and a diatom culture following ciliate and copepod infection, as a function of seawater chemistry (Ratti et al. 2013). However, grazer-induced changes in the NPQ levels have not yet been established as a useful early indicator of predation.

Chlorophyll *a* fluorescence is a commonly used technique to probe various parameters of photosynthesis and photophysiology in algae and higher plants. Commonly measured parameters are maximum quantum yield (F_v/F_m) in the dark-adapted state, often used as an indicator of stress, and effective quantum yield in the light-adapted state ($F_{v'}/F_{m'}$). Both measurements indicate the efficiency of photon absorption by chlorophyll and accessory pigments, which is further translated into electron flow in the electron transport chain. Therefore, effective quantum yield can help in an estimation of the rate of electron transport, which is highly dependent on absorptance of the cells, though relative electron transport rates ($rETR_{max}$) can be determined in cases where absorptance is unknown and is often excluded (Figueroa et al. 2003, Kalaji et al. 2017, Johnsen and Sakshaug 2007). In-depth information about light harvesting efficiency, alpha, and electron transport rates can be obtained by constructing photosynthesis irradiance curves (Rubio et al. 2003).

This chapter aims to investigate photophysiology-based measurements, particularly NPQ, as an early indicator of *O. marina* infestation in *D. tertiolecta* cultures and subsequent culture crash. A ciliate, *Euplotes* sp., is used as an alternative predator in some experiments to test the effectiveness NPQ measurements for early detection of invader species.

3.2 Materials and Methods

3.2.1 Cultivation conditions of prey and predator strains

The *Dunaliella tertiolecta* (CS-175) culture was purchased from the CSIRO Culture Collection, Hobart, Tasmania, Australia and maintained axenically in F/2 seawater-based medium at pH 8. The predator strains, *Oxyrrhis marina* and *Euplotes* sp. were isolated from seawater collected from the west coast of Gujarat, India and maintained in the same F/2 medium as used for the prey alga, *D. tertiolecta*. *O. marina* and *Euplotes* sp., were fed on *D. tertiolecta*. Grazing cultures were established using prey cells which were harvested during late exponential phase and centrifuged at 1500 g for 10 min followed by a wash with fresh F/2 media to remove cell debris. Similarly, predator cultures were harvested and washed to minimise carry-over of bacterial load. Predator and prey were then mixed in the required proportions to establish the grazing cultures. Unless otherwise stated, a prey-predator concentration of 100:1 was set up using the respective cell densities at the time of inoculation where the initial prey cell concentration was ~10^5 cells ml^{-1}. The cell concentration was monitored daily to understand the prey-predator population dynamics and a visible clearance of prey cells in a grazing culture was considered as a 'culture crash'. Unless mentioned otherwise, 200 ml grazing cultures were cultivated in 500 ml Erlenmeyer flasks (Borosil) and incubated at 25^{O}C under 30–50 µmol photons m^{-2} s^{-1} cool white fluorescent light (Philips, Eindhoven, Netherlands) fixed at ~35 cm above the culture flasks. The crash assay conditions, cell density and other related parameters were optimized in preliminary experiments. Light intensity was measured using a light sensor (LI-210R, LI-COR, USA). Morphological features of all the strains were observed under a phase contrast microscope (Leica DM2000, Germany). Prey and predator cells were fixed in Lugol's iodine for cell counts using an Improved Neubauer haemocytometer and Sedgwick rafter chamber, respectively. Predator cell concentrations <10^3–10^4 cells ml^{-1} were mostly undetected in microscopic counts and required additional sample harvesting in order to obtain detectable level of predator numbers. The ingestion rates were calculated by using eq. 3.1–3.8 described by Jeong et al. (2001).

$$I = C' * F \tag{3.1}$$

where, I is ingestion rate (prey cells $predator^{-1}$ d^{-1}), C' is the mean prey cell concentration (cells ml^{-1}) and F is the clearance rate (prey cells d^{-1}).

$$F = V * g * PD'^{-1} \tag{3.2}$$

where F is the clearance rate (prey cells d^{-1}), v is the volume (ml) of the culture, PD' is the predator mean concentration (cells ml^{-1}), g is the predator growth constant

$$C' = \frac{C_0(e^t(k-g)-1)}{t(k-g)} \tag{3.3}$$

where C' is the mean prey cell concentration (cells ml^{-1}), C_0 is the initial prey concentration (cells ml^{-1}) in grazing flasks, K is the prey growth constant, g is the predator growth constant, and t is $t_2 - t_1$, that is, t_2 is final time-point and t_1 is initial time-point

$$PD' = \frac{PD_0(e^{PD*t}-1)}{PD*t} \tag{3.4}$$

where PD_0 is the initial predator cell number (cells ml^{-1}) and PD is the predator growth rate (cells d^{-1})

$$K = \frac{\ln\left(\frac{C_t}{C_0}\right)}{t} \tag{3.5}$$

where K is the prey growth constant, C_t is the final prey cell concentration (cells ml^{-1}) in control bottles, and C_0 is the initial prey cell concentration (cells ml^{-1}) in experimental bottles

$$g = K - \frac{\ln\left(\frac{C_{t'}}{C_0}\right)}{t} \tag{3.6}$$

where g is the predator growth constant and $C_{t'}$ is final prey cell concentration (cells ml^{-1}) in grazing flasks

$$P = \frac{\ln\left(\frac{N_t}{N_0}\right)}{t} \tag{3.7}$$

where P is the specific growth rate of prey (d^{-1}), N_t is the final prey cell concentration (cells ml^{-1}) at t_2, and N_0 is the initial number of prey cells at t_1

$$PD = \frac{\ln\left(\frac{M_t}{M_0}\right)}{t} \tag{3.8}$$

where PD is the specific growth rate of the predator (d^{-1}), M_t is the final predator cell concentration (cells ml^{-1}) at t_2 and M_0 is the initial number of predator cells (cells ml^{-1}) at t_2

3.2.2 Chlorophyll *a* fluorescence measurements

The grazing cultures of *O. marina* feeding on *D. tertiolecta* were operated in batch mode. Ungrazed cultures of *D. tertiolecta* served as controls. The prey-predator cell concentration was monitored daily by manual cell counting, and cells from the control and grazing flasks were harvested for measurements of chlorophyll *a* fluorescence using a PhytoPAM II (Walz, Germany). A preliminary method optimisation process was performed to minimise the background signal using the auto-gain and zero-offset controls of the PAM. Additionally, the settings of the saturation pulse were optimised to obtain maximum fluorescence rise and a stable plateau. Other parameters were set as per the manufacturer's instructions (Walz 2003). For F_v/F_m and NPQ measurements, 3 ml of algal samples were dark adapted for 15 min. Photosynthetic measurements were then performed using the PhytoPAM II with a measuring light intensity of 2 µmol photons m^{-2} s^{-1}, which was followed by a saturation pulse (SP) that had an intensity of 8,000 µmol photons m^{-2} s^{-1} and width of 350 ms. The minimum fluorescence (F_0) in the measuring light and maximum fluorescence (F_m) from the saturating pulse were determined, allowing calculation of the variable fluorescence following dark adaptation (F_v) and maximum photosynthetic yield (F_v/F_m) using eq. 3.9 and eq. 3.10, respectively. Subsequently, actinic light (AL) of 480 µmol photons m^{-2} s^{-1} was switched on after the first SP and SPs then delivered at intervals of 20 s until steady values for light-adapted maximum fluorescence (F_m') were attained. The NPQ values were computed using the 'Stern–Volmer' formula, eq. 3.11. For $rETR_{max}$ and alpha estimation, the RLCs were constructed using the built-in PhytoWin software by applying incremental actinic illumination (16–610 µmol photons m^{-2} s^{-1}) in twenty steps, with each intensity applied for 20 s. The derived parameters alpha was computed by the in-built PAM, PhytoWin, software which uses the model reported by (Peeters and Eilers 1978) to fit the RLC using relative rate of electron transport (rETR) values calculated by eq. 3.12 (Figueroa et al. 2003, Johnsen and Sakshaug 2007) in which Y(II) is effective quantum yield of photosystem II and E_{PAR} is irradiance intensity. All the assays were performed with three replicate experiments, each involving three technical replicates.

$$F_v = (F_m - F_0) \tag{3.9}$$

$$F_v/F_m = F_m - F_O/F_m \tag{3.10}$$

$$NPQ = (F_m/F_{m'}) - 1 \tag{3.11}$$

$$\text{rETR} = \text{Y(II)} * E_{PAR} \tag{3.12}$$

3.2.3 Single-cell chlorophyll *a* fluorescence measurement

To investigate grazing-mediated effects on NPQ levels at the single cell level, starved cells of *O. marina* were fed on *D. tertiolecta* to establish the grazing culture that was compared with the control, containing *D. tertiolecta* cells only. Chlorophyll *a* fluorescence measurement were made daily using a Walz microscopy-PAM on a) the control that is *D. tertiolecta* cells alone; b) prey cells that were ingested inside the predator and c) prey cells outside the predator (uneaten prey cells in grazed cultures). For F_v/F_m and NPQ determination, 10 µl sample aliquots from control and grazing cultures were mounted on poly L-lysine-coated slides (Thermoscientific-Menzel-Glaser, Germany) for 10-15 min dark acclimatisation. Single-cell photosynthetic measurements were performed with a PAM-CONTROL unit using a Hundwetzlar (Germany) fluorescence microscope under a 15x objective lens. Measuring light (ML) of 2 µmol photons m^{-2} s^{-1} followed by a 0.8 s long SP of 8,000 µmol photons m^{-2} s^{-1} intensity was applied to a sample. Actinic light (AL) of 570 µmol photons m^{-2} s^{-1} was switched on for 8 min and, in the presence of AL, repeated SPs were given with an interval of 20 s. NPQ was calculated using eq. 3.11, once F_m' values had stabilized. A prior optimisation was done to determine the ideal incubation time (20 min) for cells to adhere to poly L-lysine-coated slides and emit a signal between 300–3500 fluorescence intensity. A longer incubation time affected the cell viability and hence yielded poor fluorescence values below 300 units. Higher signals, above 3500 units, were non-linear and overestimated photosynthetic parameters. Artefactual light effects and the background signal in the absence of cells were corrected by the F-offset function using the poly L-lysine slide alone. The current of the photomultiplier detector and photomultiplier gain were kept minimal to improve signal-to-noise ratio and ensure no ambient light contributed to the signal. At every saturation pulse, the fluorescence-induction kinetics was observed for the fluorescence rise and stable plateau formation. All the other settings were set as per the instruction manual (Walz 2000).

3.2.4 Effect of prey-cell concentration on NPQ levels

Grazing cultures were established using different prey, *D. tertiolecta* and predator, *O. marina*, concentrations to fall into the categories of high-level infestation 1:1, moderate level 100:1, low level 1000:1 and very low-level infestation 10000:1. A further grazing experiment was setup, in which additional prey cells were added to grazing cultures on day 2 (pulse-prey treatment). The NPQ profiles of the grazing cultures along with the control flasks were monitored daily until complete removal of prey cells was observed.

3.2.5 Effect of elevated growth light and low salinity on NPQ profiles under the influence of *O. marina* grazing

Conditions such as elevated light for growth (150 µmol photons m^{-2} s^{-1}) and low salinity (16.5 practical salinity units, PSU) were assessed for their effect on the NPQ profiles to determine if suboptimal growth conditions affected the responses of NPQ to grazing. The elevated light intensity was chosen as a supra-saturating intensity based on a rapid-light curves (RLC). The NPQ levels were recorded daily as described above until the culture crash occurred. Light intensity and salinity were monitored using a light sensor (LI-210R, LI-COR) and salinity refractometer (Ade advance optics), respectively.

3.2.6 Effect of *Euplotes* sp. grazing on NPQ profiles of prey cells

To validate that altering NPQ levels were due to grazing pressure, a different species of predator, *Euplotes* sp., was fed on *D. tertiolecta* cells. The NPQ levels and ingestion rates were estimated at intervals of 24 h using the techniques outlined above.

3.2.7 Statistical analysis

The statistical significance of the difference between the control and the grazer-infested group across different time-points was analysed using GraphPad software 7.02 (GraphPad Software Inc, CA, USA) for carrying out an unpaired two-sample t-test. The level of statistical significance for all the analyses was $P < 0.05$.

3.3 Results

3.3.1 Prey and predator numbers

In the 'crash' experiments, *O. marina* grazed at an average rate of ~9.47 x 10^{11} prey cells $predator^{-1}$ d^{-1}, and 92 % ($P < 0.0001$) prey depletion (Figure 3.1a) was observed by day 2. From the third day onwards, the population of *O. marina* significantly ($P < 0.0001$) exceeded the concentration of prey cells, which resulted in a culture crash, and prey cells were completely cleared on day 4.

The ingestion rate of *O. marina* increased across three days but halted after the crash. *Euplotes* sp. grazed at a rate of ~1.76 x 10^{14} prey cells $predator^{-1}$ d^{-1} and on day 2 ($P = 0.035$) 57 % prey depletion was observed (Figure 3.1b). The maximum clearance, 94 %, was observed on day 3 ($P < 0.0001$) leading to a culture crash. The ingestion ability of *O. marina* (Figure

3.2c) and *Euplotes* sp. (Figure 3.1d) peaked on the third day and halted thereafter (Figures 3.2a and b). Henceforth, day 3 will be referred to as a crash day.

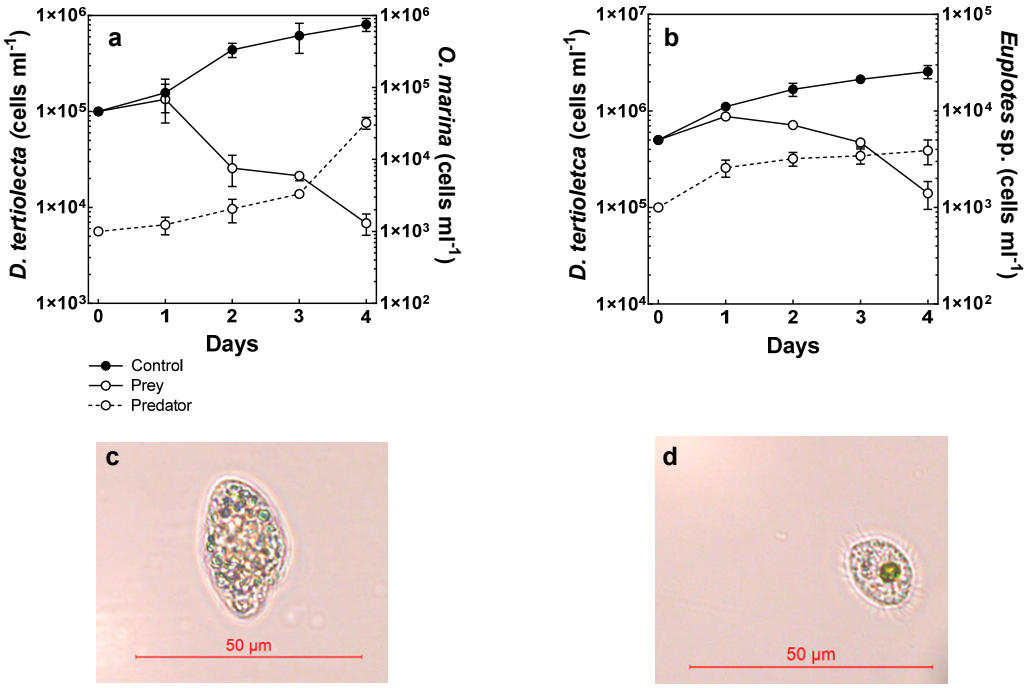

Figure 3.1 Change in prey, *D. tertiolecta*, concentration upon a, c) *O. marina* and b, d) *Euplotes* sp. infestation as a function of time. 'Control' is prey cell concentration alone, 'prey' and 'predator' indicate respective cell concentration in mixed culture. Data represent means ± SD, n = 3

3.3.2 Chlorophyll *a* fluorescence measurements

The NPQ profiles were found to be strongly affected in predated cultures. As shown in Figure 3.2a, algal cultures infested with *O. marina* showed a statistically significant ~55 and 74 % reduction ($P < 0.0001$) in NPQ on days 1 and 2, respectively. Additionally, a significant increase in the rate of *O. marina* ingestion was observed over this time. The NPQ levels continued to decline moderately after day 2 in comparison to the initial time points until the culture crash occurred. Similar to grazing by *O. marina*, reductions of ~35 and 60 % in NPQ levels in *Euplotes*-infested cultures were observed on days 1 and 2, respectively (Figure 3.2b).

From day 1 to 3, a moderate negative correlation between the ingestion rate and the NPQ levels were found in the grazing cultures of both (Figures 3.2c and d) *O. marina* (R^2 = 0.955) and *Euplotes* sp. (R^2 = 0.713). *O. marina*-mediated grazing did not alter the F_v/F_m (Figure 3.3a) of *D. tertiolecta* cells across all time points. An increasing $rETR_{max}$ was observed

in the grazing group in which an increment (P = 0.0011) of 50 % was seen on day 3. In contrast, alpha, the initial slope of the rapid light curve, was reduced by 20 % (P < 0.0001) and 11 % (P = 0.0009) on days 2 and 3 (Figure 3.3b).

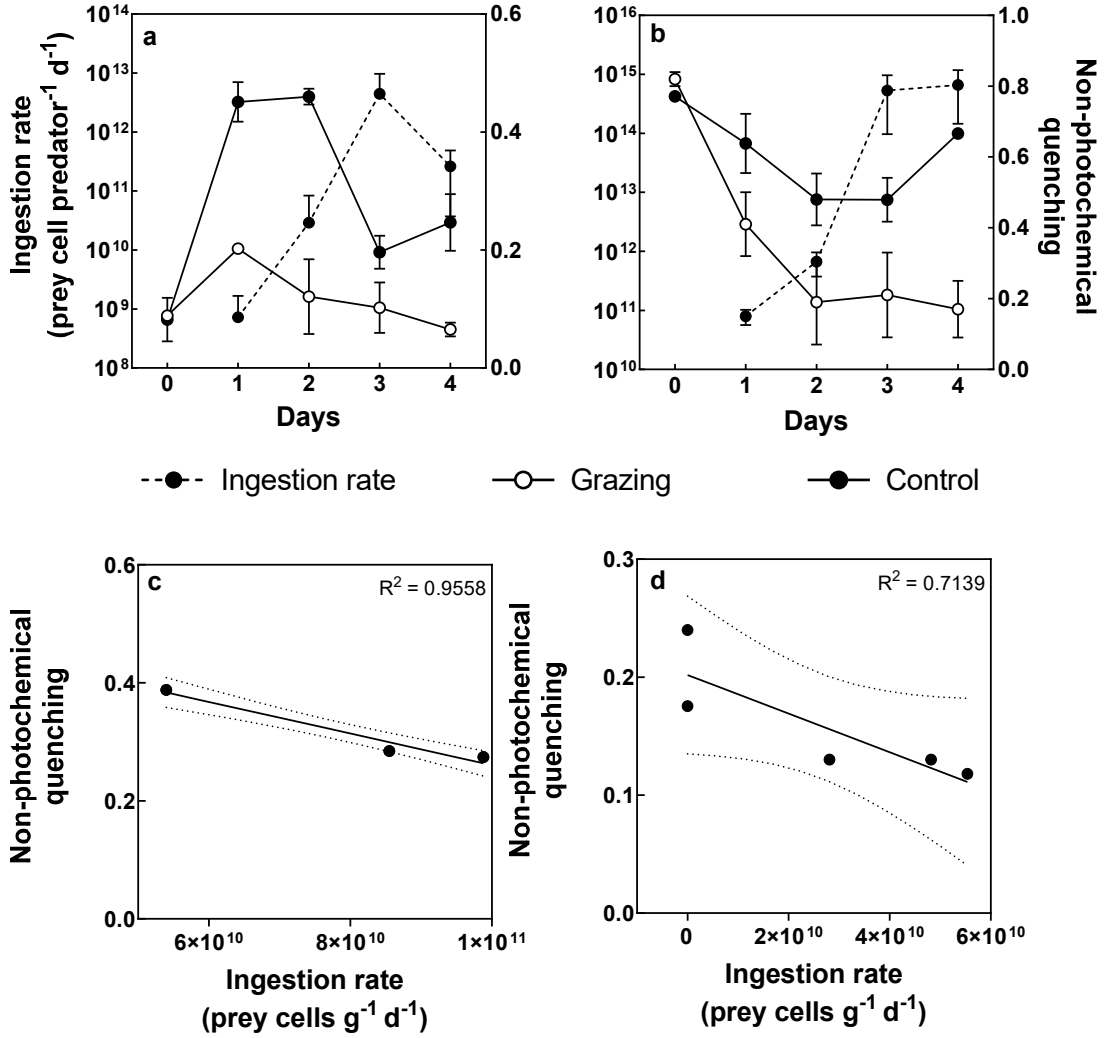

Figure 3.2 Effect of predator ingestion a, c) *O. marina* and b, d) *Euplotes* sp. and its correlation with non-photochemical quenching levels of *D. tertiolecta* cells. 'Control' is prey cell concentration alone, 'Grazing' indicates prey and predator in mixed culture. Solid black lines and dotted lines indicates line fit and 95 % confidence interval limits, respectively. Data represent means ± SD, n = 3

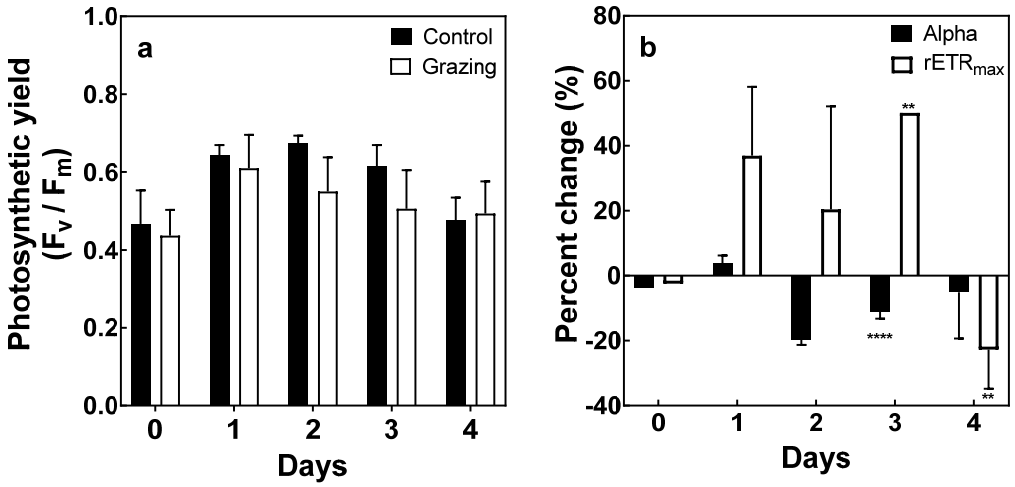

Figure 3.3 *O. marina*-mediated changes in a) maximum photosynthetic yield and b) light harvesting efficiency alpha, relative electron transport maximum ($rETR_{max}$) of *D. tertiolecta* cells as a function of time in control and grazing cultures. Level of significance 0.05, P values are ≤ **0.0021, ****0.0001. Data represent means ± SD, n = 3

3.3.3 Single-cell chlorophyll a fluorescence measurement

In Figure 3.4a, no significant difference was observed in NPQ levels of control and prey cells (outside predator) until day 1. However, prey cells engulfed by predators showed significantly lower (P = 0.0002) NPQ levels. From the second day onwards, un-engulfed prey cells, that remain outside the predators, showed a decline of 54 % in NPQ levels (P = 0.0446) in comparison to control cells, whereas, prey cells inside predator cells showed 84 % NPQ reduction (P = 0.0004). The trend of declining NPQ was further observed in both uneaten prey (outside predator) and engulfed prey (inside predator) cells until the culture crash. No significant differences (Figure 3.4b) in F_v/F_m levels were found between control and prey cells (outside predator) until the prey cells were completely cleared in the grazing culture on day 3; whereas F_v/F_m levels of prey cells (inside predator) were consistently low after day 0.

3.3.4 Effect of prey-cell concentration on NPQ levels

The culture that was highly infested (1:1) crashed on day 2 (Figure 3.5) and showed 69 % lower NPQ levels (P = 0.0001) in comparison to the control, 24 h prior to the crash. The moderately infested culture (100:1) showed a 52 % (P = 0.0004) to 72 % (P < 0.0001) decline in NPQ levels from day 1 onwards, and complete prey cell displacement occurred on day 3. In low grazer density (1000:1) cultures, a reduction of 56 % (P = 0.0025) in NPQ levels was

observed on day 2, with a delayed culture crash on day 4. Cultures with very low grazer (10000:1) infestation crashed on day 5 and showed a declining NPQ trend ~43 % (P = 0.0194) from day 3 onwards (Table 3.1). Overall, reductions in the NPQ levels were observed in all grazer-infested groups at least 24–48 h, prior to the crash.

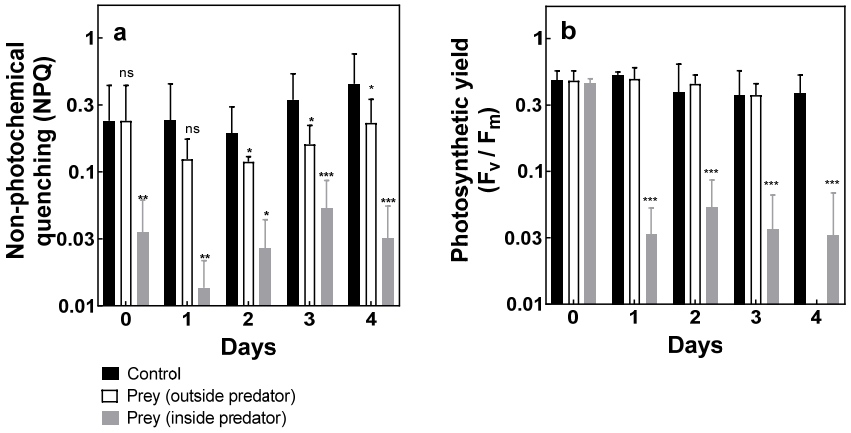

Figure 3.4 a) Non-photochemical quenching and b) maximum photosynthetic yield of single prey, *D. tertiolecta*, cell under grazing pressure of *O. marina*. 'Control' is prey cells alone, Prey (inside predator) is cell ingested by predator and prey (outside predator) is uneaten prey cells in grazing culture. Level of significance 0.05, P values are ≤ ^{ns}0.1234, *0.0332, **0.0021, ***0.0002. Data represent means ± SD, n = 10

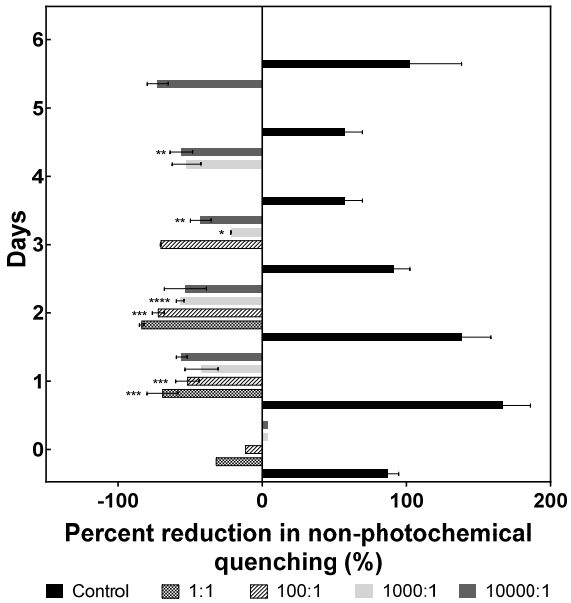

Figure 3.5 Crash predictive potential of non-photochemical quenching (NPQ) levels under increasing prey-cell concentrations. Prey-predator cell concentration ratios are high level 1:1, moderate level 100:1, low level 1000:1, and very low level 10000:1. Level of significance 0.05. P values are ≤ *0.0332, **0.0021, ***0.0002. Data represent means ± SD, n = 3

Table 3.1 Percent reduction in non-photochemical quenching (NPQ) levels of *D. tertiolecta* 24 and 48 h before the crash in grazing cultures with increasing prey cell concentrations. Prey-predator cell concentration ratios resulting in infection level high 1:1, moderate 100:1, low 1000:1, and very low 10000:1.

	Percent reduction in NPQ profiles (%)	
Level of infection	**48 h**	**24 h**
1: 1	0	69
100: 1	52	72
1000: 1	56	43
10000: 1	43	56

In a 'prey-pulsing experiment' (Figure 3.6), additional prey cells were provided on day 2, which resulted in an increased ($P = 0.0017$) prey population and 69 % increase ($P = 0.0073$) in NPQ levels in prey cells in the pulsed group in-comparison to the non-prey-pulsed group on day 3. However, a declining NPQ trend was observed in the pulsed group after day 3 until the crash, which was similar to the non-pulsed group. Overall, from day 2 onwards, NPQ levels of both the pulsed and the non-pulsed group were significantly ($P < 0.0001$) lower than those of the control group.

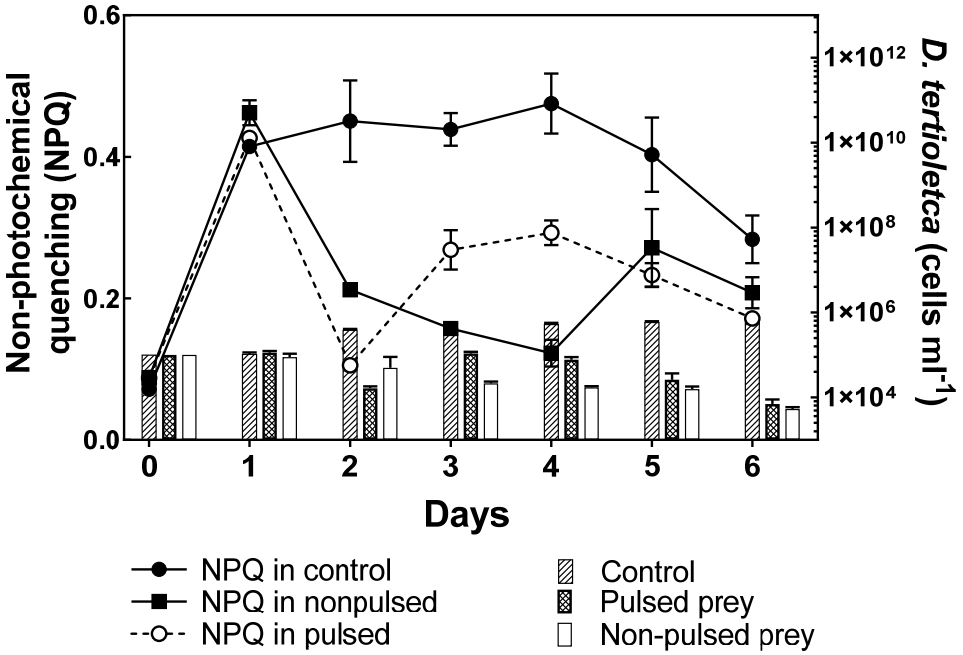

Figure 3.6 Crash predictive potential of non-photochemical quenching (NPQ) levels under prey-pulsed (additional prey added after day 2) and non-pulsed conditions. Data represent means ± SD, n = 3

3.3.5 Effect of elevated growth light and low salinity on NPQ profiles under the influence of *O. marina* grazing

On day 0, NPQ levels in both elevated growth light level (150 µmol photons m^{-2} s^{-1}) and low salinity (16.5 PSU) were higher as compared to other days. On day 2, the grazing group showed a significant reduction in both conditions. The elevated light (Figure 3.7a) and low salinity (Figure 3.7a) resulted in a decline of 47 % (P = 0.0057) and 40 % (P = 0.0266), respectively, in the NPQ levels. The culture crash in both the groups occurred on day 3, with declining NPQ profiles from day 1 until the day of the crash. The growth rate of *D. tertiolecta* cells in control group were found to be low in both elevated light and low salinity conditions as compared to under optimal growth conditions (Table 3.2).

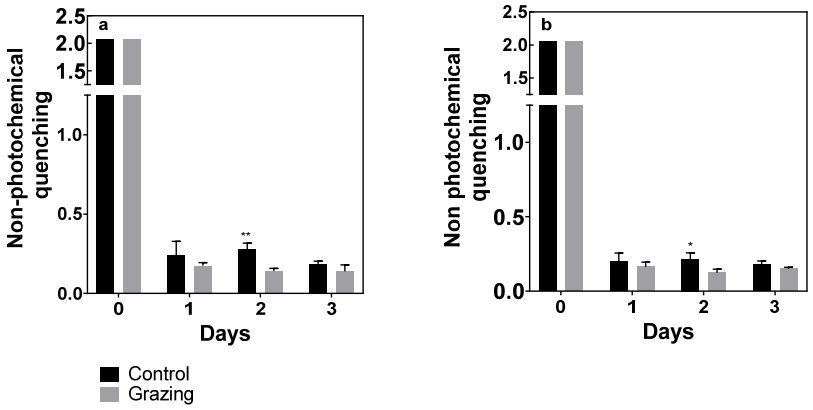

Figure 3.7 The combined effect of grazing and a) elevated light, b) low salinity on non-photochemical quenching levels of *D. tertiolecta* in control and grazing cultures. Level of significance 0.05, P values are ≤ *0.0332, **0.0021. Data represent means ± SD, n = 3

Table 3.2 *D. tertiolecta* growth rate (µ d^{-1}) under (a) optimal conditions (OC) - 30 µmole photons m^{-2} s^{-1} and 32 PSU salinity (b) elevated light (EL) - 150 µmole photons m^{-2} s^{-1} and (c) low salinity (LS) - 30 µmole photons m^{-2} s^{-1} and 16.5 PSU salinity. Control group indicates only *D. tertiolecta* cells and grazing indicates *O. marina* infested *D. tertiolecta* culture. Crash indicates total displacement of *D. tertiolecta* cells in grazing culture. Numbers indicate mean value ± SD, n = 3

	Day 0		Day 1		Day 2		Day 3	
	Control	Grazing	Control	Grazing	Control	Grazing	Control	Grazing
OC	0	0	0.7±0.1	0.05±0.2	0.89±0.08	0.2±0.3	0.8±0.1	-2.3±0.6
EL	0	0	0.6±0.4	-0.7±0.1	0.45±0.3	-4.9±0.2	0.4±0.1	Crash
LS	0	0	0.4±0.2	-0.37±0.09	0.2±0.1	-6.1±0.3	0.2±0.05	Crash

3.4 Discussion

Algal predation is a process of sequential prey capture, processing and digestion that manifests in the degradation of the algal pigments and in the storage of digested products in food vacuoles. Upon predation, the algal prey cells also undergo cellular and metabolic responses. For instance, both prey capture and predation-specific stimuli alter the photosynthetic pigment content of prey (Feinstein et al. 2002). In this study, we investigated possible photosynthetic alterations in *D. tertiolecta* cultures under grazing pressure which can provide insights into potential predator outbreaks so that preventative measures can be deployed.

Photosynthetic parameters such as F_v/F_m, $rETR_{max}$ and NPQ are measured in order to monitor the overall physiological state of algal cultures. F_v/F_m is a measure of the maximum quantum yield of photosystem II, which reflects the ability to perform photochemistry. The maximum photosynthetic yield has been reported to be negatively affected due to presence of 'weed' (contaminating) algae (Winckelmann et al. 2015). However, in the present study, no significant alterations were observed in F_v/F_m under grazing pressure (Figure 3.3a), which correlates with the experiments on grazing of diatom and cyanobacterial cultures reported by Ratti et al. (2013). This can occur due to the relatively higher proportion of healthy and ungrazed prey cells at initial time points in the PAM measurement of the bulk sample. The low photosynthetic yield after day 3 in the control and grazing cultures may be attributed to decreased photosynthetic function during the late log and stationary phases mostly due to nutrient exhaustion (Fogg 1957) as experiments were operated in a batch mode. Similarly, (Young and Beardall 2003) reported a drop in F_v/F_m values in *Dunaliella tertiolecta* culture under nitrogen depletion and recovery on restoration of nitrogen replete conditions. However, potential of F_v/F_m as an indicator of stress is debatable (Kruskopf and Flynn 2006). $rETR_{max}$ is a measure of the capacity for electron transport rate between reaction centre and electron carriers of PSII; it is reported to be negatively affected under abiotic stress conditions such as nutrient depletion (Malapascua et al. 2014, Zhao et al. 2017) and other factors such as salinity stress (Karthikaichamy et al. 2018). In contrast, exposure of *D. tertiolecta* cells to biotic stress caused by *O. marina* grazing resulted in an overall increase in $rETR_{max}$ levels from day 1 until the culture crash on day 3 although alpha, that is, the light-harvesting efficiency, was reduced in the *O. marina*-infested culture in comparison to the control (Figure 3.3.b). Another photosynthetic parameter, reflecting the photo-protective ability of an algal cell, is NPQ. Hence, it is an important measurement for monitoring the state of accessory pigments and stress

responses of algae. Under the grazing pressure from *O. marina* and *Euplotes* sp., NPQ levels dropped compared to the control culture (Figures 3.2a and b). A sequential NPQ reduction was observed from day 1 to day 3 as the predator population increased exponentially with a reduction in the prey concentration. Similarly, an alteration of the NPQ levels was reported in grazed cultures of a diatom and cyanobacterium as a function of seawater chemistry, in which Euplotes sp.-mediated grazing reduced NPQ levels in *Tetraselmis suecica* and increased NPQ in *Synechococcus* sp. cultures (Winckelmann et al. 2015). A negative correlation between the light-harvesting efficiency and $rETR_{max}$ levels coupled with increasing NPQ levels is reported in various algal strains upon exposure to various abiotic stress conditions (Nitschke et al. 2012, Serodio et al. 2006). The exposure to biotic stress such as algal grazing in this study shows a similar negative correlation between the light-harvesting efficiency and $rETR_{max}$, but in contrast to previous studies (Nitschke et al. 2012, Serodio et al. 2006), NPQ levels were instead significantly reduced.

In addition to NPQ levels, the ETR/NPQ ratio is reported to decrease in macroalgae with incremental exposure to UVB irradiance (Figueroa et al. 2014). In contrast, ETR/NPQ ratio significantly increased under grazing pressure from *O. marina*. Although this ratio can potentially indicate the presence of a predator in this study, currently deployed photosynthesis measurement devices do not capture the ratio in a relatively straightforward manner as compared to the 'Stern-Volmer' equation-based NPQ calculation. This underlines the need for further investigation of changes in the ETR/NPQ ratio in a variety of algal prey-predator combinations and possible improvements in the device algorithm for the estimation of the ETR/NPQ ratio (Deore et al. 2020b).

A decreased capacity to utilise electrons in carbon assimilation (manifest as a decreased $rETR_{max}$) is reported to activate NPQ, driven by proton (pH) gradient formation and xanthophyll cycle activation. An increased proton gradient across the thylakoid membrane leads to activation of an enzyme, violaxanthin de-epoxidase (VDX), which triggers conversion of violaxanthin to zeaxanthin. Zeaxanthin is reported to assist in disspiation of excess photos as heat, a process reflected in NPQ activation (Serodio et al. 2006, Genty et al. 1990). Increased alpha and $rETR_{max}$ brings NPQ relaxation as electrons are efficiently carried through the electron transport chain and utilised (Serodio et al. 2006). In contrast, the moderately reduced alpha, elevated $rETR_{max}$ and lower NPQ values in the grazing culture as compared to the control (Figures 3.2 and 3.3) may indicate possible alterations in proton gradient formation across the thylakoid membrane. A similar observation was made upon addition of proton gradient

uncouplers in algal cultures and isolated chloroplasts (Cao et al. 2013, Markou et al. 2016). This suggests the possibility of a similar effect being caused by the invasion of *O. marina* and *Euplotes* sp. However, experimental validation is required to deduce the exact cause of the NPQ decrease in the grazing cultures of *D. tertiolecta*. The observations of the present study however suggest that the monitoring of NPQ levels can provide an early indication of an outbreak of *O. marina* and *Euplotes* sp.

Single-cell microscopy PAM was deployed to investigate further the reduction in NPQ levels as an outcome of the grazing-specific response of prey cells. Both uneaten (outside predator) and grazed (inside predator) prey cells from the experimental grazing cultures showed significantly lower NPQ levels than the control (Figure 3.4). Interestingly, the NPQ levels of uneaten (outside predator) prey cells started to decline from day 2 and followed the same trend until the crash. This suggests that NPQ reduction can be a strong indicator of grazing of *D. tertiolecta* cells and that the declining trend is related to the exponential increase of the population of *O. marina*. Microalgal prey cells are reported to exert metabolic responses against grazing stimuli (Amato et al. 2018) and the trend of declining NPQ in *D. tertiolecta* cells outside the predator may indicate a similar possibility of predator-mediated secretion of extracellular cues which may directly or indirectly alter NPQ levels. Our preliminary hypothesis is that ammonia excreted by grazers (Dolan 1997) may act as a photosynthetic uncoupler (Crofts 1967), thereby reducing NPQ levels (see chapter 4). The predator, *O. marina* is heterotrophic and non-photosynthetic in nature and therefore fails to show chlorophyll *a* fluorescence (Slamovits and Keeling 2008). Therefore, the possibility of NPQ reduction due to the mere presence of grazers in a prey culture can be overruled. On day 0, predator cells are starved or have limited prey cells consumed, therefore NPQ levels were low. Although freshly consumed prey cells continue to emit chlorophyll fluorescence, degradation of pigments due to digestion of prey inside the predator (Feinstein et al. 2002) can reduce the chlorophyll *a* fluorescence response. Pigment or prey degradation inside the predator is reflected in reduced F_v/F_m values from day 1 and continued to drop until the culture crash.

Currently practiced grazer monitoring methods such as microscopy and continuous flow-cytometry fail to detect very low predator concentrations; such methods, moreover, are not deployed on-site (Day et al. 2012). Cultures with different prey and predator intensities crash on different days, which could be due to the severity of the *O. marina* infestation (Figure 3.5). The very high (1:1) predator concentration, which is caused by the higher grazing rate that results in a crash on day 2, can be traced to 69 % reduction in NPQ 24 h prior to the crash.

Similarly, moderate (100:1), low (1000:1), and very low (10000:1) levels of infestation show 72 %, 43% and 56 % reduction in NPQ levels, respectively, 24 h prior to the crash (Table 3.1). Experiments with different prey-predator intensities indicate that relative reduction in the NPQ level can be detected 24–48 h prior to the crash for as low as 10^4 grazer cells ml^{-1} of algae culture.

NPQ levels have been found to be elevated in algal strains due to various abiotic stress conditions (Harker et al. 1999, Serodio et al. 2006). Chapter 3 reports decreased NPQ levels under biotic stresses such as predator invasion in *D. tertiolecta* cultures (Figure 3.7). In outdoor mass cultures, both biotic and abiotic stresses are inevitable and NPQ levels can be modulated under cumulative stress conditions. Under elevated growth light exposure conditions, NPQ levels increase by ~10 fold on day 0 in both control and grazing cultures. This reflects the activation of the NPQ mechanism as a part of the protective response. Further, this NPQ elevation relaxes from day 1 onwards. Similar NPQ relaxation after stress exposure has been reported in a study that describes the manner in which *D. tertiolecta* operates with multiple photo-protective mechanisms (Segovia et al. 2015, Ihnken et al. 2011). The reduction in NPQ levels in the grazing culture under abiotic stress conditions is consistent with the observations from the grazing experiments alone.

This chapter demonstrates a consistent reduction of NPQ levels in the *D. tertiolecta* culture in both bulk and single-cell PAM measurements 24–48 h prior to the culture crash following introduction of predators (Figures 3.2 and 3.4). At the large-scale microalgae cultivation platform various environmental conditions exist which can induce changes in photosynthetic parameters such as NPQ. As a result, grazer-induced changes in NPQ profiles of the prey cells may go unnoticed due to the dynamic nature of the photosynthetic process. Therefore, development of an array of potential diagnostic measures in addition to NPQ profiling could provide a more accurate indication of grazing. Other energy dissipation measures of photosynthesis are regulated (YNPQ) and passive (YNO) heat loss that are demonstrated to be affected under stress in addition to NPQ levels (Blain and Shears 2019). Similarly, the effects of biotic stress on YNPQ and YNO can be investigated and further explored as potential photosynthesis-based tools for investigating algal predation. An integrated approach of NPQ assessment along with traditional microscopy and molecular methods would enable the deployment of preventive strategies to avoid biomass loss in mass cultures. Different algal species have different acclimation potential and can respond to stress

conditions differently (Segovia et al. 2015). Therefore, the development of NPQ as an indicator of grazing requires systematic testing across different prey and predator species.

3.5 Conclusion

The results in this chapter suggest the possibility of detection of grazer invasion based on the photosynthetic signature, NPQ, which can be recorded in combination with currently used grazer detection methods. Online and real-time monitoring of the photosynthetic signature would be an ideal approach to monitor contamination at large-scale microalgal cultivation platforms. Currently, only a few handheld devices, such as AquaPen, FluroPen, etc., are available to record photosynthetic measurements including NPQ. However, to obtain real-time data with high quality temporal resolution requires better guided sensors, probes and software integration. There is a possibility to leverage image- and remote sensing-based chlorophyll *a* fluorescence measurement that can reflect NPQ levels of cultures in real-time. The decline in NPQ levels of algal prey under grazing pressure also indicates the possible underlying changes at cellular level. The potential role of ammonia as a driver for the observed changes in NPQ in grazing cultures is investigated further in the chapter 4.

References

Amato A, V Sabatino, GM Nylund, J Bergkvist, S Basu, MX Andersson, R Sanges, A Godhe, T Kiørboe, and E Selander. 2018. "Grazer-induced transcriptomic and metabolomic response of the chain-forming diatom *Skeletonema marinoi*." *The ISME Journal* 12 (6):1594.

Blain CO, and NT Shears. 2019. "Seasonal and spatial variation in photosynthetic response of the kelp *Ecklonia radiata* across a turbidity gradient." *Photosynthesis Research* 140 (1):21-38.

Cao S, X Zhang, D Xu, X Fan, S Mou, Y Wang, N Ye, and W Wang. 2013. "A transthylakoid proton gradient and inhibitors induce a non-photochemical fluorescence quenching in unicellular algae *Nannochloropsis* sp." *FEBS Letters* 587 (9):1310-1315.

Crofts AR. 1967. "Amine uncoupling of energy transfer in chloroplasts I. Relation to ammonium ion uptake." *Journal of Biological Chemistry* 242 (14):3352-3359.

Day JG, Y Gong, and Q Hu. 2017. "Microzooplanktonic grazers – A potentially devastating threat to the commercial success of microalgal mass culture." *Algal Research* 27:356-365. doi: https://doi.org/10.1016/j.algal.2017.08.024.

Day JG, NJ Thomas, UE Achilles-Day, and RJ Leakey. 2012. "Early detection of protozoan grazers in algal biofuel cultures." *Bioresource Technology* 114:715-719.

Demory D, C Combe, P Hartmann, A Talec, E Pruvost, R Hamouda, F Souillé, P Lamare, M Bristeau, and J Sainte-Marie. 2018. "How do microalgae perceive light in a high-rate pond? Towards more realistic Lagrangian experiments." *Royal Society Open Science* 5 (5):180523.

Deore P, A Karthikaichamy, J Beardall, and S Noronha. 2020. "Non-photochemical quenching, a non-invasive probe for monitoring microalgal grazing: an early indicator of predation by *Oxyrrhis marina* and *Euplotes* sp." *Applied Phycology* 1 (1):20-31.

Dolan JR. 1997. "Phosphorus and ammonia excretion by planktonic protists." *Marine Geology* 139 (1):109-122.

Eggert A, S Raimund, D Michalik, J West, and U Karsten. 2007. "Ecophysiological performance of the primitive red alga *Dixoniella grisea* (Rhodellophyceae) to irradiance, temperature and salinity stress: growth responses and the osmotic role of mannitol." *Phycologia* 46 (1):22-28.

Feinstein TN, R Traslavina, M Sun, and S Lin. 2002. "Effects of light on photosynthesis, grazing, and population dynamics of the heterotrophic dinoflagellate *Pfiesteria piscicida* (Dinophyceae)." *Journal of Phycology* 38 (4):659-669.

Figueroa FL, R Conde-Alvarez, and I Gómez. 2003. "Relations between electron transport rates determined by pulse amplitude modulated chlorophyll fluorescence and oxygen evolution in macroalgae under different light conditions." *Photosynthesis Research* 75 (3):259-275.

Figueroa FL, B Domínguez-González, and N Korbee. 2014. "Vulnerability and acclimation to increased UVB radiation in three intertidal macroalgae of different morpho-functional groups." *Marine Environmental Research* 97:30-38.

Fogg GE. 1957. "Relationships between metabolism and growth in plankton algae." *Journal of General Microbiology* 16 (1):294-297.

Fundel B, H Stich, H Schmid, and G Maier. 1998. "Can phaeopigments be used as markers for Daphnia grazing in Lake Constance?" *Journal of Plankton Research* 20 (8):1449-1462.

Genty B, J Harbinson, J Briantais, and NR Baker. 1990. "The relationship between non-photochemical quenching of chlorophyll fluorescence and the rate of photosystem 2 photochemistry in leaves." *Photosynthesis Research* 25 (3):249-257.

Harker M, C Berkaloff, Y Lemoine, G Britton, A Young, J Duval, N Rmiki, and B Rousseau. 1999. "Effects of high light and desiccation on the operation of the xanthophyll cycle in two marine brown algae." *European Journal of Phycology* 34 (1):35-42.

Ihnken S, JC Kromkamp, and J Beardall. 2011. "Photoacclimation in *Dunaliella tertiolecta* reveals a unique NPQ pattern upon exposure to irradiance." *Photosynthesis Research* 110 (2):123-137.

Jeong HJ, SK Kim, JS Kim, ST Kim, YD Yoo, and JY Yoon. 2001. "Growth and grazing rates of the heterotrophic dinoflagellate *Polykrikos kofoidii* on red-tide and toxic dinoflagellates." *Journal of Eukaryotic Microbiology* 48 (3):298-308. doi: doi:10.1111/j.1550-7408.2001.tb00318.x.

Johnsen G, and E Sakshaug. 2007. "Biooptical characteristics of PSII and PSI in 33 species (13 pigment groups) of marine phytoplankton, and the relevance for pulse-amplitude-modulated and fast-repetition-rate fluorometry 1." *Journal of Phycology* 43 (6):1236-1251.

Kalaji HM, G Schansker, M Brestic, F Bussotti, A Calatayud, L Ferroni, V Goltsev, L Guidi, A Jajoo, and P Li. 2017. "Frequently asked questions about chlorophyll fluorescence, the sequel." *Photosynthesis Research* 132 (1):13-66.

Karthikaichamy A, P Deore, S Srivastava, R Coppel, D Bulach, J Beardall, and S Noronha. 2018. "Temporal acclimation of *Microchloropsis gaditana* CCMP526 in responce to hypersalinity." *Bioresource Technology* 254:23-30.

Kok B. 1956. "On the inhibition of photosynthesis by intense light." *Biochimica et Biophysica Acta* 21 (2):234-244.

Kruskopf M, and KJ Flynn. 2006. "Chlorophyll content and fluorescence responses cannot be used to gauge reliably phytoplankton biomass, nutrient status or growth rate." *New Phytologist* 169 (3):525-536.

Malapascua JR, CG Jerez, M Sergejevová, FL Figueroa, and J Masojídek. 2014. "Photosynthesis monitoring to optimize growth of microalgal mass cultures: application of chlorophyll fluorescence techniques." *Aquatic Biology* 22:123-140.

Markou G, O Depraetere, and K Muylaert. 2016. "Effect of ammonia on the photosynthetic activity of *Arthrospira* and *Chlorella*: a study on chlorophyll fluorescence and electron transport." *Algal Research* 16:449-457.

Müller P, X Li, and KK Niyogi. 2001. "Non-photochemical quenching. A response to excess light energy." *Plant Physiology* 125 (4):1558-1566.

Nitschke U, S Connan, and DB Stengel. 2012. "Chlorophyll a fluorescence responses of temperate Phaeophyceae under submersion and emersion regimes: a comparison of rapid and steady-state light curves." *Photosynthesis Research* 114 (1):29-42. doi: 10.1007/s11120-012-9776-z.

Peeters JCH, and P Eilers. 1978. "The relationship between light intensity and photosynthesis—a simple mathematical model." *Hydrobiological Bulletin* 12 (2):134-136.

Ratti S, AH Knoll, and M Giordano. 2013. "Grazers and phytoplankton growth in the oceans: an experimental and evolutionary perspective." *PLoS One* 8 (10):e77349. doi: 10.1371/journal.pone.0077349.

Rubio FC, FG Camacho, JF Sevilla, Y Chisti, and EM Grima. 2003. "A mechanistic model of photosynthesis in microalgae." *Biotechnology and Bioengineering* 81 (4):459-473.

Segovia M, T Mata, A Palma, C García-Gómez, R Lorenzo, A Rivera, and FL Figueroa. 2015. "*Dunaliella tertiolecta* (Chlorophyta) avoids cell death under ultraviolet radiation by triggering alternative photoprotective mechanisms." *Photochemistry and Photobiology* 91 (6):1389-1402.

Serodio J, S Vieira, S Cruz, and H Coelho. 2006. "Rapid light-response curves of chlorophyll fluorescence in microalgae: relationship to steady-state light curves and non-photochemical quenching in benthic diatom-dominated assemblages." *Photosynthesis Research* 90 (1):29-43.

Shelly K, D Holland, and J Beardall. 2010. "Assessing nutrient status of microalgae using chlorophyll a fluorescence." In *Chlorophyll a fluorescence in aquatic sciences: Methods and applications*, edited by Prášil Ondřej and Borowitzka M.A., 223-235. Dordrecht: Springer.

Slamovits CH, and PJ Keeling. 2008. "Plastid-derived genes in the nonphotosynthetic alveolate *Oxyrrhis marina*." *Molecular biology and evolution* 25 (7):1297-1306.

Walz H. 2000. "WinControl window software for PAM fluorometers." *Users manual. Walz, H. BmbH Effeltrich*.

Walz H. 2003. "Phytoplankton Analyzer Phyto-PAM and Phyto-Win software V 1.45, System Components and Principles of Operation." *Ó Heinz Walz GmbH, Germany*:47-64.

Winckelmann D, F Bleeke, B Thomas, C Elle, and G Klöck. 2015. "Open pond cultures of indigenous algae grown on non-arable land in an arid desert using wastewater." *International Aquatic Research* 7 (3):221-233. doi: 10.1007/s40071-015-0107-9.

Young EB, and J Beardall. 2003. "Photosynthetic function in *Dunaliella tertiolecta* (Chlorophyta) during a nitrogen starvation and recovery cycle." *Journal of Phycology* 39 (5):897-905.

Zhao L, K Li, Q Wang, X Song, H Su, B Xie, X Zhang, F Huang, X Chen, B Zhou, and Y Zhang. 2017. "Nitrogen Starvation Impacts the Photosynthetic Performance of

Porphyridium cruentum as Revealed by Chlorophyll *a* Fluorescence." *Scientific Reports* 7 (1):8542. doi: 10.1038/s41598-017-08428-6.

Chapter 4

Oxyrrhis marina-mediated total ammonia-nitrogen as an early grazing marker and its implication for non-photochemical quenching levels of *Dunaliella tertiolecta*.

A reformatted version of this chapter is currently accepted in the journal *Applied Phycology* as: Deore, P, Beardall J and Noronha S. 2020. "Non-photochemical quenching, a non-invasive probe for monitoring microalgal grazing: influence of grazing-mediated total ammonia-nitrogen" (in press).

4.1 Introduction

Algal prey and predators co-exist in the pelagic food web: algae are primary producers and predators are consumers and such interactions result in nutrient recycling where the excretion products of consumers are an important source of nutrients to the producer. One such example is zooplankton-mediated nitrogen recycling in the form of ammonia-nitrogen (NH_3–N and NH_4^+–N), referred to henceforth as Total Ammonia Nitrogen (TAN). TAN affects biomass (Tam and Wong 1996), chemosensory mechanisms (Martel 2009) and photosynthetic processes of the microalgal prey (MacLachlan et al. 1994). The preferential uptake of ammonia over other forms of nitrogen sources by *Dunaliella* sp. (Dortch 1990) and its effect on photosynthesis, particularly NPQ, is extensively reported (Markou et al. 2016). The components and significance of NPQ formation is outlined in detail in chapter 2 (Section 2.5.1.2). Full activation of NPQ is inhibited in presence of free ammonia (NH_3) by affecting the water splitting reaction (Velthuys 1980) and sequestering H^+ ions, thereby disrupting proton gradient formation across the thylakoid membrane (Crofts 1967). As result, violaxanthin de-epoxidase activation and quenching complex formation in NPQ activation are compromised. Similarly, free ammonia as a result of grazer-mediated TAN dissociation can mediate photosynthetic uncoupling which may lead to the observed reduction in NPQ levels of *Dunaliella tertiolecta* (Chapter 3).

A clear link between grazing-mediated TAN and its consequential effect on NPQ levels of the microalgal prey has not yet been reported. In addition to the causal relationship, the estimation of ammonia-nitrogen released by the predator and NPQ levels as a function of time

in grazer infested cultures can be further leveraged to develop TAN as an early marker of grazing of *D. tertiolecta* mediated by *O. marina*. It is anticipated that significant levels of TAN must be accumulated prior to a quantifiable inhibition in NPQ formation as described in chapter 3. The current chapter aims to validate the crash-predictive potential of TAN, along with NPQ levels, as a marker of microalgal grazing. To our knowledge, this is the first demonstration that nitrogen recycling in the form of ammonia-nitrogen can alter NPQ levels and indicate the presence of a predator, in this case *Oxyrrhis marina*, in *Dunaliella tertiolecta* cultures.

4.2 Materials and Methods

4.2.1 Prey and Predator strain

The *Dunaliella tertiolecta* (CS-175) and *Oxyrrhis marina* strains were cultivated as described in chapter 3 (Section 3.2.1) The culture pH was monitored daily using a Jenway 3510 pH probe (HACH). Maximum specific growth rate for prey cells and predator population growth rate of predator were computed using formulae described in chapter 3. All experiments were terminated (as per the findings of chapter 3) on day 4 following the total disappearance of prey cells from the grazing flask.

4.2.2 Chlorophyll *a* fluorescence

Chlorophyll *a* fluorescence, measured using a Walz PhytoPAM II, was used to derive the photosynthetic parameters F_v/F_m, $rETR_{max}$, alpha and NPQ as described in chapters 2 and 3. To investigate the effects of ammonium chloride on NPQ levels, a healthy *D. tertiolecta* culture was treated with increasing concentrations of ammonium chloride, 0–50 mM, and incubated in the dark for 5 min prior to recording the chlorophyll *a* fluorescence response. All the mentioned parameters were computed using equations described in chapter 3. (Section 3.2.2)

Q_A re-oxidation kinetics were recorded using a PSI FL-3000 Fluorometer (Photon System Instruments, Drasov, Czech Republic). The total duration of the measurement was 60 s, and the actinic flash and measuring light voltages were set to 100 and 30 %, respectively. The actinic flash duration was adjusted to 30 µs. The decay kinetics were determined by fitting the raw fluorescence data to a three-phase exponential decay model. The decay model involves three phases: fast, medium and slow. Each phase reflects a redox state of Q_A, Q_B and plastoquinol (PQ). The fast phase reflects Q_A re-oxidation through Q_A to Q_B or Q_B^-. The middle phase is characterised by Q_A re-oxidation by PQ molecules. The slow phase is associated with

the reduction of the donar side of photosystem II (PSII) by Q_A (charge recombination). Experiments were independently performed three times and raw data from the three biological replicates (separate cultures) of each experiment were averaged. The half-life for each phase was computed according to eq. 4.1 using ExpDec3, the exponential function in OriginPro2016 software. Additionally, Q_A re-oxidation kinetics were measured with healthy *D. tertiolecta* cultures in the presence of 100 nM 3-(3,4–di-chlorophenol)-1,1-dimethylurea (DCMU) and ammonium chloride.

$$Y = A1 * \exp(-x/t_1) + A2 * \exp(-x/t_2) + \ A3 * \exp(-x/3) + \ Y^0 \quad (4.1)$$

where A is an amplitude, t is time (s) and x is decay constant

4.2.3 Effect of the predator-infested spent medium on NPQ levels of *D. tertiolecta*

A grazing culture of 500 ml in 1000 L transparent glass bottle inoculated using a prey-predator ratio of 1:1 was incubated until prey cells were totally cleared in 3-4 h. The control (predator-free) and grazing cultures were harvested and centrifuged at 4500 x g for 10 min. The supernatant, that is the spent medium, was harvested, replenished with fresh F/2 nutrients, then used for cultivation of *D. tertiolecta* cells only. The spent media was used to check the possibility that extracellular products of *O. marina* might affect NPQ levels of *D. tertiolecta*. The NPQ levels of *D. tertiolecta* in fresh F/2 media, predator-free spent medium and predator-infested spent medium were measured using the techniques outlined in section 3.2.2.

4.2.4 Estimation of reactive oxygen species (ROS)

ROS levels were estimated using the method described by Marxen et al. (2007). Briefly, 5 ml aliquots of culture samples were stained with 0.02 mM 2',7'-dichlorodihydrofluorescein diacetate (DCF-DA) dissolved in dimethyl sulfoxide (DMSO). Stained samples were incubated at room temperature (25^{o}C) for an hour, and fluorescence was recorded at 485 nm excitation and 530 nm emission using a Hitachi F7000 fluorescence spectrophotometer. Arbitrary fluorescence units indicating ROS levels were normalized to prey cell concentration and are expressed as ROS-induced fluorescence per cell.

4.2.5 Estimation of total ammonia-nitrogen (TAN) in grazing cultures

Over the course of the culture crash, TAN accumulation in the grazing culture was estimated using the method described by Strikland and Parsons (1972). Briefly, 10 ml aliquots of culture were centrifuged at 1500 x g for 10 min. To the supernatant, 2 mg of phenol prepared

in 95 % ethyl alcohol was added, followed by the addition of 50 mg of sodium nitroprusside. An oxidising reagent, consisting of 200 mg sodium citrate, 10 mg sodium hydroxide and 6.5 ml sodium hypochlorite (32 %) solution, was freshly prepared. Immediately after the addition of the sodium nitroprusside, 1 ml of the oxidising reagent was added. Samples were incubated at room temperature for an hour. Formation of a blue indo-phenol complex was recorded at a wavelength of 640 nm in a CARY50 Bio UV visible spectrophotometer. A standard curve was prepared using ammonium sulphate to estimate the total concentration of ammonia-nitrogen as described by Strikland and Parsons (1972).

4.2.6 Effect of nitrogen source on NPQ profiles of grazing culture

Grazing and control (healthy *D. tertiolecta*) cultures were established separately using nitrate, ammonium chloride or urea as the nitrogen source in F/2 seawater-based media. The NPQ levels were monitored in control and grazing flasks throughout the culture crash.

4.2.7 Statistical analysis

The statistical significance of the difference between the control and the grazer-infested group across time was analysed using GraphPad software 7.02 (GraphPad Software Inc, CA, USA) in order to perform an unpaired two-sample t-test. The level of statistical significance for all the analyses was $P < 0.05$. All experiments were performed independently three times with three independent biological replicates (discrete cultures) for each experiment.

4.3 Results

4.3.1 Prey and predator cell concentrations

The growth (cell concentration) of prey cells was reduced by grazing pressure, when compared to control cultures. Active *O. marina* grazing led to prey cell numbers being depleted by 14, 80, 94 and 96 % on days 1, 2, 3 and 4, respectively. The maximum clearance, 96 %, was observed on day 4 leading to a culture crash. Hence, day 4 is henceforth referred to as 'crash day' (Figure 4.1). The maximum specific growth rate of *D. tertiolecta* was 1.27 d^{-1} and -0.76 d^{-1} (for net growth rate) in control and grazing cultures, respectively, and the maximum specific growth rate of the predator was 1.72 d^{-1}. As the prey concentration was depleted by 96 % on day 4, predator population growth also ceased. *O. marina* grazed at an average rate of 8.84 x 10^{12} prey cells $predator^{-1}$ d^{-1}. As predators ingested more prey cells the pH of grazing culture dropped compared to the control (Figure 4.2).

4.3.2 Chlorophyll *a* fluorescence

A five-minute exposure of *D. tertiolecta* to different concentrations of ammonium chloride resulted in a significant reduction in NPQ levels. The minimum ammonium chloride

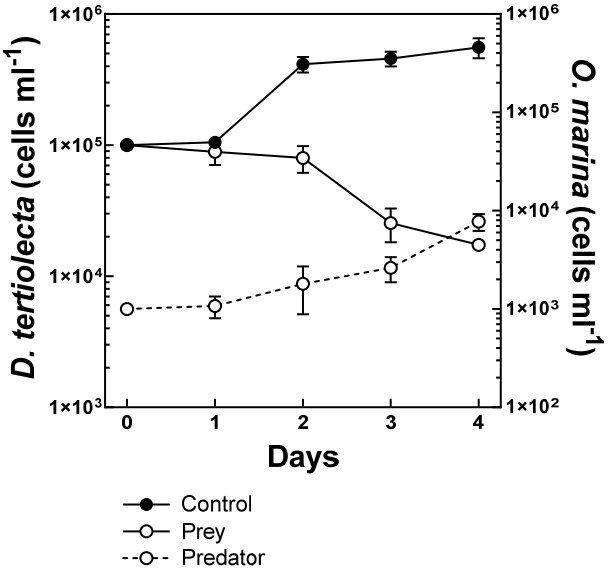

Figure 4.1 Prey and predator growth dynamics in grazing cultures of *Oxyrrhis marina*. "Control" is prey cell concentration alone, "prey" and "predator" indicate respective cell concentration in mixed culture. Data represent means ± SD, n = 9

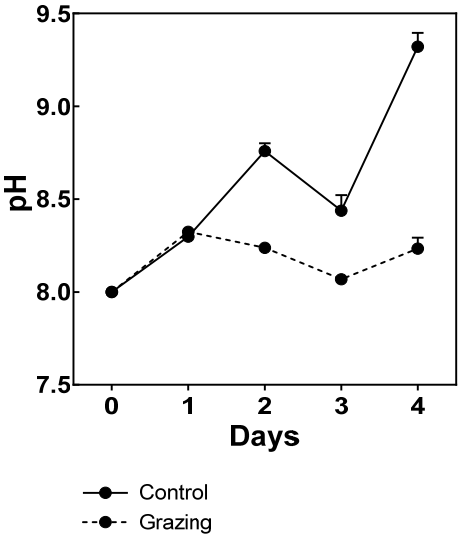

Figure 4.2 Effect of predator invasion on pH of control and grazing cultures as a function of time. Data represent means ± SD, n = 9

concentration required to create significant alterations to NPQ was found to be ~1 mM, which is theoretically equivalent to ~0.21 mM of free ammonia (NH_3) at pH 8.1, salinity 35 PSU, and

25°C. Greater NPQ inhibition was seen with increasing concentrations of ammonium chloride in the healthy culture of *D. tertiolecta* (Figure 4.3).

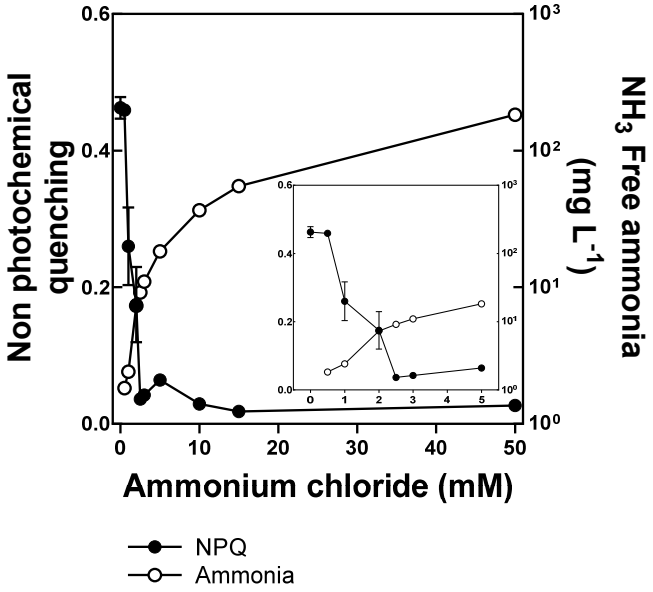

Figure 4.3. Theoretical estimation of free ammonia (NH_3) accumulation and its effect on non-photochemical quenching levels (NPQ) of healthy *D. tertiolecta* culture treated with increasing concentrations of ammonium chloride (0–50 mM). Data represent means ± SD, n = 9

Table 4.1. Components of Q_A re-oxidation kinetics in *D. tertiolecta* under grazing conditions. The numbers indicate the amplitude, half-life and decay rate ± standard error. DCMU and ammonium chloride concentrations were 100 nM.

	Amplitude (A)			**Half-life (tau)**			**Decay rate (k)**		
	Fast	**Medium**	**Slow**	**Fast (µs)**	**Medium (ms)**	**Slow (s)**	**Fast (s)**	**Medium (s)**	**Slow (s)**
Control	0.655 ±0.084	0.024 ±0.001	0.018 ±0.001	398.961 ±0.000	41.230 ±0.007	1.3 ±0.2	1737.382 ±99.280	16.810 ±3.060	0.505 ±0.108
NH_4Cl	0.112 ±0.008	0.029 ±0.001	0.081 ±0.003	1240 ±0.0001	74.21 ±0.01	11.4 ±1.1	559.45 ±50.83	9.340 ±1.440	0.060 ±0.006
Grazing	0.166 ±0.017	0.0089 ±0.0004	0.0071 ±0.0003	482.948 ±0.000	32.43 ±0.00	3.9 ±0.6	1435.24 ±74.88	21.375 ±2.703	0.176 ±0.027
DCMU	0.005 ±0.002	0.083 ±0.011	0.05 ±0.01	1263 ±0.012	130.93 ±0.02	0.94 ±0.15	54.88 ±5.76	5.29 ±0.64	0.73 ±0.08

The analysis of Q_A re-oxidation kinetics revealed that the half-life of the fast phase was 21 % shorter in grazing cultures than in the controls. Similarly, the addition of ammonium chloride and DCMU to the *D. tertiolecta* culture accelerated the fast-phase kinetics by ~210 %. (Table 4.1). It was observed that the medium-phase half-life was 21 % longer in the grazing culture; however, values for this parameter increased by 210 % and 217 % in cultures treated with ammonium chloride and DCMU respectively. The half-life of the slow-phase decay increased by 185 % and 735 % in the presence of the grazer and ammonium chloride, respectively. DCMU treatment lowered the half-life of the slow phase by 31 %.

4.3.3 Effect of predator-infested spent media on NPQ levels of *D. tertiolecta*

In Figure 4.4, the NPQ levels of *D. tertiolecta* cultivated in the predator-infested spent medium were significantly (P = 0.0062) lower than in *D. tertiolecta* cells cultivated in predator-free spent medium and fresh F/2 media. Overall, a reduction of 32% in the NPQ levels was observed.

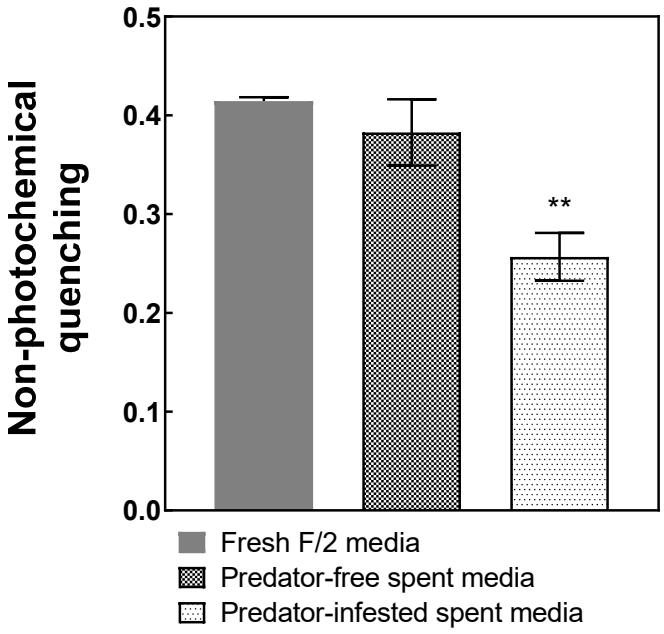

Figure 4.4. The NPQ levels of *D. tertiolecta* cultivated in predator-free and predator-infested spent media. Level of significance 0.05, P values are ≤ **0.0021. Data represent means ± SD, n = 9

4.3.4 Estimation of reactive oxygen species (ROS)

At the initial time-point (day 0), ROS levels per cell (Figure 4.5) were 38 % higher in both the control and the grazing cultures than on day 1, and concentrations significantly decreased over the course of cultivation. However, no significant difference in ROS accumulation was observed in the grazing culture when compared to the control across all time points.

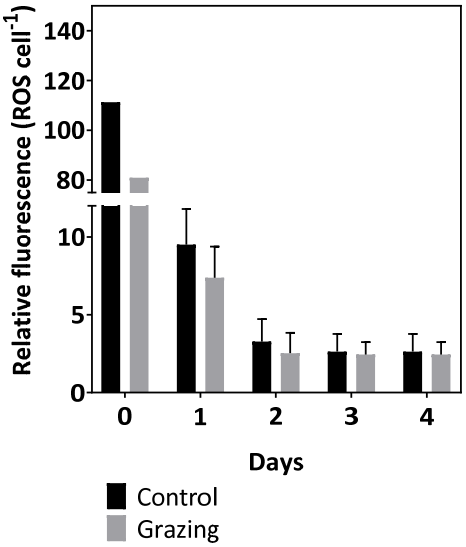

Figure 4.5. Estimation of reactive oxygen species (ROS) levels (relative concentration per cell) in control and grazing cultures. Data represent means ± SD, n = 9

4.3.5 Estimation of total ammonia-nitrogen (TAN) in grazing cultures

Ammonia is a known inhibitor of NPQ. Therefore, TAN accumulation was estimated to determine the possible cause of NPQ reduction in the presence of grazers. A significant ($P < 0.0001$) accumulation of TAN was found in the grazing culture on days 2, 3 and 4 (Figure 4.6a). On day 0, the difference in the TAN levels of the control and the grazing culture was as low as 5 %, though 43 % more TAN accumulation was seen in grazing cultures compared to the control on day 1, which increased up to 92 % to 95% over the next two days before dropping to 85 % by the end of the crash. The highest TAN accumulation of 53 mg l^{-1} was observed to coincide with the highest predator ingestion rate of 9 x 10^{12} prey cells predator^{-1} d^{-1} on day 3, that is, 24 h before the culture crash (Figure 4.6b). A significant reduction in the NPQ levels of the grazing culture was observed as ammonia accumulation and predator ingestion rate progressively increased (Figure 4.7).

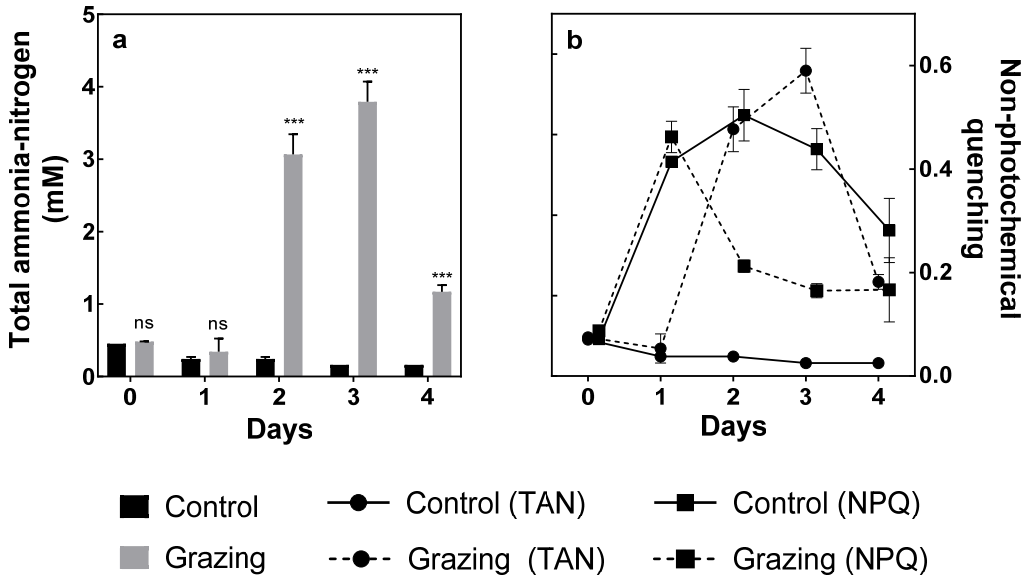

Figure 4.6 a) Total ammonia-nitrogen (TAN) accumulation and b) relative impact on NPQ levels of *D. tertiolecta* in control and grazing cultures as a function of time. Level of significance 0.05. P values are $\leq^{ns}$ 0.1234, ***0.0002. Data represent means ± SD, n = 9

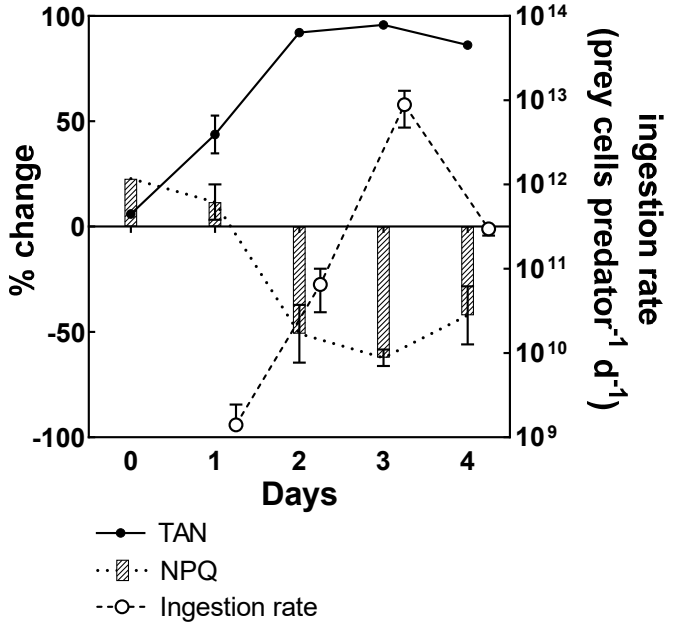

Figure 4.7 Percentage of change in the total concentration of ammonia-nitrogen (TAN), non-photochemical quenching levels and predator ingestion rate as a function of time. Data represent means ± SD, n = 9

4.3.6 Effect of nitrogen source on NPQ profiles of grazing culture

The crash assays that used ammonium chloride (Figure 4.8a) and urea (Figure 4.8b) instead of nitrate (Figure 4.8c) as the nitrogen source did alter the NPQ levels of prey cells, though the trend in NPQ was unlike that in nitrate-based medium. The grazing culture in the nitrate-based F/2 medium showed a declining trend in the NPQ ($P < 0.0001$) as the culture

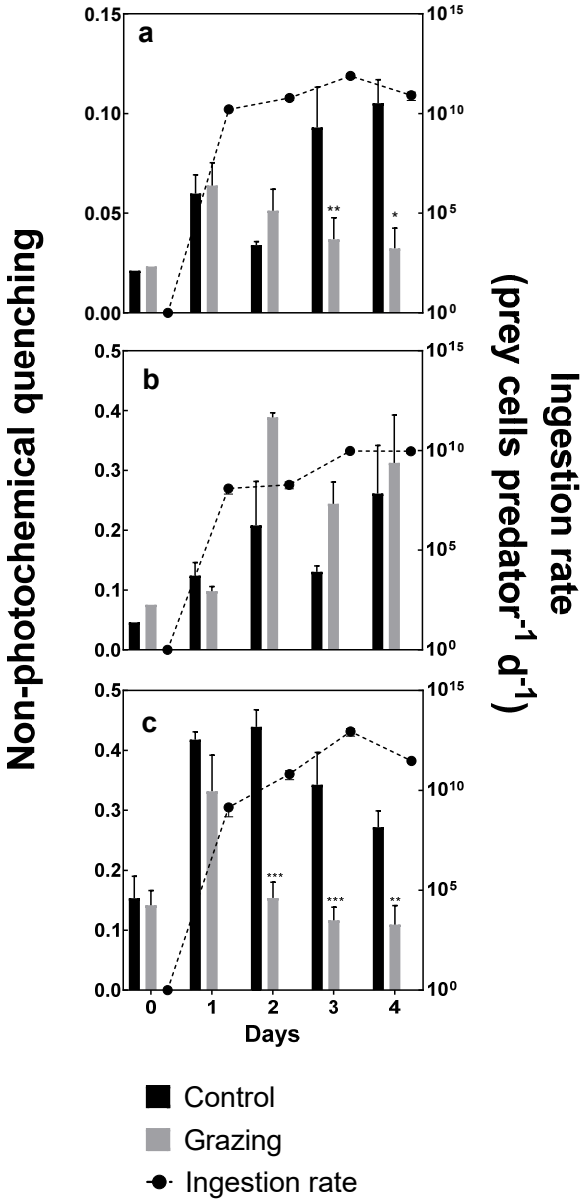

Figure 4.8 Effect of a) ammonium chloride-, b) urea-, c) nitrate-based cultivation media on non-photochemical quenching (NPQ) levels of *D. tertiolecta* and ingestion rate of *O. marina*. Level of significance 0.05. P values are ≤*0.0332, **0.0021, ***0.0002. Data represent means ± SD, n = 9

progressed towards the crash whereas the use of ammonium chloride as the N-source in the grazing culture resulted in a moderate reduction of the NPQ ($P < 0.001$) in the grazing culture when compared to the control on day 3, that is, 24 h prior to the crash day. In contrast, NPQ levels of grazing cultures were increased in the urea-based F/2 medium. The ingestion rate in both urea- and ammonium chloride-based media was similar to that in the crash assay in nitrate-based cultivation medium; however, no declining trend was observed in the NPQ in the grazing culture with urea as the N-source.

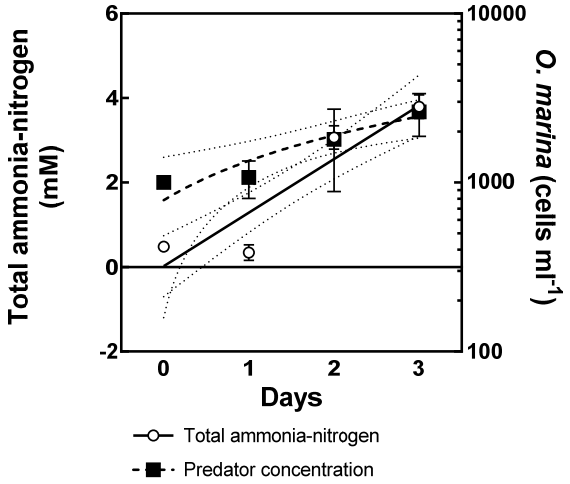

Figure 4.9 Comparison of microscopy-based predator cell ($R^2 = 0.5797$) counts with relative levels of total ammonia-nitrogen ($R^2 = 0.8424$) as a means of warning of *Oxyrrhis marina* infestation. Data represent means ± SD, n = 9. Symbols (hollow circles and solid squares) represents the data points, dashed and solid black line represent fitted lines of cell concentration and TAN, respectively, dotted line indicates 95 % confidence interval limits.

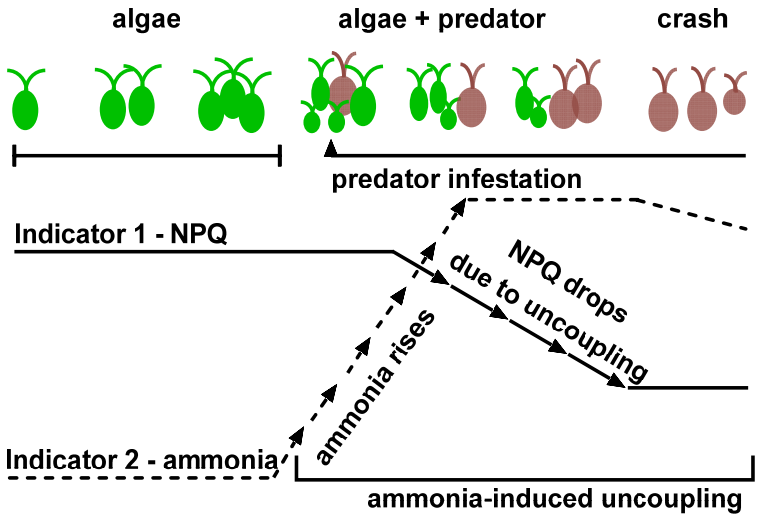

Figure 4.10 Conceptual illustration of non-photochemical quenching (NPQ) and total ammonia-nitrogen (TAN) levels as early indicators of algal grazing.

The relative levels of TAN in grazing culture positively correlate (R^2 = 0.9137) with increased *O. marina* concentration. Moreover, accumulated TAN levels appear to better indicate (R^2 = 0.8424) the presence of the predator as compared to microscopy-based (R^2 = 0.5797) counts (Figure 4.9). Figure 4.10 depicts a conceptual model of the causal relationship between NPQ and TAN, and its use as an early indicator of *Oxyrrhis marina*-mediated predation.

4.4 Discussion

In chapter 4, we investigated total ammonia-nitrogen (TAN) excreted by the predator *O. marina* as the probable cause for the reduction in NPQ level of the microalgal prey, *D. tertiolecta* (Figure 4.6). TAN accumulation with increased prey cell ingestion by the predator suggests the potential of TAN as an early marker of microalgal predation.

Nitrogen is recycled in the form of ammonia-nitrogen by the majority of zooplankton predators that are reported to infect the mass-scale cultivation of microalgae (Carney and Lane 2014). Excreted ammonia is rapidly taken up by the microalgal cells and accounts for up to 43 % of their total nitrogen requirement (Alcaraz et al. 1994). Similarly, *D. tertiolecta* is reported to preferentially take up ammonia, in this case secreted by *O. marina*, over other nitrogen sources (Dortch 1990, Fábregas et al. 1989). *O. marina*-mediated ammonia release is tightly coupled with the high glutamine/glutamate ratio of *Dunaliella* sp. cells. Ammonia uptake and its effect on intracellular amino acid pools of prey is reported as an indicator of stress in mixed population (Flynn and Fielder 1989). However, changes in the source of nitrogen are reported to alter the physiology of microalgal cells, particularly photosynthesis. Ammonia affects photosynthetic parameters such as NPQ, F_v/F_m, $rETR_{max}$, light harvesting efficiency (alpha) and Q_A re-oxidation kinetics (Markou et al. 2016, MacLachlan et al. 1994, Cao et al. 2013).

In chapter 3, we report a reduction in the NPQ levels as a function of active predation-mediated by *O. marina*. However, the photosynthetic quantum efficiency F_v/F_m remains unaffected (Figure 3.3a), which suggests that the overall photochemistry of PSII was unaltered. Similarly, modulation of NPQ and unaltered F_v/F_m in the presence of grazers are also reported by Ratti et al. (2013). In contrast, alpha was reduced moderately, the $rETR_{max}$ levels increased (Figure 3.3b) and the half-life of the medium phase of Q_A re-oxidation was enhanced in grazing cultures compared to the control (Table 4.1).

Similar effects on Q_A re-oxidation decay kinetics in the presence of the photosynthetic inhibitor DCMU and under abiotic stress conditions have been reported in other algal species (Dao and Beardall 2016, Zhang et al. 2017). Recording chlorophyll *a* fluorescence induction decay kinetics can reveal information about Q_A re-oxidation; moreover, they can provide insights into the flow of electrons from Q_A to Q_B, and the possibility of electron back-recombination with the oxygen-evolving complex of the PSII reaction center. The elevated level of electron back-recombination is typically observed in the presence of an uncoupler such as ammonia or 3-(3,4–di-chlorophenol)-1, 1-dimethylurea (DCMU), wherein electrons are readily passed on to the oxygen-evolving complex of PSII due to inhibition of Q_A. Q_A re-oxidation decay kinetics were measured to investigate the effect of grazing on electron carriers beyond PSII. The Q_A re-oxidation kinetics is composed of three phases: the fast phase reflects the electron transfer between Q_A and Q_B; the medium phase, between Q_B and PQ (plastoquinol); and the slow phase, the combination of an electron with the donor side of PSII. Any changes in phase kinetics reflect an altered redox state of electron carriers (de Wijn and Van Gorkom 2001). The three-phase exponential Q_A decay kinetics revealed that the fast and slow phases slowed in the grazer-infested culture by 21 % and 185 %, respectively. However, the medium phase accelerated by 21 % in comparison to the control, which suggests the possibility of a higher proportion of reduced PQ. The reduction in half-life in the slow phase by 185% indicates that PQ re-oxidation may not occur, due to back recombination with the donor side of PSII. Similar effects on photosynthesis were seen in other algal species (Dao and Beardall 2016) and, as a manifestation of physiological stress, photosynthesis was affected along with the accumulation of ROS. The role of ROS accumulation in prey capture by *O. marina* (Martel 2009) and grazer mortality (Flores et al. 2012) is well documented. However, the grazing culture of *D. tertiolecta* did not accumulate significant ROS in the current study (Figure 4.5). Therefore, extracellular cues for NPQ reduction were assessed, in which predator-infested spent medium was used for fresh cultivation of *D. tertiolecta*. The NPQ levels of cells that were propagated in predator-infested spent media were significantly lower than in cells that were cultivated in predator-free spent media (Figure 4.4). This indicates the possibility of extracellular secretion by the predator, recycled ammonia-nitrogen, which may cause inhibition of NPQ.

Excreted ammonia-nitrogen can exist in either free ammonia (NH_3–N) or ammonium ion (NH_4^+–N) form depending on pH of the culture and together can be measured as total ammonia-nitrogen (TAN). A systematic, time-dependent estimation revealed that TAN

accumulation is linked with the increased predator ingestion rate and decreased NPQ level of microalgal prey in grazing cultures. Overall, TAN levels in grazing cultures linearly increased from day 0 to 3 but dropped on day 4 as the predator growth and ingestion ceased due to depletion of microalgal prey cells by 96 % (Figures 4.1 and 4.7). A similar correlation between recycled nitrogen in the form of ammonia and predator growth rate is reported by Dolan (1997) and Sherr et al. (1983). Goldman et al. (1989) reported prey concentration dependent grazing of *O. marina* fed to *D. tertioleta*, *I. galbana* and *P.tricornutum*. In addition to the altered prey-predator concentrations, the pH dropped in *O. marina*-infested cultures (Figure 4.2), possibly associated with a rise in CO_2 from predator cell respiration or assimilation of ammonia secreted by predators. Fuggi et al. (1981) reported a rise in pH in algal culture upon nitrate uptake and its decrease during active ammonia assimilation, changes associated with pH regulation within cells as the different forms of nitrogen are assimilated.

To confirm further that predator-excreted ammonia-nitrogen is a sole source of NPQ inhibition, the crash assay was established in ammonium chloride- and urea-based F/2 media. Unlike nitrate-based F/2 media, the NPQ levels in urea-based cultivation media increased in the presence of the predator, whereas in ammonium chloride-based media, NPQ levels reduced on day 3 and day 4 in the grazing culture. Grazing-mediated reduction in the NPQ levels was observed as early as 48 h and 24 h prior in nitrate and ammonium chloride-based cultivation media, respectively. However, the decreasing NPQ trend was not observed in urea-based grazing cultures (Figure 4.8). Urea dissociates into ammonia and carbon dioxide with the help of two intracellular enzymes, namely urease and urea amidolyase (Bekheet and Syrett 1977)**;** however, *D. tertiolecta* lacks the former enzyme (Murphree et al. 2017). The latter enzyme, urea amidolyase, is ATP-dependent and operates under metabolic control of the substrate, urea (induction) and product, ammonia (repression). Microalgal cultures grown in the presence of ammonia plus urea are reported to have nil or minimal urea amidolyase activity (Hodson et al. 1975). Similar enzyme inhibitory conditions may exist in grazing cultures in which ammonia-nitrogen is present due to the predator activity and urea present in the cultivation media as a nitrogen source. The uncoupling effect of ammonia is reported to drastically reduce the cellular ATP pool (Krogmann et al. 1959) which is crucial for urea amidolyase activity. Increased NPQ levels of grazing cultures in urea-based cultivation media suggest the possibility of metabolic stress due to the inhibition of urea amidolyase; however, this requires further work and experimental validation.

Overall, significant accumulation of TAN and reduction in NPQ levels in grazing cultures as compared to the control were observed as early as 48 h prior to the culture crash (day 4). A moderate build-up of TAN levels due to active predation of *O. marina* appears at least 72 h prior to the culture crash (Figure 4.7). Although TAN levels are low in the initial phase, the presence of light is sufficient to trigger the preferential uptake of ammonia-nitrogen by *D. tertiolecta*. Perhaps, rapid uptake of ammonia-nitrogen (Fábregas et al. 1989) may be the probable reason for the non-significant difference in levels of TAN on day 2 in grazing culture as compared to the control. A positive correlation of TAN levels with increasing predator concentration in grazing cultures (Figure 4.6) suggests that TAN build-up occurred as a result of increased prey cells ingestion by the predator which led to nitrogen turnover.

Crofts (1967) described the role of ammonia as a uncoupler of photosynthesis. Such uncoupling is reported to inhibit NPQ formation in *Nannochloropsis* sp. (Cao et al. 2013). The predator, *O. marina* excretes ammonia which primarily exisits as ammonium ions (NH_4^+) which is converted to free ammonia (NH_3) as pH levels rise. The grazing culture pH ranges from 8 to 8.4 in the current study (Figure 4.2) which suggests the possibility of presence of free ammonia. The free form of ammonia within cells can easily diffuse across the membranes of the chloroplast and protonate in the presence of high H^+ in the lumen of the chloroplast. The proton gradient across the thylakoid membrane is thus disturbed due to H^+ sequestration. At the same time, light absorption is continued and the Hill reaction remains operational, compensating for the loss of H^+ ions (Crofts 1967). This correlates with the increased $rETR_{max}$ values in the presence of the predator (Figure 3.3). Hence, a reduction in the levels of NPQ in the presence of *O. marina* was observed. In addition to NPQ reduction, the uncoupler ammonium chloride is reported to disturb ATP synthesis, whereupon the rate of electron flow is accelerated (Müller et al. 2001). To further confirm ammonia-mediated NPQ reduction, a healthy *D. tertiolecta* culture was treated with ammonium chloride. In an aqueous solution, ammonium chloride dissociates into ammonium ions (NH_4^+) and chloride (Cl^-) ions. As mentioned above the ammonium (NH_4^+) can be converted into free ammonia (NH_3); both forms of ammonia-nitrogen can be taken up by *D. tertiolecta* cells. A steep, but non-linear, decrease in NPQ was observed as the concentration of total ammonia-nitrogen increased. Overall the enhanced $rETR_{max}$ with declining NPQ and decreased pH in grazing cultures of *O. marina* are consistent with accumulation of ammonia. The kinetics of NPQ is typically composed of three parts, namely qE, qT and qI. The first component, qE is highly dependent on the build-up of a transthylakoid proton gradient (delta pH) and is the most relevant component to the findings

of current paper. The other two components qT and qI are associated with state transitions and photoinhibition, respectively (Müller et al. 2001). Low pH conditions inside the thylakoid lumen activate qE and the xanthophyll cycle, both of which are necessary for the full expression of NPQ (Demmig-Adams et al. 1990). First, binding of H^+ ions from the lumen to the PsbS protein of PSII causes conformational change (Li et al. 2000), followed by activation of violaxanthin de-epoxidase that catalyses the conversion of violaxanthin to zeaxanthin located in the vicinity of light harvesting complexes (Jahns et al. 2009).The altered PSII state and zeaxanthin form a quenching complex that dissipates excess photon energy as heat, that is NPQ (Müller et al. 2001). Few green algal species are reported to activate qE independently of the xanthophyll cycle (Niyogi et al. 1997a). However, *D. tertiolecta* is reported to operate pH-dependent qE and xanthophyll activation for the expression of NPQ (Ihnken et al. 2011). The accumulation of ammonia interferes with the proton gradient across the membrane (Crofts 1967). As a result, the quenching complex consisting of protonated PsbS and zeaxanthin cannot form and qE is not activated, hence NPQ is compromised (Roháček et al. 2014). Similarly, the presence of ammonia in predator-infested culture of *D. tertiolecta* may interfere with qE and xanthophyll cycle activation. As a result, NPQ levels were reduced with the incremental accumulation of ammonia as the grazer population exponentially increased.

TAN-based monitoring of *O. marina* invasion can indicate a 5–10 % load of predators at least 48 h prior to the culture crash (Figure 4.9 and 4.10). Traditional microscopy-based methods are labour-intensive. Moreover, processing of small subsamples as a representative of a large volume of culture often under represents the actual load of the contaminating predators. Continuous flow-cytometry monitoring can process large samples with a detection limit of 10^8 cells ml^{-1} but this, however, requires a sophisticated laboratory setup (Day et al. 2017). Estimation of TAN levels can be leveraged to set up an online tool to monitor predator invasion. Various pH- and ion selective electrode-based sensors are commercially available which can be integrated and implemented in-line with microalgal culture to facilitate real-time monitoring of grazer invasion. Oligonucleotide-based molecular methods are sensitive to low concentration of predators (Carney et al. 2016), however they have limited application mainly due to species-specific detection. In contrast, TAN based methods can be a universal marker of microalgae grazing because ammonia, as a consequence of nitrogen recycling, is excreted by most of the zooplankton predators reported to infest the mass cultivation of microalgae.

Changes in the TAN and NPQ levels, especially in outdoor conditions, can also occur due to abiotic stress conditions such as high light, temperature and nutrient load relevant to

wastewater-based cultivation. In addition, NPQ levels and photosynthetic processes are generally subjected to adverse effects across a light:dark cycle as cells move between intense light and darkness (Demory et al. 2018). Therefore, estimation of only NPQ levels could indicate a potential false positive outcome. Similarly, TAN build-up can be under estimated especially during light-hours as the presence of light is one of the driving factors in ammonia-nitrogen uptake by microalgae (Fábregas et al. 1989). Measurement of TAN build-up together with NPQ levels as a complementary tool can overcome challenges associated with each measurement under extreme light and dark conditions. TAN and NPQ levels together can serve as an efficient early warning sign of predator invasion. However, empirical validation is required to access the effectiveness of TAN and NPQ-based measurements under light and dark phases of the day, mimicking the outdoor conditions.

4.5 Conclusion

Monitoring of algal grazing requires an integrated approach for early detection of a predator. This chapter reports grazing-induced changes in photosynthetic parameters of the prey cells. In the grazing culture, decreased levels of NPQ correlated with increasing total ammonia-nitrogen concentration before the algae culture crash occured. Total ammonia-nitrogen that was recycled by the predator was taken up by *D. tertiolecta* cells, causing NPQ inhibition. Both NPQ and ammonia detection can be automated and implemented online with algae cultivation for effective monitoring of predator infestation. Perturbed NPQ levels in microalgal cultures can be observed under a variety of stresses other than grazing. However, taken in conjunction with NPQ measurements, total ammonia-nitrogen can act as an effective marker and symptom of predator invasion. Currently a range of on-site total ammonia detection kits e.g. API® and immersion probes e.g. ISE, Hach® are available for ammonia/ammonium estimation. Immersion probes can be integrated with other microalgal health monitoring sensors such as pH, optical density etc., to develop a continuous grazer monitoring platform.

In addition to the nutrient recycling, repackaging of biomolecules is an inevitable outcome of active grazing. Chapter 5 investigates potential of repackaged biomacromolecules based on spectral information acquired using Fourier Transform Infrared Spectroscopy (FTIR) combined with chemometrics method as means of fault detection.

References

Alcaraz M, E Saiz, and M Estrada. 1994. "Excretion of ammonia by zooplankton and its potential contribution to nitrogen requirements for primary production in the Catalan Sea (NW Mediterranean)." *Marine Biology* 119 (1):69-76.

Bekheet IA , and PJ Syrett. 1977. "Urea-degrading enzymes in algae." *British Phycological Journal* 12 (2):137-143.

Cao S, X Zhang, D Xu, X Fan, S Mou, Y Wang, N Ye, and W Wang. 2013. "A transthylakoid proton gradient and inhibitors induce a non-photochemical fluorescence quenching in unicellular algae *Nannochloropsis* sp." *FEBS Letters* 587 (9):1310-1315.

Carney LT, and TW Lane. 2014. "Parasites in algae mass culture." *Frontiers in Microbiology* 5:278-286. doi: 10.3389/fmicb.2014.00278.

Carney LT, JS Wilkenfeld, PD Lane, OD Solberg, ZB Fuqua, NG Cornelius, S Gillespie, KP Williams, TM Samocha, and TW Lane. 2016. "Pond Crash Forensics: Presumptive identification of pond crash agents by next generation sequencing in replicate raceway mass cultures of *Nannochloropsis salina*." *Algal Research* 17:341-347. doi: https://doi.org/10.1016/j.algal.2016.05.011.

Crofts AR. 1967. "Amine uncoupling of energy transfer in chloroplasts I. Relation to ammonium ion uptake." *Journal of Biological Chemistry* 242 (14):3352-3359.

Dao L, and J Beardall. 2016. "Effects of lead on two green microalgae *Chlorella* and *Scenedesmus*: photosystem II activity and heterogeneity." *Algal Research* 16:150-159.

Day JG, Y Gong, and Q Hu. 2017. "Microzooplanktonic grazers – A potentially devastating threat to the commercial success of microalgal mass culture." *Algal Research* 27:356-365. doi: https://doi.org/10.1016/j.algal.2017.08.024.

de Wijn R, and HJ Van Gorkom. 2001. "Kinetics of electron transfer from QA to QB in photosystem II." *Biochemistry* 40 (39):11912-11922.

Demmig-Adams B, WW Adams, U Heber, S Neimanis, K Winter, A Krüger, F Czygan, W Bilger, and O Björkman. 1990. "Inhibition of zeaxanthin formation and of rapid changes in radiationless energy dissipation by dithiothreitol in spinach leaves and chloroplasts." *Plant Physiology* 92 (2):293-301.

Demory D, C Combe, P Hartmann, A Talec, E Pruvost, R Hamouda, F Souillé, P Lamare, M Bristeau, and J Sainte-Marie. 2018. "How do microalgae perceive light in a high-rate pond? Towards more realistic Lagrangian experiments." *Royal Society Open Science* 5 (5):180523.

Dolan JR. 1997. "Phosphorus and ammonia excretion by planktonic protists." *Marine Geology* 139 (1):109-122.

Dortch Q. 1990. "The interaction between ammonium and nitrate uptake in phytoplankton." *Marine ecology progress Series. Oldendorf* 61 (1):183-201.

Fábregas J, J Abalde, and C Herrero. 1989. "Biochemical composition and growth of the marine microalga *Dunaliella tertiolecta* (Butcher) with different ammonium nitrogen concentrations as chloride, sulphate, nitrate and carbonate." *Aquaculture* 83 (3-4):289-304.

Flores HS, G Wikfors, and H Dam. 2012. "Reactive oxygen species are linked to the toxicity of the dinoflagellate *Alexandrium* spp. to protists." *Aquatic Microbial Ecology* 66:199-209. doi: 10.3354/ame01570.

Flynn KJ, and J Fielder. 1989. "Changes in intracellular and extracellular amino acids during the predation of the chlorophyte *Dunaliella primolecta* by the heterotrophic dinoflagellate *Oxyrrhis marina* and the use of the glutamine/glutamate ratio as an indicator of nutrient status in mixed populations." *Marine Ecology Progress Series. Oldendorf* 53 (2):117-127.

Fuggi A, VM Rigano, V Vona, and C Rigano. 1981. "Nitrate and ammonium assimilation in algal cell-suspensions and related pH variations in the external medium, monitored by electrodes." *Plant Science Letters* 23 (2):129-138.

Goldman JC, MR Dennett, and H Gordin. 1989. "Dynamics of herbivorous grazing by the heterotrophic dinoflagellate *Oxyrrhis marina*." *Journal of Plankton Research* 11 (2):391-407.

Hodson RC, SK Williams, and WR Davidson. 1975. "Metabolic control of urea catabolism in *Chlamydomonas reinhardi* and *Chlorella pyrenoidosa*." *Journal of Bacteriology* 121 (3):1022-1035.

Ihnken S, JC Kromkamp, and J Beardall. 2011. "Photoacclimation in *Dunaliella tertiolecta* reveals a unique NPQ pattern upon exposure to irradiance." *Photosynthesis Research* 110 (2):123-137.

Jahns P, D Latowski, and K Strzalka. 2009. "Mechanism and regulation of the violaxanthin cycle: the role of antenna proteins and membrane lipids." *Biochimica et Biophysica Acta (BBA)-Bioenergetics* 1787 (1):3-14.

Krogmann DW, AT Jagendorf, and M Avron. 1959. "Uncouplers of spinach chloroplast photosynthetic phosphorylation." *Plant Physiology* 34 (3):272.

Li X, O BjoÈrkman, C Shih, AR Grossman, M Rosenquist, S Jansson, and KK Niyogi. 2000. "A pigment-binding protein essential for regulation of photosynthetic light harvesting." *Nature* 403 (6768):391.

MacLachlan DJ, JHA Nugent, JT Warden, and MCW Evans. 1994. "Investigation of the ammonium chloride and ammonium acetate inhibition of oxygen evolution by Photosystem II." *Biochimica et Biophysica Acta (BBA)-Bioenergetics* 1188 (3):325-334.

Markou G, O Depraetere, and K Muylaert. 2016. "Effect of ammonia on the photosynthetic activity of *Arthrospira* and *Chlorella*: a study on chlorophyll fluorescence and electron transport." *Algal Research* 16:449-457.

Martel CM. 2009. "Conceptual Bases for Prey Biorecognition and Feeding Selectivity in the Microplanktonic Marine Phagotroph *Oxyrrhis marina*." *Microbial Ecology* 57 (4):589-597. doi: 10.1007/s00248-008-9421-8.

Marxen K, KH Vanselow, S Lippemeier, R Hintze, A Ruser, and U Hansen. 2007. "Determination of DPPH radical oxidation caused by methanolic extracts of some microalgal species by linear regression analysis of spectrophotometric measurements." *Sensors* 7 (10):2080-2095.

Müller P, X Li, and KK Niyogi. 2001. "Non-photochemical quenching. A response to excess light energy." *Plant Physiology* 125 (4):1558-1566.

Murphree CA, JT Dums, SK Jain, C Zhao, DY Young, N Khoshnoodi, A Tikunov, J Macdonald, G Pilot, and H Sederoff. 2017. "Amino Acids Are an Ineffective Fertilizer for *Dunaliella* spp. Growth." *Frontiers in Plant Science* 8:847.

Niyogi KK, O Bjorkman, and AR Grossman. 1997. "Chlamydomonas xanthophyll cycle mutants identified by video imaging of chlorophyll fluorescence quenching." *The Plant Cell* 9 (8):1369-1380.

Ratti S, AH Knoll, and M Giordano. 2013. "Grazers and phytoplankton growth in the oceans: an experimental and evolutionary perspective." *PLoS One* 8 (10):e77349. doi: 10.1371/journal.pone.0077349.

Roháček K, M Bertrand, B Moreau, B Jacquette, C Caplat, A Morant-Manceau, and B Schoefs. 2014. "Relaxation of the non-photochemical chlorophyll fluorescence quenching in diatoms: kinetics, components and mechanisms." *Philosophical Transactions of the Royal Society B: Biological Sciences* 369 (1640):20130241.

Sherr BF, EB Sherr, and T Berman. 1983. "Grazing, growth, and ammonium excretion rates of a heterotrophic microflagellate fed with four species of bacteria." *Applied and Environmental Microbiology* 45 (4):1196-1201.

Strikland JDH, and TR Parsons. 1972. *A practical handbook of seawater analysis*. Edited by JC Stevenson. Second ed. Canada: The Alger Press Ltd.

Tam NFY, and YS Wong. 1996. "Effect of ammonia concentrations on growth of *Chlorella vulgaris* and nitrogen removal from media." *Bioresource Technology* 57 (1):45-50.

Velthuys BR. 1980. "Mechanisms of electron flow in photosystem II and toward photosystem I." *Annual Review of Plant Physiology* 31 (1):545-567.

Zhang X, F Ma, X Zhu, J Zhu, J Rong, J Zhan, H Chen, C He, and Q Wang. 2017. "The acceptor side of photosystem II is the initial target of nitrite stress in *Synechocystis* sp. strain PCC 6803." *Applied and Environmental Microbiology* 83 (3):e02952-16.

Chapter 5

FTIR-based spectral signature in combination with chemometrics tools as an early marker of *Oxyrrhis marina* contamination in *Dunaliella tertiolecta* cultures

5.1 Introduction

Bioprocess monitoring tools at commercial-scale microalgae cultivation settings, for both open and closed platforms, are evolving to enable online and real-time monitoring of various physiochemical parameters of algal growth. In recent years, cultivation setups are increasingly integrating optical probes and sensors to measure cell density, pH, dissolved oxygen levels, chlorophyll fluorescence etc., that are indirect measures of algal growth (Havlik et al. 2013). In addition to these sensors, Fourier Transform Infrared (FTIR) spectroscopy-based approaches have been reported for monitoring intracellular and extracellular metabolite accumulation (Kosa et al. 2017, Lammers et al. 2017), nutrient stress (Stehfest et al. 2005), algal growth (Jebsen et al. 2012), algal biodiversity (Domenighini and Giordano 2009), bio-macromolecule accumulation (Kansiz et al. 1999, Mayers et al. 2013) and characterization of algal biomass (Sudhakar and Premalatha 2015). Girard et al. (2013) reported the *in-situ* deployment of Attenuated Total Reflectance FTIR (ATR-FTIR) spectroscopy with a fiber optic probe for online monitoring of sugars in a *Scenedesmus obliquus* culture. Application of FTIR spectroscopy in an off-line mode in combination with chemometric methods, such as Principal Component Analysis (PCA) and Partial Least Square Regression (PLSR), are extensively reported for estimation of algal growth, chemical characterization and quantitation of biomacromolecules (Vongsvivut et al. 2013). Another study reported time-resolved changes in *Dunaliella parva* cultures to investigate the effect of chemical environment on bio-molecular composition using a horizontal ATR-cuvette placed in-line with the cultures (Vogt and White 2015).

Screening of microalgal populations and bioprospecting of algal strains are the most widely reported applications of FTIR spectroscopy owing to its ability to discriminate between microalgal strains (Sigee et al. 2002, Giordano et al. 2009) with subtle changes in bio-macromolecular composition (Mayers et al. 2013). However, the discriminatory potential of FTIR spectroscopy combined with the chemometric methods has not been studied in relation to screening of contaminating microbes, including predators, in algal culture. The current

chapter focuses on studying the potential of the FTIR spectroscopy-based approach, in combination with chemometric process tools, as a means of possible fault detection that indicates the presence of predators in an algal culture.

5.2 Materials and method

5.2.1 Microalgal strains and growth conditions

Microalgal prey and predator strains were cultivated and maintained as described in section 3.2.1.

5.2.2 Grazing assay

D. tertiolecta cells were inoculated (at 10^5 cells ml^{-1}) in 200 ml of fresh F/2-based medium in 500 ml conical flasks and incubated for 6 days prior to introduction of *O. marina* (10^2 cells ml^{-1}) on the seventh day. Over the course of the experiment, culture flasks containing only *D. tertiolecta* cells served as a 'control' and were compared with 'grazing' flasks containing *D. tertiolecta* culture infested with the predator. Prey and predator from control and grazing flasks were monitored daily to estimate cell concentrations, growth and ingestion rate as described in section 3.2.1. Total disappearance of prey cells from the grazing flasks were declared as a 'culture crash' and the assay was terminated. Samples were sampled for FTIR spectroscopy measurements every second day (day 0, 2, and 4) until the infestation of the predator on day 7, and were subsequently sampled daily (days 7, 8, 9, 10, 11 and 12) until the culture crash. In addition to this, a fixed concentration of *D. tertiolecta* cells (10^6 cells ml^{-1}) were mixed with an incremental load (10^4–10^6 cells ml^{-1}) of the predator cells such that samples contained 0, 1, 3, 7, 5,10, 20, 30, 40, 50, 60, 70, 80 and 100 % of predator concentration. All samples were subjected to FTIR spectroscopy measurements as described below in section 5.2.4. All experiments were performed with three independent replicates.

5.2.3 Biochemical methods

5.2.3.1 Lipid estimation

Total lipids were extracted and quantified using the method described by Bligh and Dyer (1959). Briefly, 2 ml of chloroform and methanol (1:1) were added to 1 ml of control and grazing sample and vortexed for 30 sec. Chloroform and MiliQ water were then added (1 ml of each) sequentially and the sample vortexed for a further 30 sec. The mixture was centrifuged

at 3000 x g for 5 min and the supernatant collected. The supernatant was allowed to form two layers where the top layer of methanol was discarded. The lower, chloroform, layer was dried at 50^{O}C and the dry matter weighed. A standard curve was prepared using 16-hydroxyhexadecanoic acid (Sigma) and this was used to estimate the concentration of total lipids (µg ml^{-1}) normalized to cell concentration.

5.2.3.2 Carbohydrate estimation

Total carbohydrates were estimated using the method described by Dubois et al. (1956) wherein 5 % of phenol in the presence of concentrated sulfuric acid was added to samples and incubated at 35^{O}C for 30 min. The formation of the pale-golden yellow product was recorded at 483 nm. A standard curve was prepared using D-glucose (Sigma) and used to estimate carbohydrate concentration (µg ml^{-1}) normalized to cell concentration.

5.2.4 FTIR spectroscopy

5.2.4.1 Sample pre-processing

A silicon wafer, polished on one side, of 100 mm diameter and 0.5 mm thickness was cut into smaller pieces of 33 x 33 mm that completely covered the infrared irradiance beam window of the FTIR spectrophotometer (Thermo Scientific, Nicolet^{TM} iS5). The silicon wafers were sequentially treated with RCA cleansers 1 and 2 as described by Kern (1993) to remove silicon di-oxide layer that can interfere in the resultant spectra due to its strong absorption in the mid-infrared region (Milekhin et al. 2006). Briefly, RCA cleanser solution 1 was prepared by mixing 65 ml of ammonium hydroxide (27 %) in 325 ml distilled water. The solution of heated at 70^{o}C using hotplate followed by addition of 65 ml of Hydrogen peroxide (30 %). Pre-cut silicon wafers were soaked into RCA cleanser 1 for 15 min followed by distilled water wash prior to hydrogen fluoride (2.5 % v/v) treatment for 5 min. RCA cleanser solution 2 were prepared by mixing 65 ml of hydrochloric acid (37 %) in 260 ml distilled water and heated at 70^{o}C followed by addition of 65 ml of hydrogen peroxide (30 %). Silicon wafers pre-treated with solution 1 were soaked in the solution 2 for 15 mins and were cleaned with distilled water. The wafers were blow dried using nitrogen gas. The RCA-treated wafers were stored under vacuum and routinely checked for metasilicate, Si-OH and Si-O-Si bond absorption at wavenumbers 740, 800 and 1100 cm^{-1}, respectively, to determine if a silicon dioxide layer was formed and contaminated wafers were discarded. A preliminary optimization was performed where 10^{6} cells were washed twice with 200 mM ammonium formate (BioUltra, Sigma) to

remove salts and were deposited onto the RCA-treated silicon wafers (Sigma) followed by drying at 50°C for 15 min in a vacuum chamber to obtain an even layer of algal film (from control and grazing samples) film prior to spectra acquisition.

5.2.4.2 Spectral acquisition

Spectra were acquired using a bench top Fourier Transform Infrared (FITR) spectrophotometer (Thermo Scientific, Nicolet^{TM} iS5) coupled with transmission accessory, iD5, and a DTGS detector operated at room temperature. The transmission spectra were collected in the mid-infrared region (4000–800 cm^{-1}) at a spectral resolution of 4 cm^{-1} with 256 scans co-added and converted to absorbance spectra through OMNIC^{TM} (Thermo Scientific) software. Background spectra using empty silicon wafers were acquired prior to each measurement.

5.2.4.3 Spectral pre-processing and multivariate analysis of spectral data

All spectra were imported, pre-processed and analyzed using the spectral multivariate data analysis software Unscrambler 10 (Camo Analytics, Oslo, Norway). Raw spectra were transformed to second derivative spectra using the Savitsky-Golay algorithm to resolve spectral peaks, which are often obscured, and eliminate broad baseline sloping in raw spectra. The resultant second derivative spectra were corrected for interference due to scattering effects and differences in sample thickness using the Extended Multiplicative Signal Correction (EMSC) method (Heraud et al. 2006). The resultant spectra post EMSC correction were trimmed to eliminate strong water vapor and atmospheric carbon dioxide interference, yielding post-processed spectra spanning wavenumbers 1000–1430, 1700–1770 and 2800–3050 cm^{-1} that were further used in multivariate analysis.

The post-processed spectra were used for principal component analysis (PCA) to identify trends and classification in datasets. Any outliers strongly influencing the PCA model were eliminated to yield the first few important Principal Components (PC). Further, scores and loading plots were used to visualize data clustering and identify the most influential wavenumbers contributing to variance in the datasets, respectively. In addition to PCA, the post-processed spectra were used for Partial Least Square Regression (PLSR) analysis to identify signature wavenumbers, as predictors, indicating the predator load in the algae culture. Regression coefficient plots were used to visualize wavenumbers that influenced the PLSR model developed for grazing conditions. The predictive PLSR model was built using a Non-

Iterative Partial Least Square (NIPALS) algorithm and lipid, carbohydrate concentrations estimated using the methods described in sections 5.2.3 and 5.2.4. The dataset was divided into a calibration set (two-thirds of the original dataset) and a validation set (one-third of the original dataset) (Wold et al. 2001).

Relative abundances of bio-macromolecules were estimated using the area-under-the-curve of peaks assigned to each bio-macromolecule (Table 5.1) in EMSC-corrected spectra according to the Beer-Lambert law that describes a positive correlation between absorbance and concentration of analytes (Mayers et al. 2013, Wagner et al. 2010). Analytical standards D-glucose (Sigma) and Lyso-PE (Avanti) were used to check the linear range of the FTIR spectrophotometer.

5.2.5 Statistical analysis

All univariate statistical analysis to estimate significance of difference between control and grazing cultures were performed using unpaired two-sample t-tests in GraphPad Prism 7 software (CA, USA). The level of statistical significance for all the analyses was $P < 0.05$.

Table 5.1 FTIR band assignment associated with chemical functional groups in microalgae.

Wavenumber (cm^{-1})	Band assignment	Reference
~3013 (shift 3012)	υ(C–H) of *cis* C=CH- of unsaturated fatty acids	(Guillen and Cabo 1997)
~2960	υ_{as}(C–H) of methyl (CH_3) groups primarily from lipids	(Socrates 2001)
~2925	υ_{as}(C–H) of methylene (CH_2) groups primarily from lipids	(Socrates 2001)
~2872	υ_{s}(C–H) of methyl (CH_3) groups primarily from lipids	(Socrates 2001)
~2852 (shift 2850)	υ_{s}(C–H) of methylene (CH_2) groups primarily from lipids	(Socrates 2001)
~1745	υ(C=O) esters of lipid triglycerides and fatty acids	(Guillen and Cabo 1997)
~1717	υ(C=C) of free fatty acids	(Guillen and Cabo 1997)
~1640	Amide I of proteins	(Vongsvivut et al. 2013)

Wavenumber (cm^{-1})	Band assignment	Reference
~1532	Amide II of proteins	(Vongsvivut et al. 2013)
~1409	Amino acid side chains and υ_S(COO-) group of proteins	(Barth 2007)
~1382	$\delta_s(CH_3)$ and $\delta_s(CH_2)$ of lipids and proteins	(Guillen and Cabo 1997)
~1363	$\delta_s(CH_3)$ of cholesteryl ester and fatty acids radicals	(Gupta et al. 2014)
~1346 (shift 1335)	$\gamma_{wag}(CH_2)$ of polymethylene chains	(Gupta et al. 2014)
~1330	Amide III: α helix	(Barth 2007)
~1261 (shift 1243)	$\upsilon_{as}(SO_3)$ Sulfatides or sulpholipids	(Dreissig et al. 2009)
~1232	$\upsilon_{as}(PO_2^-)$ of phosphodiester of nucleic acids	(Wong et al. 1991)
~1083	$\upsilon_s(PO_2^-)$ of phosphodiester of nucleic acids and phospholipids	(Wong et al. 1991)
~1065	υ_s(R–O–O–O–R') of carbohydrates and υ(C–O–H) spingolipids	(Wong et al. 1991)
~1024	υ(C–C) of carbohydrates and υ(C–O–P) of phosholipids	(Wong et al. 1991)

υ = stretching; υ_s = symmetric stretch; υ_{as} = asymmetric stretch; δ_s = symmetric bend; γ_{wag}= out-of-plane deformation bend.

5.3 Results

5.3.1 Population dynamics of prey and predator

After predator infestation in *D. tertiolecta* cultures on day 7 there was a depletion of prey cells by 6, 21, and 89 % on day 8, 9 and 10, respectively, inside grazing flask as compared to the control (Figure 5.1). On day 11, almost 99 % prey cells were cleared from grazing flask hence day 11 were declared as 'culture crash'. The maximum ingestion rate of the predator was

2 x 10^{11} prey cells predator^{-1} day^{-1}. The maximum growth rates of the *D. tertiolecta* cells in control cultures and of the predator in grazing cultures were 1.54 d^{-1} and 4.59 d^{-1}, respectively.

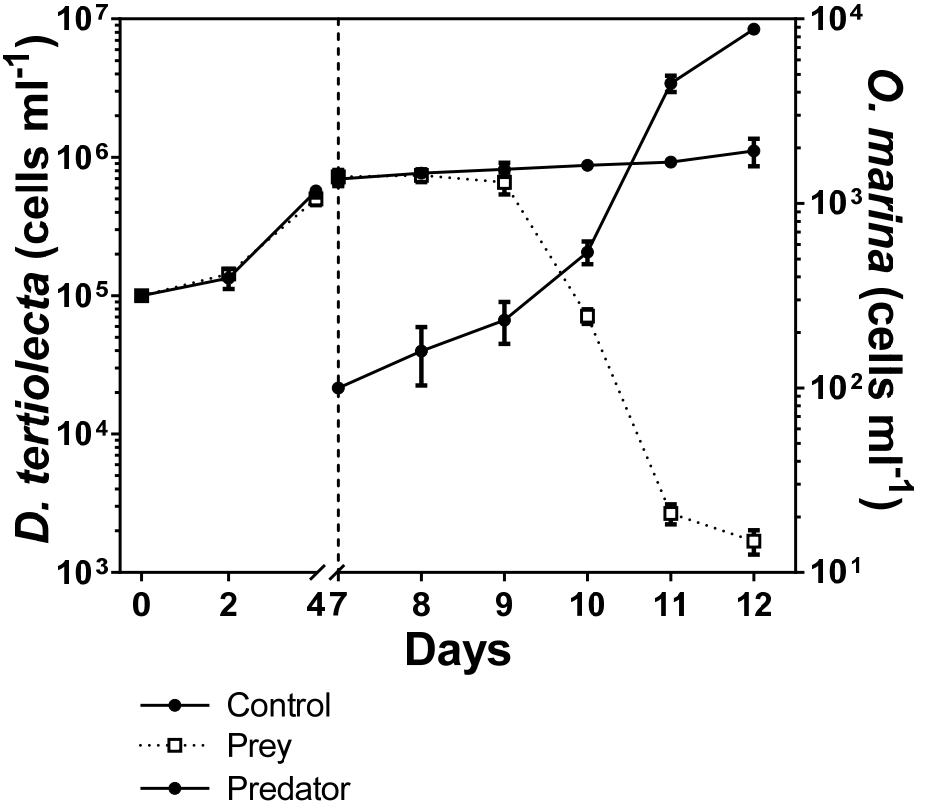

Figure 5.1 Population dynamics of prey, *D. tertiolecta*, and predator, *O. marina*, based on cell concentrations. A 'control' indicates only *D. tertiolecta* cells, 'prey' and 'predator' indicates *D. tertiolecta* and *O. marina* cell concentrations, respectively, in grazing cultures. Dashed line indicates addition of the predator in *D. tertiolecta* cultures on day 7. Data represent mean. n = 3

5.3.2 Determination of microalgal lipids and carbohydrates using FTIR

A strong linear (R^2 = 0.95) correlation (Figures 5.2a) for lipid estimation was observed between FTIR-absorbance (1745 cm^{-1}) and wet-chemistry method. In contrast, the correlation between FTIR absorbance (1024, 1066, 1083 cm^{-1}) and carbohydrate concentration appears to be weak, based on R^2 = 0.55 (Figures 5.2b).

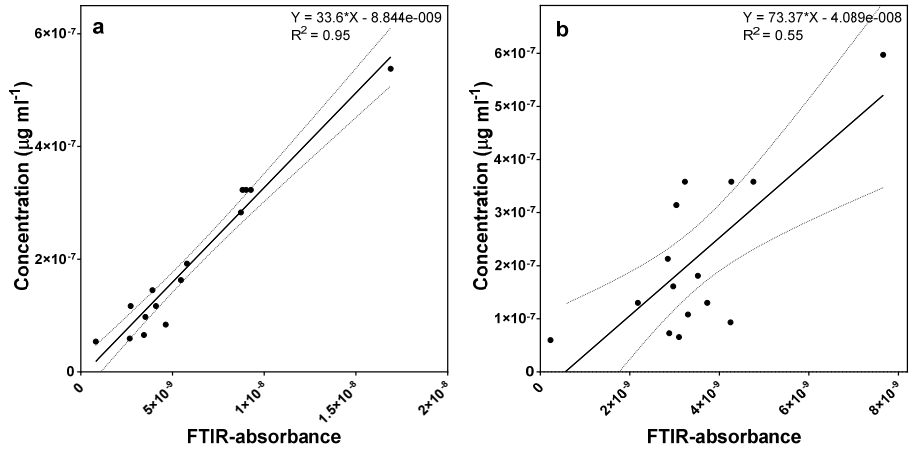

Figure 5.2 Correlation of FTIR absorbance-based on area-under waveband for (a) lipid and (b) carbohydrate estimation with traditional wet-chemistry methods. The data represents means, n = 3

5.3.3 Multivariate analysis of FTIR data

5.3.3.1 Principal Component Analysis (PCA) and Partial Least Square Regression (PLSR) models of grazing cultures

The scores and loadings plot (PC-1 77 %) of the PCA represents the general trend (Figure 5.3a) and multivariate nature of the spectral data (Figure 5.3c), respectively, in the active algal grazing samples across all time-points from days 7–12. The positively loaded wavebands (1066, 1093, 1349 and 1382 cm^{-1}) mostly contribute to clustering of control groups except on day 10 and 12. In contrast, negatively loaded wavebands (1024, 1065, 1159 and 1365 cm^{-1}) contribute to clustering of grazing cultures except on day 9 (Figure 5.3b). The PLSR coefficient plot (Figure 5.3d) highlights wavebands that are mostly associated with carbohydrates (1024, 1065 and 1083 cm^{-1}), cholesteryl esters (1363 cm^{-1}) and polyethylene chains (1382 cm^{-1}) which appear to significantly contribute to the regression model. The influence of the wavebands, 1346, 1363, 1382 cm^{-1}, in classification of *D. tertiolecta* cultures, the control, from predator- infested cultures were consistent across all experiments. The peak centered at 1363 cm^{-1} were contributed from samples containing high predator concentration. Therefore, the relative abundance of the waveband at 1363 cm^{-1}, based on the peak area with respect to grazer ingestion rate across all time-points was investigated. The PLSR model indicates overall good correlation (R^2 = 0.8941) between measured and predicted levels of lipids (Figure 5.4a) as compared to carbohydrates (Figure 5.4b).

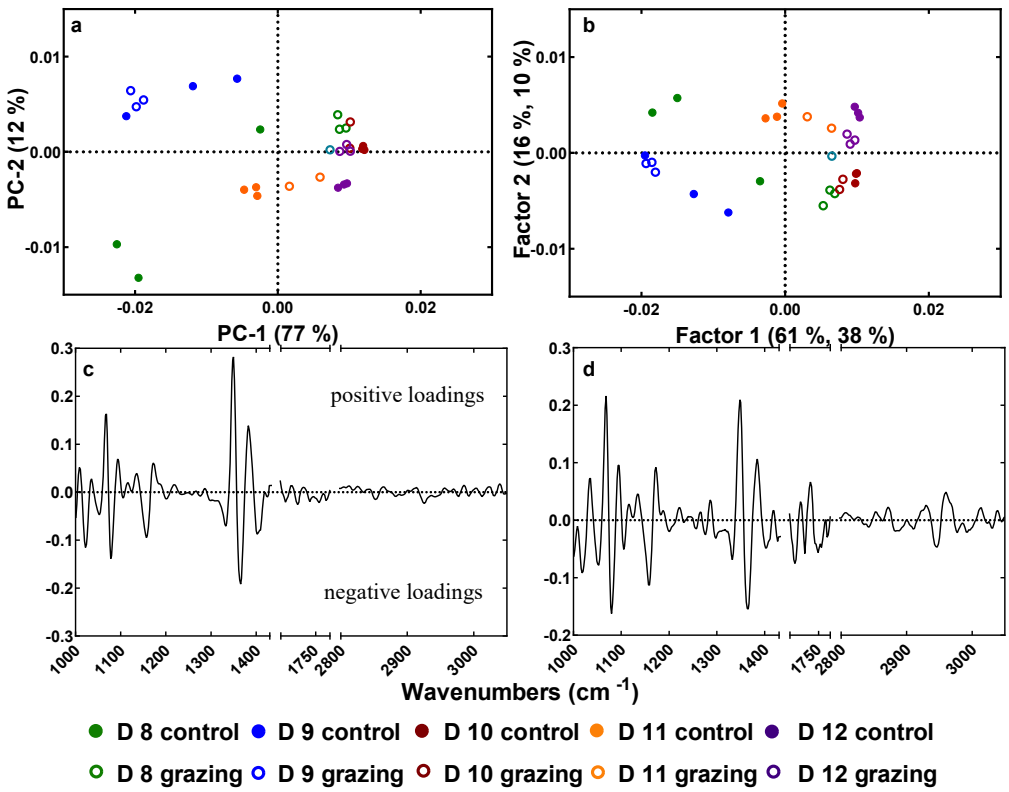

Figure 5.3 Multivariate analysis of *D. tertiolecta* cultures infested with *O. marina* (active grazing cultures) on day 7 revealing the signature spectra as an indicator of contamination. a) scores and c) loading plot of Principal Component Analysis (PCA). b) scores and d) raw coefficient plot of Partial Least Square Regression (PLSR) model.

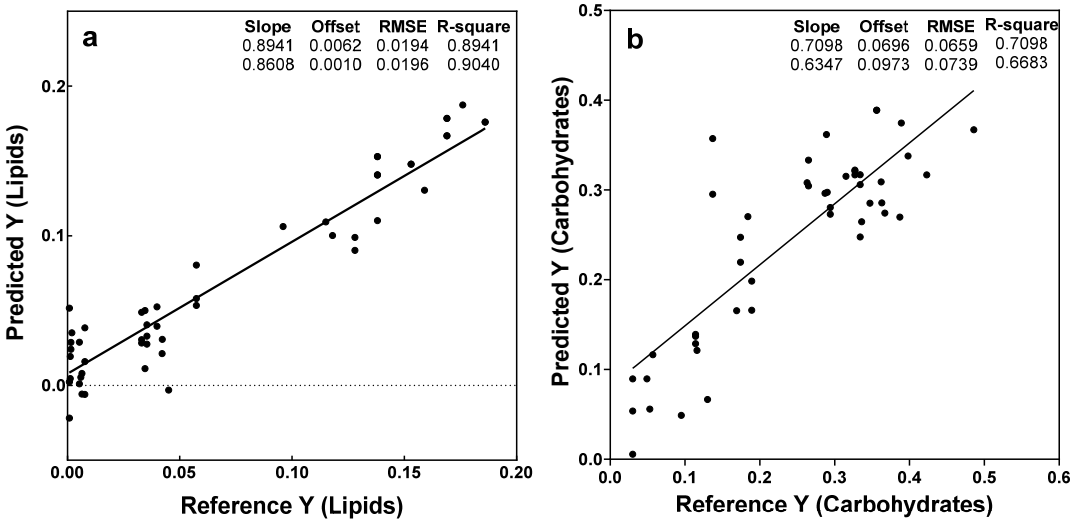

Figure 5.4 Partial Least Square regression model of active grazing cultures estimated using (a) lipid and (b) carbohydrate concentration concentrations as a predictor for both calibration (n = 35) and validation (n = 46) datasets.

5.3.3.2 PCA of only prey and predator cultures

Figure 5.5a indicates very low relative abundance of carbohydrate-related wavebands 1024, 1065, 1083 cm^{-1} in both prey and predator cells. However, there was a relatively higher abundance of absorbance at 1261, 1346, 1363 and 1382 cm^{-1} wavebands in prey-only compared to predator-only samples. In contrast, predator-only cells showed a higher abundance of the waveband at 1745 cm^{-1}, associated primarily with carbonyl esters of lipids and those at 2852, 2925, 2960 cm^{-1} associated with vibrations of CH_2 and CH_3 in proteins and lipids. In addition, a peak at 3012 cm^{-1}, that is primarily assigned to C–H band stretching of olefin chains present in unsaturated fatty acids, was observed to be abundant in predator-only samples. The scores plot from the PCA (Figure 5.5b) distinctly separates prey-only samples from predator-only samples based on the initial difference in relative biomolecular composition estimated using the spectral features in the 1000–1400, 1700–1770 and 2900–3050 cm^{-1} waveband ranges. In

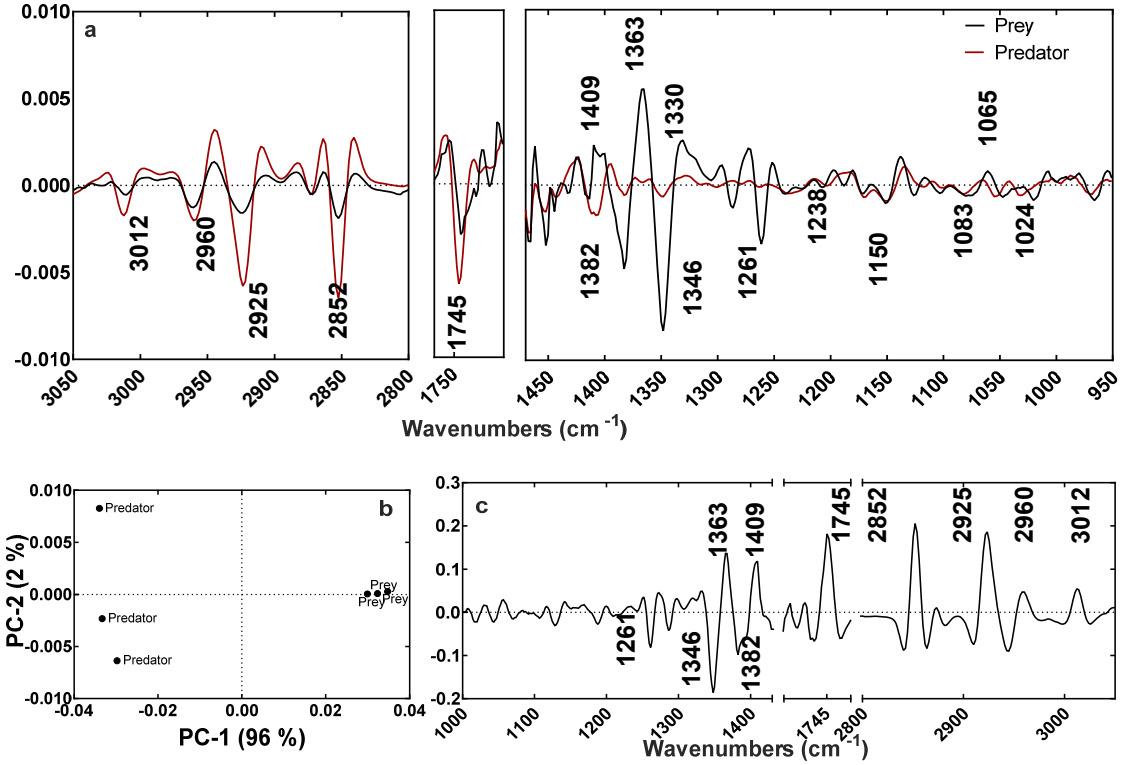

Figure 5.5c,

Figure 5.5 Comparison of only prey, *D. tertiolecta*, and predator, *O. marina*, cells for identification of classifier biomolecules based on a) EMSC corrected spectra b) scores and d) loadings of wavebands of Principal Component Analysis (PCA). n = 3

the loadings plot indicates the negatively loaded wavebands (1261, 1346 and 1382, cm^{-1}) that discriminate prey-only samples from the predator cells cluster based on cell composition, whereas other, positively loaded wavebands (1363, 1409, 1745, 2850 and 2925 cm^{-1}), were influenced by the predator-only group.

5.3.3.3 PCA and PLSR model of *D. tertiolecta* cultures containing incremental (0–100 %) predator load

Figure 5.6a shows that *D. tertiolecta* cells infested with incremental load of predator (0–100%) clustered into low-to-moderate (0–30%) and high level (40–100%) of infestation along PC-1 (61%), based on three wavebands 1346, 1363 and 1382 cm^{-1}. The negatively loaded 1363 cm^{-1} waveband was associated with groups that are infested with a high concentration of predator (40, 50, 60, 70, 80, 100 %). In contrast, positively loaded wavebands at 1346 and 1382 cm^{-1} were mostly influenced by the biomass composition of prey cells in samples containing a low-to-moderate level of predator infestation (0–30 %). The PLSR model (Figure 5.6c and d) was constructed for predication of the extent of grazer concentrations wherein samples infested

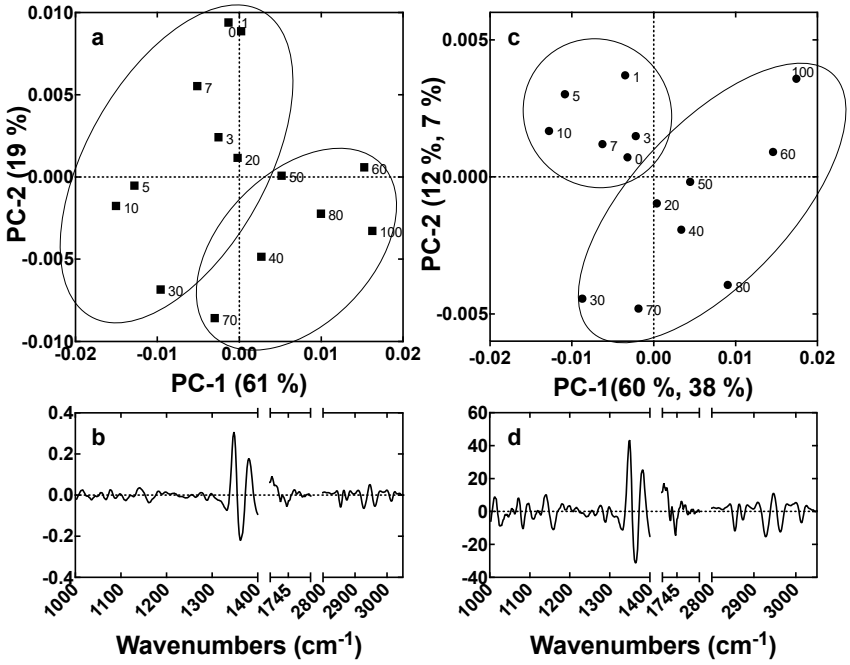

Figure 5.6 Multivariate analysis of *D. tertiolecta* cultures infested with incremental (0– 100 %) predator load (inactive cultures) and influence of 1000–1400, 1700–1770 and 2900–3050 cm^{-1} wavebands. a) Scores and c) loading plot of principal component analysis (PCA). b) Scores and d) raw coefficient plot of partial least square regression analysis (PLSR) model.

with low-to-moderate level of predators clustered (top-left quadrant) along negative scores, whereas samples with a high-level of predators distinctly clustered along positive scores PC-1 (60 %, 38 %).

The raw coefficient plot (Figure 5.6d) of the PLSR (R^2 = 0.9) model indicates that the variation in cell spectra of each sample is multivariate, with contributions mostly from 1346, 1363, 1382 cm^{-1} wavebands that are roughly associated with proteins, lipids, cholesteryl esters and fatty acid radicals as observed in the loadings plot (Figure 5.6b) of the PCA. Although PCA and PLSR indicates the contribution of 1346, 1363, 1382 cm^{-1} wavebands in a distinct classification between low-to-moderate and high predator infested groups, no collinearity was observed between intensity (area-under-waveband) of the three wavebands (variables) and the level of predator load in samples.

5.3.3.4 Relative abundance of predator specific 1363 cm^{-1} wavenumber in grazing culture

The relative abundance of signature wavebands (1346, 1363, 1382 cm^{-1}) varied across time-points in grazing cultures compared to the control. In particular, the waveband 1363 cm^{-1} appears to be primarily associated with the increase in the predator cell concentration and

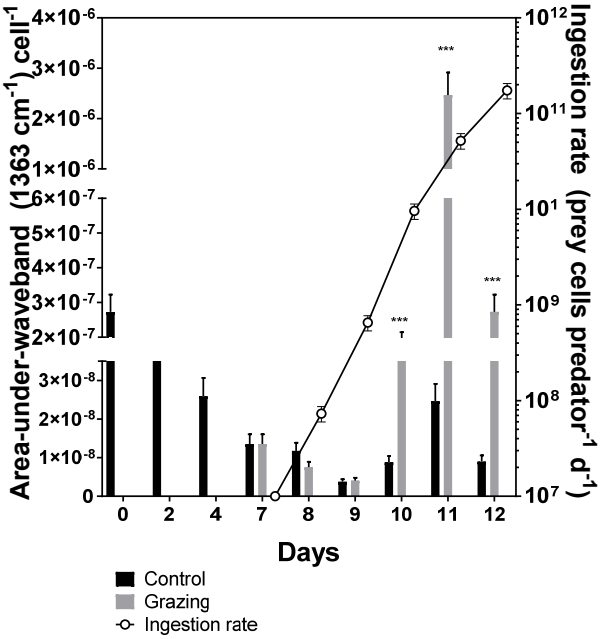

Figure 5.7 Changes in relative abundance of signature wavenumber 1363 cm^{-1} based on area-under-waveband and rate of prey ingestion as a function of time in active grazing cultures infested with *O. marina* on day 7. Level of significance 0.05, P values are ***0.002. The data represents means ± SD, n = 3

accordingly reflected in PCA and PLSR models. The relative abundance of the 1363 cm^{-1} waveband (Figure 5.7), that is primarily associated with in-plane deformation of CH_3 in cholesteryl and fatty acids radicals, was reduced by 96 % on day 8 and increased by 73 %, 171 %, and 68 % on day 9, 10 and 11, respectively.

5.3.4 Spectral features in pre- and post-processed FTIR spectra

Primary inspection of average raw, pre-processed and EMSC corrected spectra (Figure 5.8) indicates the relative abundance of biomolecules assigned to bands in the spectral range 3050–2800, 1770–1700 and 1450–950 cm^{-1} as given in Table 5.1. Peaks of bands centered at 3012 and 1745 cm^{-1} are primarily associated with unsaturated fatty acids (UFA) and carbonyl ester (C=O), respectively. Moreover, both peaks were predominant in samples with relatively higher concentration of the predator, *O. marina*. Quantitative proportions of bands at 3012, 2960, 2925, 2852 and 1745 cm^{-1} were highest, whereas the spectral features at 1024, 1060 and

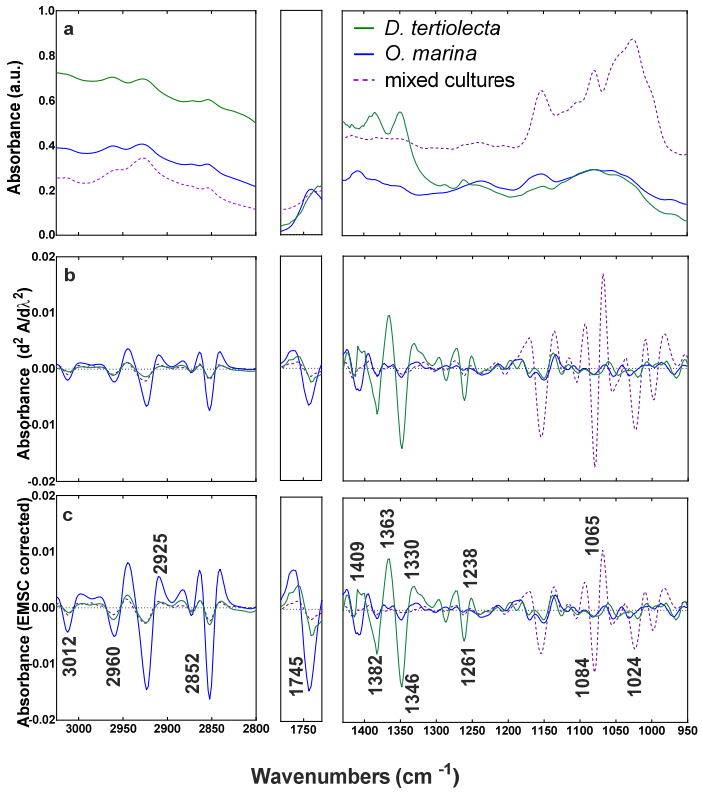

Figure 5.8 Representative spectral features in a) raw b) second derivative and c) EMSC corrected spectra of *D. tertiolecta* (day 0), *O. marina* and mixed cultures (prey and predator – day 10). Each spectrum represents the average of three replicates and bold numbers indicate wavebands cm^{-1}. Biomolecule assignments to each waveband is given in Table 5.1.

1083 cm^{-1}, that are characteristic of carbohydrates (C-O-C), were relatively less abundant in samples that exclusively contained predator cells compared to the control, *D. tertiolecta*.

The peak centered at waveband 1238 cm^{-1} represents the P=O bonds that are predominant in the phosphodiester backbone of nucleic acids and phospholipids and appears to be in equal in proportion across control and predator-infested samples. The other unique features of the spectra consisted of bands at 1261 cm^{-1}, that is associated with carboxylic acids and sulfolipids, and at 1330 cm^{-1}, which is a characteristic of amide III modes (α helix) in proteins, that were mostly prevalent in samples with high prey cell concentration. Other distinct spectral features include a peak centered at 1346 cm^{-1} characteristic of out-of-plane deformation of $-CH_2$ groups of polymethylene chains present in cell membranes; a peak at 1365 cm^{-1} associated with cholesteryl esters and fatty acid radicals; a band at 1382 cm^{-1} associated with $-CH_3$ and $-CH_2$ of proteins and lipids; a peak at 1409 cm^{-1} representative of the influence of amino acid side chains on protein structure. The peaks centered at wavebands 1261,1330 and 1363 cm^{-1} are well resolved in the pre-processed EMSC-corrected (Figure 5.8b) and second derivative spectra (Figure 5.8c) but appear to be hidden otherwise. Overall, raw and processed spectra, especially from multiple samples, appears to be inconclusive. Application of multivariate analysis helps to identify important variables (wavenumbers) indicating underlying changes such as grazing.

5.4 Discussion

The potential of FTIR, in combination with multivariate analysis, to discriminate the presence of *O. marina* was investigated to identify spectral markers of algal grazing. PCA and the PLSR model suggests that the wavebands 1346, 1363 and 1382 cm^{-1} represent signature spectra and are the important variables that are associated with the presence of *O. marina* (Figures 5.3, 5.5 and 5.6). The incremental high loading of the peak centered at 1363 cm^{-1} is associated with cholesteryl esters (Gupta et al. (2014) and positively correlates with the increasing rate of prey ingestion by the predator (day 9–12) in active grazing cultures (Figure 5.8). However, the relative absorbance of the 1363 cm^{-1} peak was significantly lower in predator-only samples as compared to grazing cultures (Figure 5.5). This suggests the possibility that accumulation of cholesteryl ester primarily from cholesterol molecules is an outcome of metabolic growth of the predator due to increased grazing activity. Similarly, the peak also influenced the clustering of samples infested with high concentrations of predator (50–100%). The peak at 1363 cm^{-1} (sometimes found at 1372 cm^{-1} due to a wavenumber shift)

is reported as one of the characteristic wavebands of sterols in brown algae (Bouzidi et al. 2008) and pure cholesterol (Paradkar and Irudayaraj 2002). Phytoplankton such as *D. tertiolecta* are rich in phytosterols such as ergosterol and 7-dehydroproliferasterol that are precursors of cholesterol synthesis. *O. marina* is reported to synthesize cholesterol either by using phytosterols or via a *de novo* pathway if the diet is devoid of the precursors. Growth of *O. marina* is also reported to be positively correlated with cholesterol accumulation (Chu et al. 2008). The phytosterol and cholesterol molecules are reported as to be potential biomarkers to classify members of the Dinophyceae. Similarly, the current study reports the cholesteryl esters waveband, 1363 cm^{-1}, as a potential marker of presence of *O. marina* which is also a member of Dinophyceae. The relative changes in 1363 cm^{-1} (based on area-under-the peak) suggest that the shift in phytosterol to cholesterol pool as a function of grazing can be observed 72 h prior to the culture crash (Figures 5.1 and 5.8). Microalgae culture collapses are sudden, as predators outcompete prey cells within 24–48 h after detection of first sign of invasion using currently practiced monitoring methods (Day et al. 2017). Early warning signs to detect the risk of predator outbreak as early as 72 h prior to a crash can greatly assist in the timely implementation of grazer-mitigation strategies.

The other wavebands of signature spectra, 1346 and 1382 cm-1, were mostly contributed in clustering of samples (Figure 5.3) containing a high level of *D. tertiolecta* cells (controls). Polymethylene chains that are predominantly present in algal lipids (Jones 1962) contribute to the vibrations associated with the waveband at 1346 cm^{-1}, whereas, the 1382 cm^{-1} waveband indicates relative changes in protein and lipids (Guillen and Cabo 1997). No collinearity was found in relative abundance of wavebands, 1346 and 1382 cm^{-1}, and predator concentration. Microalgal lipids are reported to be a contributor of polymethylene chains found in kerogen (Ishiwatari and Machihara 1982, Metzger et al. 1991). Kerogen is complex mixture of hydrocarbons and formed by extensive cross-linking of polymethylene chains which originates from condensation of unsaturated oxygenated lipids and the phytyl component of chlorophyll (Walter 1976). The formation of oxygenated lipids can be triggered by reactive oxygen species (ROS) generated under stress conditions (Nikookar et al. 2005). Biotic stress such as microalgal grazing is reported to activate ROS (Potin 2008) which can further react with biomolecules, including lipids, leading to the formation of oxygenated lipids (Vileno et al. 2010). Interaction of oxygenated lipids with chlorophyll molecule may contribute to the observed changes in the 1346 cm^{-1} waveband. However, further experimental validation is required to confirm the role of the polymethylene chain in grazing cultures. The other feature,

at 1382 cm^{-1}, appears to be associated with the differential accumulation of proteins in control samples as compared to grazing cultures. The changes observed in the relative abundance of lipids and proteins is in agreement with the study reported by Ratti et al. (2013) in which the bio-macromolecular composition of microalgal prey, *T. suecica*; *T. weissflogii* and *Synechococcus* sp. were found to be altered under the grazing pressure of *Euplotes* sp.

The PLSR models developed using lipids and carbohydrate concentrations as a predictor suggests strong influence of the wavebands (variables) of signature spectra on observations - active and inactive grazing cultures (Figures 5.3 and 5.5). The models were built using a cross-validation approach in which PLSR-lipid model suggests good linearity as indicated by value of co-efficient of determination (R^2 = 0.8941), whereas the PLSR-carbohydrate model provided a less satisfactory value of co-efficient of determination (R^2 = 0.7098).

In addition to the signature spectra, wavebands 1745, 2925 2960 and 3012 cm^{-1} appear to be indicative of high predator concentration (Figure 5.6). The observed changes in these wavebands indicates the possibility of a differential accumulation of lipids as a function of variable incremental predator concentration observed in this study. Although the vibrations associated with 2925 and 2960 cm^{-1} wavebands is also contributed by proteins, the observed incremental concentrations of total lipids suggest that the observed changes in the wavebands (2925 and 2960 cm^{-1}) mostly due to lipids in the current study. A similar observation is reported by Dao et al. (2017) wherein lipids appeared to contribute more to these wavebands as compared to proteins. In active grazing cultures the difference in relative intensity of the 3012 cm^{-1} peak was minimal until day 9, despite the increased predator concentration. Exposure of *D. tertiolecta* cells to the predator may possibly activate ROS-mediated lipid peroxidation leading to the destruction of unsaturated fatty acids (3012 cm^{-1}) and as result the overall intensity of the 3012 cm^{-1}waveband was affected contributing to negligible differences in relative abundance at 3012 cm^{-1} between grazing and control cultures until day 9 (Figure 5.3). Similar changes in 3012 cm^{-1} abundance due to activation of lipid peroxidation during the hemodialysis process have been reported (Oleszko et al. 2015). Systematic investigation is required to gain more understanding about predator-mediated cholesterol accumulation and induction of lipid peroxidation. PCA and the PLSR model consistently indicate that *D. tertiolecta* accumulated overall less lipid as compared to *O. marina*. Parrish et al. (2012) reported a similar trend wherein the heterotrophic *O. marina* accumulated higher lipid and fatty acid levels compared to autotrophic algae. Therefore, wavebands associated with lipids were

expected to contribute to the multivariate models more than others. In contrast, in this study the FTIR feature associated with only dietary lipid, cholesteryl ester, contributed the most as an indicator of incremental load of *O. marina*. The potential of fatty acid and lipid profiles as a chemotaxonomic biomarker to determine the community structure of marine microalgae, bacteria and fungi are widely reported (Cañavate 2019).

The peak centered at 1409 cm^{-1} is yet another distinct feature that is associated with amino acid composition of proteins (Figure 5.8). The peak appears to be loaded differently in prey and predator samples (Figure 5.5). The observed differences in waveband 1409 cm^{-1} loading is reported to vary due to amino acid side-chain vibration of proteins and the protonation state which is directly linked to environmental conditions such as pH and organic solvents (Joachim and Haris 2009). Grazing activity of *O. marina* and its excreted nitrogen-ammonia is found to be associated with changes in pH (chapter 4). However, it is crucial to understand the overall contribution of amide-I and II bands (proteins) to deduce the overall effect of algal grazing on protein composition. These wavebands are prone to low signal-to-noise ratio due to the presence of water vapor and were, therefore, eliminated from the data analysis. Acquiring the spectra containing wavebands (1500–1700 cm^{-1}) that are mostly affected by water vapor can pose a great challenge in on-site implementation of FTIR-based method especially at outdoor cultivation platforms. Alternatively, Attenuated Total Reflectance (ATR-FTIR) optical probes can be integrated to monitor microalgal cultures that typically have very high water to biomass ratio (Amaro et al. 2017, Mayers et al. 2013) to facilitate measurement at wavebands that are sensitive to water vapour interference.

In addition to the wavebands of signature spectra, the peaks centered at 1024, 1068 and 1083 cm^{-1} suggest a contribution from ring vibrations (R-O-P-O-R') in the PLSR model of an active grazing culture (Figure 5.3). These wavebands are reported to be mostly associated with abundance of carbohydrates in microalgae (Wagner et al. 2010). However, poor correlation was observed between the intensity of the 1024, 1068, and 1083 cm^{-1} wavebands and carbohydrates that were estimated using wet-chemistry methods (Figure 5.1). This suggests an influence of the ring vibration originating from other biomolecules. Certain classes of lipids such as phospholipids, sulfatides and sphingolipids are known to influence the vibration at 1024, 1068, and 1083 cm^{-1} wavebands (Dreissig et al. 2009). The influence of these wavebands in the PLSR model suggest that the observed change is likely to be contributed from the above-mentioned classes of lipids as opposed to carbohydrates. In addition, oxygenated lipids generated as an outcome of grazing pressure are also likely to contribute to the ring vibrations.

Changes in the relative intensity of candidate wavebands across different time-points in grazing cultures suggests that the biomolecular composition of an algal grazing culture is dynamic (Figure 5.8). As a consequence, identifying a particular biomolecule as a chemotaxonomic marker is challenging. At large scale cultivation, the presence of abiotic stress can also modulate levels of a particular biomolecule as is observed under grazing pressure. Therefore, the present study suggests investigating FTIR-based spectra in combination with multivariate analysis to identify important wavebands (variables) that can indicate the potential risk of grazers. The present study is proof-of-concept that FTIR-based screening in combination of multivariate analysis can be implemented to monitor early signs of predator invasion. The current study did not account for environmental factors, prevalent in large-scale cultivation, that may trigger changes in the macromolecule composition. However, exposure to stress environmental conditions are likely to cumulatively affect the both prey and predator yielding spectral patterns that can be resolved using multivariate tools such as partial least square regression.

Maes et al. (2018) reported hyperspectral reflectance-based spectral feature, 708 nm, as a marker of *Poterioochromonas* sp. and diatom contamination in *Chlorella vulgaris* culture. Changes in the relative intensity of feature associated with 708 nm is attributed to chlorophyll catabolism. Degradation products, particularly originated from chlorophyll, are prevalent under variety of stress conditions. Therefore, monitoring of such breakdown products as means of contaminant invasion can result in false positive outcome. Moreover, activation of catabolic pathway can be a delayed a cellular response which may occur after a significant biomass loss. This can delay the implementation of grazer mitigation strategies. As oppose to this, the spectral feature, 1363 cm^{-1}, associated with sterol synthesis as a function of predator growth have a distinctive advantage over the spectral feature that are indicative of catabolic products. Therefore, shift in the biomacromolecule composition probed with FTIR can server as a reliable marker of predator infestation in microalgal culture.

5.5 Conclusion

Infrared based sensors are being integrated to enable monitoring of various microalgal processes. Implementation of a wide range of infrared sensors in combination with appropriate chemometrics tools could potentially reveal more information beyond algal growth and biomass composition. The scale and nature of the microalgal cultivation platform is dynamic which poses a great challenge to pinpoint a single measurement, for example photosynthetic

yield or chemotaxonomic marker, as an indicator of algal grazing. An integrated approach is required wherein multiple microalgal process such as photosynthesis, growth, biomass composition and other physiochemical variables can be monitored simultaneously. Importantly, it is vital to understand the importance of measurements holistically with respect to microalgal prey-predator interaction. For example, metabolic activity of the predator such as nitrogen recycling can show cascading effects where excreted nitrogen-ammonia can alter the pH of a culture, a factor that is likely to affect photosynthesis and overall macromolecular composition. The current chapter suggests the use of 1363 cm^{-1} waveband as a potential marker for *O. marina*-mediated grazing in *D. tertiolecta* culture. To our knowledge this is the first demonstration of use of FTIR for screening of microalgal grazing. Findings of chapter 5 suggests the potential of an on-line implementation of FTIR-based temporal screening to monitor changes in overall biomolecular composition that is known to occur under grazing pressure. Further, targeted sensors aimed at detecting spectral signatures can be developed and integrated in-line with microalgal cultures.

References

Amaro HM, I Sousa-Pinto, FX Malcata, and AC Guedes. 2017. "Microalgal fatty acids—From harvesting until extraction." In *Microalgae-Based Biofuels and Bioproducts*, edited by Gonzalez-Fernandez C and Muñoz R, 369-400. Woodhead Publishing.

Barth A. 2007. "Infrared spectroscopy of proteins." *Biochimica et Biophysica Acta (BBA)-Bioenergetics* 1767 (9):1073-1101.

Bligh EG, and WJ Dyer. 1959. "A rapid method of total lipid extraction and purification." *Canadian Journal of Biochemistry and Physiology* 37 (8):911-7. doi: 10.1139/o59-099.

Bouzidi N, Y Daghbouche, M El Hattab, Z Aliche, G Culioli, L Piovetti, S Garrigues, and M de la Guardia. 2008. "Determination of total sterols in brown algae by Fourier transform infrared spectroscopy." *Analytica Chimica Acta* 616 (2):185-189.

Cañavate JP. 2019. "Advancing assessment of marine phytoplankton community structure and nutritional value from fatty acid profiles of cultured microalgae." *Reviews in Aquaculture* 11 (3):527-549.

Chu FE, ED Lund, PR Littreal, KE Ruck, E Harvey, J Le Coz, Y Marty, J Moal, and P Soudant. 2008. "Sterol production and phytosterol bioconversion in two species of heterotrophic protists, *Oxyrrhis marina* and *Gyrodinium dominans*." *Marine biology* 156 (2):155-169.

Dao L, J Beardall, and P Heraud. 2017. "Characterisation of Pb-induced changes and prediction of Pb exposure in microalgae using infrared spectroscopy." *Aquatic Toxicology* 188:33-42.

Day JG, Y Gong, and Q Hu. 2017. "Microzooplanktonic grazers – A potentially devastating threat to the commercial success of microalgal mass culture." *Algal Research* 27:356-365. doi: https://doi.org/10.1016/j.algal.2017.08.024.

Domenighini A, and M Giordano. 2009. "Fourier transform infrared spectroscopy of microalgae as a novel tool for biodiversity studies, species identification, and the assesment of water quality." *Journal of Phycology* 45 (2):522-531.

Dreissig I, S Machill, R Salzer, and C Krafft. 2009. "Quantification of brain lipids by FTIR spectroscopy and partial least squares regression." *Spectrochimica Acta Part A: Molecular and Biomolecular Spectroscopy* 71 (5):2069-2075.

Dubois M, KA Gilles, JK Hamilton, PT Rebers, and F Smith. 1956. "Colorimetric method for determination of sugars and related substances." *Analytical Chemistry* 28 (3):350-356.

Giordano M, S Ratti, A Domenighini, and F Vogt. 2009. "Spectroscopic classification of 14 different microalga species: first steps towards spectroscopic measurement of phytoplankton biodiversity." *Plant Ecology & Diversity* 2 (2):155-164.

Girard J, J Deschênes, R Tremblay, and J Gagnon. 2013. "FT-IR/ATR univariate and multivariate calibration models for in situ monitoring of sugars in complex microalgal culture media." *Bioresource Technology* 144:664-668. doi: https://doi.org/10.1016/j.biortech.2013.06.094.

Guillen MD, and N Cabo. 1997. "Characterization of edible oils and lard by Fourier transform infrared spectroscopy. Relationships between composition and frequency of concrete bands in the fingerprint region." *Journal of the American Oil Chemists' Society* 74 (10):1281-1286.

Gupta U, VK Singh, V Kumar, and Y Khajuria. 2014. "Spectroscopic studies of cholesterol: fourier transform infra-red and vibrational frequency analysis." *Materials Focus* 3 (3):211-217.

Havlik I, P Lindner, T Scheper, and KF Reardon. 2013. "On-line monitoring of large cultivations of microalgae and cyanobacteria." *Trends in Biotechnology* 31 (7):406-414.

Heraud P, BR Wood, J Beardall, and D McNaughton. 2006. "Effects of pre-processing of Raman spectra on in vivo classification of nutrient status of microalgal cells." *Journal of Chemometrics: A Journal of the Chemometrics Society* 20 (5):193-197.

Ishiwatari R, and T Machihara. 1982. "Algal lipids as a possible contributor to the polymethylene chains in kerogen." *Geochimica et Cosmochimica Acta* 46 (8):1459-1464.

Jebsen C, A Norici, H Wagner, M Palmucci, M Giordano, and C Wilhelm. 2012. "FTIR spectra of algal species can be used as physiological fingerprints to assess their actual growth potential." *Physiologia Plantarum* 146 (4):427-438.

Joachim AH, and PI Haris. 2009. *FTIR spectroscopy for analysis of protein secondary structure*. Edited by A Barth and PI Haris. Vol. 2, *Biological and biomedical infrared spectroscopy*. Amsterdam: IOS press.

Jones RN. 1962. "The effects of chain length on the infrared spectra of fatty acids and methyl esters." *Canadian Journal of Chemistry* 40 (2):321-333.

Kansiz M, P Heraud, B Wood, F Burden, J Beardall, and D McNaughton. 1999. "Fourier transform infrared microspectroscopy and chemometrics as a tool for the discrimination of cyanobacterial strains." *Phytochemistry* 52 (3):407-417.

Kern W. 1993. "Handbook of semiconductor wafer cleaning technology." In, 111-196. J New Jersey: Noyes Publication.

Kosa G, V Shapaval, A Kohler, and B Zimmermann. 2017. "FTIR spectroscopy as a unified method for simultaneous analysis of intra-and extracellular metabolites in high-throughput screening of microbial bioprocesses." *Microbial Cell Factories* 16 (1):195.

Lammers PJ, M Huesemann, W Boeing, DB Anderson, RG Arnold, X Bai, M Bhole, Y Brhanavan, L Brown, and J Brown. 2017. "Review of the cultivation program within

the National Alliance for Advanced Biofuels and Bioproducts." *Algal Research* 22:166-186.

Maes D, TA Reichardt, TJ Jensen, TA Dempster, JA McGowen, K Poorey, T Hipple, T Lane, and JA Timlin. 2018. Spectroradiometric Detection of Competitors and Predators in Algal Ponds. United States: Sandia National Lab.(SNL-NM), Albuquerque, NM (United States); Sandia.

Mayers JJ, KJ Flynn, and RJ Shields. 2013. "Rapid determination of bulk microalgal biochemical composition by Fourier-Transform Infrared spectroscopy." *Bioresource Technology* 148:215-220.

Metzger P, C Largeau, and E Casadevall. 1991. "Lipids and macromolecular lipids of the hydrocarbon-rich microalga *Botryococcus braunii*. Chemical structure and biosynthesis. Geochemical and biotechnological importance." In *Progress in the Chemistry of Organic Natural Products*, 1-70. Vienna: Springer.

Milekhin AG, C Himcinschi, M Friedrich, K Hiller, M Wiemer, T Gessner, S Schulze, and DRT Zahn. 2006. "Infrared spectroscopy of bonded silicon wafers." *Semiconductors* 40 (11):1304-1313. doi: 10.1134/s1063782606110108.

Nikookar K, A Moradshahi, and L Hosseini. 2005. "Physiological responses of *Dunaliella salina* and *Dunaliella tertiolecta* to copper toxicity." *Biomolecular Engineering* 22 (4):141-146.

Oleszko A, S Olsztyńska-Janus, T Walski, K Grzeszczuk-Kuć, J Bujok, K Gałecka, A Czerski, W Witkiewicz, and M Komorowska. 2015. "Application of FTIR-ATR spectroscopy to determine the extent of lipid peroxidation in plasma during haemodialysis." *BioMed Research International* 2015.

Paradkar M, and J Irudayaraj. 2002. "Determination of cholesterol in dairy products using infrared techniques: 1. FTIR spectroscopy." *International Journal of Dairy Technology* 55 (3):127-132.

Parrish CC, VM French, and MJ Whiticar. 2012. "Lipid class and fatty acid composition of copepods (*Calanus finmarchicus*, *C. glacialis*, *Pseudocalanus sp*., *Tisbe furcata* and *Nitokra lacustris*) fed various combinations of autotrophic and heterotrophic protists." *Journal of Plankton Research* 34 (5):356-375.

Potin P. 2008. "Oxidative burst and related responses in biotic interactions of algae." In *Algal chemical ecology*, 245-271. Heidelberg: Springer.

Ratti S, AH Knoll, and M Giordano. 2013. "Grazers and phytoplankton growth in the oceans: an experimental and evolutionary perspective." *PLoS One* 8 (10):e77349. doi: 10.1371/journal.pone.0077349.

Sigee DC, A Dean, E Levado, and MJ Tobin. 2002. "Fourier-transform infrared spectroscopy of *Pediastrum duplex*: characterization of a micro-population isolated from a eutrophic lake." *European Journal of Phycology* 37 (1):19-26. doi: 10.1017/S0967026201003444.

Socrates G. 2001. *Infrared and Raman characteristic group frequencies: tables and charts*. Third ed. England: John Wiley & Sons.

Stehfest K, J Toepel, and C Wilhelm. 2005. "The application of micro-FTIR spectroscopy to analyze nutrient stress-related changes in biomass composition of phytoplankton algae." *Plant Physiology and Biochemistry* 43 (7):717-726.

Sudhakar K, and M Premalatha. 2015. "Characterization of Micro Algal Biomass Through FTIR/TGA /CHN Analysis: Application to *Scenedesmus* sp." *Energy Sources, Part A: Recovery, Utilization, and Environmental Effects* 37 (21):2330-2337. doi: 10.1080/15567036.2013.825661.

Vileno B, S Jeney, A Sienkiewicz, PR Marcoux, LM Miller, and L Forró. 2010. "Evidence of lipid peroxidation and protein phosphorylation in cells upon oxidative stress photo-generated by fullerols." *Biophysical Chemistry* 152 (1-3):164-169.

Vogt F, and L White. 2015. "Spectroscopic analyses of chemical adaptation processes within microalgal biomass in response to changing environments." *Analytica Chimica Acta* 867:18-28. doi: https://doi.org/10.1016/j.aca.2015.02.005.

Vongsvivut J, P Heraud, A Gupta, M Puri, D McNaughton, and C Barrow. 2013. "FTIR microspectroscopy for rapid screening and monitoring of polyunsaturated fatty acid production in commercially valuable marine yeasts and protists." *Analyst* 138 (20):6016-6031.

Wagner H, Z Liu, U Langner, K Stehfest, and C Wilhelm. 2010. "The use of FTIR spectroscopy to assess quantitative changes in the biochemical composition of microalgae." *Journal of Biophotonics* 3 (8-9):557-566. doi: 10.1002/jbio.201000019.

Walter MR. 1976. *Stromatolites*. Vol. 20: Elsevier.

Wold S, M Sjöström, and L Eriksson. 2001. "PLS-regression: a basic tool of chemometrics." *Chemometrics and Intelligent Laboratory Systems* 58 (2):109-130.

Wong PT, RK Wong, TA Caputo, TA Godwin, and B Rigas. 1991. "Infrared spectroscopy of exfoliated human cervical cells: evidence of extensive structural changes during carcinogenesis." *Proceedings of the National Academy of Sciences* 88 (24):10988-10992.

.

Chapter 6

Untargeted profiling of *D. tertiolecta* exo-metabolome under grazing pressure of *Oxyrrhis marina*.

6. 1 Introduction

Extracellular metabolites serve as a chemical cue in prey-predator interactions leading to either prey capture or predator avoidance. The nature and occurrence of the disturbance, damage-release, prey and predator recognition signals are described in section 2.5.4. The extracellular metabolites of microalgal prey-predator interactions are mainly short peptides (Kearns and Hunter 2001), toxins (Adolf et al. 2007), fatty acids (Tambiev et al. 1989) and alkaloids (Volk et al. 2009), compounds that are known to exert either positive, stimulation, and negative, inhibition, impacts on the growth of the antagonistic species (Mendes and Vermelho 2013). Detection of predator recognition signals often triggers the release of compounds that are either inhibitory or act merely as a stress signal by prey cells. The inhibitory compounds offer a great potential in designing predator mitigation strategies, whereas the dynamics of the stress signals could potentially suggest the possibility of predator outbreak. In-depth profiling of the extracellular metabolic signals and their target site thus can help to devise grazer mitigation and monitoring strategies (Reese et al. 2019, Achyuthan et al. 2017).

Mendes and Vermelho (2013) reported a grazer mitigation approach wherein a parasitic Chytrid fungal interaction with its prey, *Haematococcus fluvialis*, is minimised by addition of external carbohydrates that saturates prey binding sites on the cell wall of the fungus, thereby reducing microalgal attachment. Other predator mitigation strategies can be developed by applying algal toxins. Numerous lethal microalgal toxins against the predator, *O. marina*, are documented that could be engineered into other microalgal host to avoid biomass loss due to predation. Strains of microalgae such as *E. huxleyi* (Wolfe et al. 1994), *C. polylepis* (John et al. 2002), *K. veneficum* (Adolf et al. 2007) and *P. parvum* (Tillmann 2003) have evolved to release toxic chemicals that deter their ingestion by the dinoflagellate, *O. marina.* In addition to toxins, polyunsaturated aldehydes such as oxylipins are also reported to be lethal against predators. Oxylipins are oxygenated cell membrane lipids produced by many diatom species which act as a grazer-activated signalling molecule and interferes with reproductive process of predators (Caldwell 2009).

Predators have also evolved to detect and discriminate between toxic and non-toxic strains of prey by using metabolic cues, infochemicals also known as kairomones, secreted by the microalgae (Achyuthan et al. 2017). For example, *O. marina* detects prey-derived infochemicals such as amino acids and amino sugars (Flynn and Fielder 1989) via a G-couple protein cell surface receptor (Roberts et al. 2010). The attachment of the infochemicals supresses the chemosensory response of *O. marina* and thereby lowers the rate of prey ingestion (Hartz et al. 2008). The role of prey recognition signals such as free amino acids in the onset of predator ingestion can be exploited for monitoring the underlying stress situation. The dynamics of such signals in relation to predator abundance can reveal the early warning potential of extracellular metabolites as a marker of the culture crash.

The importance of extracellular cues in prey-predator interactions is evident by studies that use cell-free exudates (He et al. 2016) to stimulate the chemosensory behaviour of *O. marina* (Martel 2006). The swimming behaviour and turning velocity of the predator is reported to positively change in the presence of intact prey cells, *Isochrysis galbana* and *D. tertiolecta*, as compared to cell-free exudates (Martel 2006). In addition, grazer encounter scan also trigger morphological adaptation in *Scenedesmus* sp. wherein colony formation renders them unpalatable by *Daphnia* sp. (Lürling 2003). These studies suggest that extracellular cues can directly induce behavioural changes in prey and predator cells. Therefore, detection of onset of exudates, extracellular chemicals, can serve as an indirect marker of the presence of contaminants, in this case *O. marina*.

Despite the remarkable importance of extracellular chemical cues involved in prey-predator interactions, information about the chemical ecology of metabolites with respect to marine microalgal ponds is limited. Reese et al. (2019) have reported Volatile Organic Compounds (VOC), oxidative metabolites of β-carotene, as markers of *B. pilicatilis* grazing in *Microchloropsis salina* culture. Oxidative VOC such as β-ionone and β-cyclocitral are essentially breakdown products of the pigment β-carotene. Such a pigment breakdown is an outcome of prey cell digestion by the predator whereas detection of extracellular signalling cues can provide information about early onset of prey detection by predator. The profiling of the extracellular cues, intrinsic to the interaction, can thus provide insights into water soluble chemical environment prior to the microscopically quantifiable physical capture of prey by predator eventuates. Based on the population dynamics of the prey and predator reported in previous chapters, this study hypothesised that the signalling interaction ought to occur prior to the significant ingestion of the prey cells. Therefore, it is vital to study the exo-metabolome

dynamics in a time-specific manner. Intracellular metabolites are less desirable as a marker of contamination as it requires samples with high cell concentration. (Sue et al. 2011). The purpose of predator detection at its lowest concentration is thus hindered in the case of exploring dynamics of intracellular metabolites. The current chapter aims to profile the temporal variation in metabolic footprints of *O. marina*-mediated grazing on *D. tertiolecta* cells using untargeted Liquid Chromatography- Mass Spectrometry (LC-MS) approach.

6.2 Materials and Methods

6.2.1 Preparation of grazing cultures

Microalgal grazing cultures were prepared using the prey and predator strains and cultivation conditions described in section 3.2.1.

A pilot experiment was performed to optimise the metabolite extraction method and test the extraction limit in order to determine the optimal cell concentration for the experiment. Supernatants of trial cultures with incremental cell concentration (10^5, 10^6 and 10^8 cells ml^{-1}) of 1:100 predator and prey ratio were extracted (section 6.2.3) for LC-MS analysis (section 6.2.4). The intensity of the detected metabolites was found to be positively correlated with increased cell concentration.

6.2.2 Sample harvesting and experimental design

Culturing flasks containing 700 ml of only *D. tertiolecta* and *O. marina* cells in 1000 ml glass bottles served as a 'Prey control' and 'Predator control' respectively, whereas uninoculated sterile F/2 medium was used as a 'baseline control'. Cells used for 'predator only' control contained healthy (motile) *O. marina* cells starved for 6 days. Supernatants were collected separately from independent prey and predator cell cultures and mixed together prior to metabolite extraction, which served as a 'Supernatants only' control. Supernatants only control would lack predator-specific signalling metabolites as the prey was never exposed to the predator attack. Experimental flasks with *D. tertiolecta* cells infested with *O. marina* served as 'Grazing' cultures that were used to capture metabolites elicited as an extracellular response against the predator attack. All cultures were cultivated in five independent replicate bottles. In addition, *D. tertiolecta* cells were treated with 10 mM of freshly prepared ammonium chloride as a proxy for ammonia-nitrogen excreted by the predator (Figure 6.1).

For harvesting, a volumetric equivalent based on cell concentration in respective flasks was harvested every on 0, 4, 8, 12, 16, 20, 24, 36 and 48 h from all cultures, except the ammonium chloride treated group, based on cell concentration of prey and predator in the

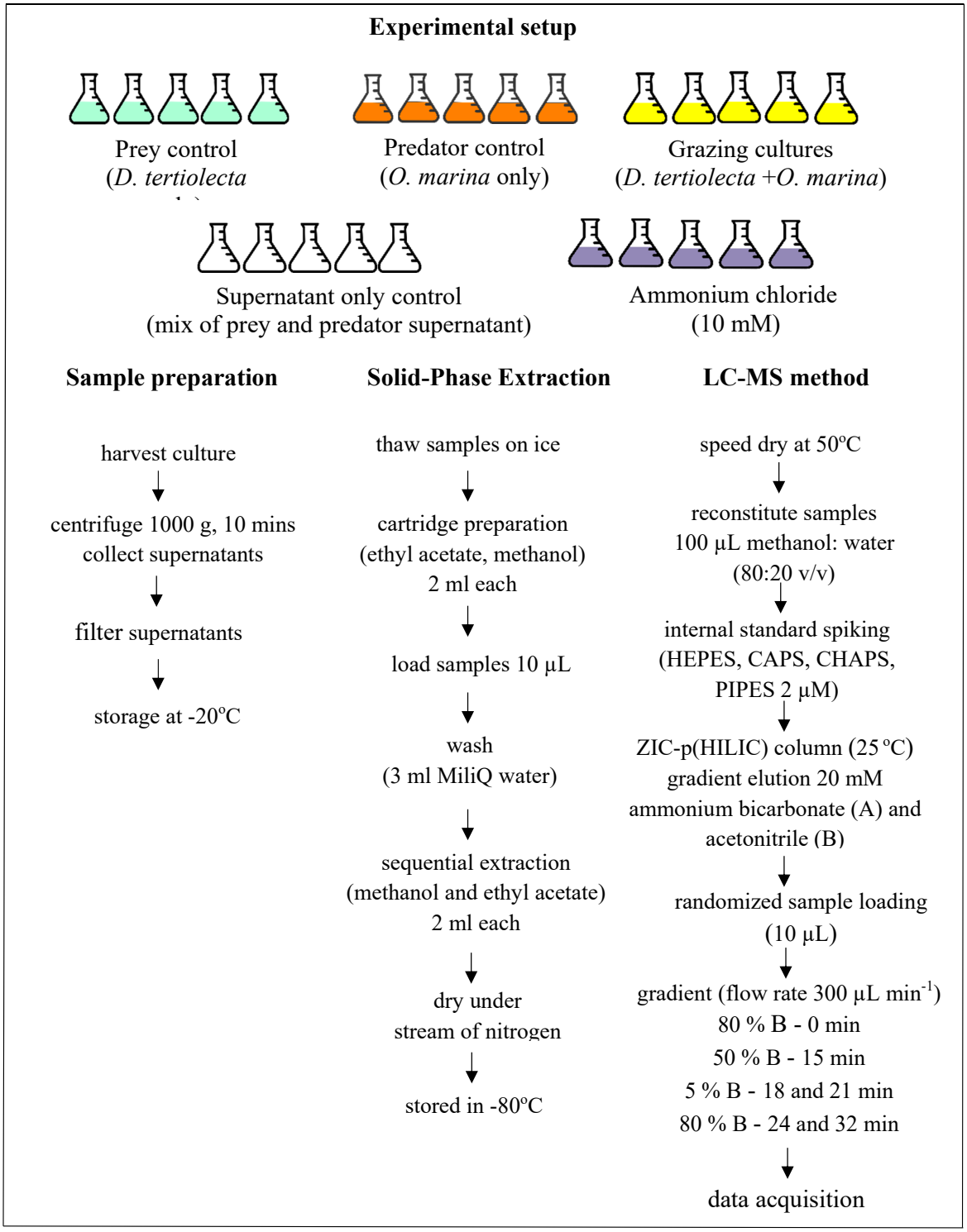

Figure 6.1. Flow chart indicating steps in sample preparation, extracellular metabolite extraction and LC-MS method.

grazing cultures. The ammonium chloride treated microalgal cells were harvested at the end of the 4th hour for metabolite extraction. For all samples, microalgal cell biomass was centrifuged at 1000 g for 10 mins and the supernatant filtered through a glass microfiber (GF/F GE healthcare 2-micron, 47 mm diameter) filter. The filtrate was stored at -20^{o}C until extraction.

6.2.3 Solid-Phase Extraction (SPE) of waterborne compounds

The stored supernatant (Section 6.2.2) was allowed to thaw on ice prior to the extraction. Metabolites were extracted using a SPE cartridge, Oasis HLB column (Waters) that was assembled in extraction chamber with a vacuum manifold. The cartridges were conditioned by adding 3 ml ethyl acetate (Thermo Fisher, MS grade) followed by 3 ml methanol (Sigma, MS grade). Cartridges were equilibrated by adding 3 ml of ultrapure MiliQ water (Sigma). Samples were loaded onto equilibrated cartridges and extracted at a flow rate of ~1 ml min^{-1}. Cartridges were washed with 4 ml of ultrapure MiliQ water. The extract was sequentially eluted and re-eluted using 2 ml of methanol and ethyl acetate. The total 8 ml of the elute was collected in detergent-free glass vials and dried under a stream of nitrogen until about 1 ml elute remained. The remaining elute was transferred from glass tubes into detergent-free Eppendorf tubes (Eppendrof LoBind, Sigma) and stored at -80^{o}C until the analysis. All samples were dried using a Speed Vac at 50^{o}C and reconstituted using 100 µl of methanol:water (80:20 v/v) prior to the LC-MS analysis. All samples were spiked with a mix of internal standards (HEPES, CAPS, CHAPS, PIPES) at 2 µM final concentration.

6.2.4 Liquid chromatography and Mass Spectrometry (LS-MS)

Extracellular metabolites across all samples were profiled in an untargeted manner using hydrophilic interaction liquid chromatography (Dionex Ultimate, Thermo Scientific) coupled with a Quadrupole-Orbitrap Mass Spectrometer (QExactive, Thermo Scientific) according to the method of Stoessel et al. (2016). The chromatography method used a ZIC-p(HILIC) column at 25^{o}C with a gradient elution using 20 mM ammonium bicarbonate (A) and acetonitrile (B). The solvent scheme was set with variable % of B and a linear gradient time such that 80 % of B was on hold for 0 min and was sequentially ramped to 50 % of B over 15 min followed by 5 % of B for 18 and 21 min and 80 % of B for 24 and 32 min. The flow rate was maintained at 300 µL min^{-1} and 10 µL of sample was injected for the analysis. Resolution of the MS was set to 35000 and operated with rapid switch between positive (4 kV) and negative (-3.5 kV) mode electrospray ionisation. Capillary temperature was set to 300^{o}C with sheath, Aux and sweep gas temperatures of 50, 20 and 2^{o}C, respectively, whereas the

probe temperature was maintained at 120°C. All samples were randomised and processed in a single batch with intermittent analysis of pooled quality-control samples to ensure reproducibility and minimise variation. To facilitate accurate metabolite identification a standard library of ~300 metabolites was analysed before the sample testing and accurate retention time for each standard was recorded. Additional retention time for metabolites lacking authentic standards were computationally predicated as described by Zhang et al. (2012).

6.2.5 Data pre-processing and analysis

Spectral processing was performed using MzMime 2.32 for peak picking (minimum feature intensity of 5000). The retention time for each feature in samples and standard library were extracted and reviewed manually. The dataset was then imported into IDEOMv20 software for noise elimination and metabolite identification (Creek et al. 2012). The metabolite identification was performed using default IDEOMv20 settings for positive and negative mode with a m/z window of 6 ppm. Resulting residual m/z were inspected for error in positive and negative mode wherein all points with m/z error <-0.4 ppm and >2 ppm, respectively, were eliminated from the analysis. Further re-identification was performed using a mass tolerance window of 3.0 ppm. The putatively identified features from positive (#1174) and negative (#741) mode were combined for estimation of metabolites elevated under grazing conditions.

As a quality control test, median feature intensities from each replicate and time point were compared across all groups to observe the possibility of variation associated with extraction or instrumentation. The median intensity of all samples of the 24 h time-point was significantly lower than those of other time-points. Therefore, the 24 h time-point was eliminated from further analysis.

The resultant peak list was further filtered to include features that were present in at least 3 out of 5 replicates, elevated in two-consecutive time-points or more and where the feature intensity was 100-fold or more than time-matched controls. The fold change of the feature intensity in grazing cultures was calculated using the respective feature intensity of the equivalent time-point in control cultures. A list of a total of 76 metabolites (specific to grazing cultures) was generated using the criteria mentioned above. This list was further annotated using a confidence score, regarding the identification of each metabolite. Confidence score indicates extent of metabolite identification accuracy based on spectral matches between features of unknown sample with database entries. Standards used in this study was given confidence score of 10 indicating exact match with database entry. Unknown features with

confidence scores less than 5 were eliminated. The 24 metabolites were putatively identified by matching with the range of a biological database using IDEOMv20 and univariate statistical analysis was performed using GraphPad Prism software.

6.3 Results

6.3.1 Grazing results

No significant differences in the cell concentration of *D. tertiolecta* in control and grazing cultures were observed until 20 h post *O. marina* infestation. Prey cell concentrations in grazing cultures were depleted by 36, 50 and 80 % at 24, 36 and 48h, respectively, whereas *O. marina* concentration exponentially increased from 12 h onwards with an average specific growth rate of 0.6 d^{-1} (Figure 6.2).

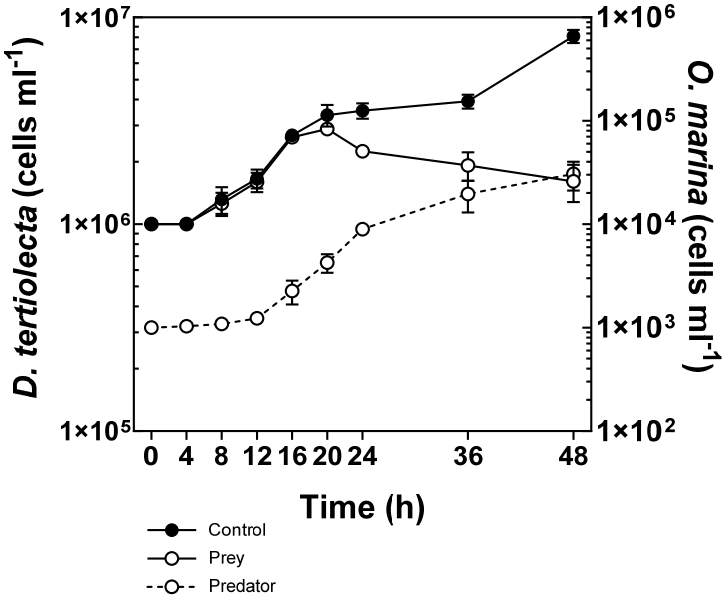

Figure 6.2. Prey-predator population dynamics in grazing cultures of *O. marina.* 'Control' is prey cell concentration alone, 'prey' and 'predator' indicate respective cell concentration in grazing culture. Data represent means ± SD, n = 5

6.3.2 Estimate of fold change of putatively identified metabolic features

A total of 1174 compounds were putatively identified, out of which only 74 metabolites were 10-fold elevated compared to the controls. Further, only 24 metabolites passed a filtering criterion of elevated accumulation in at least two consecutive time-points with a confidence score of 5 and above. The exo-metabolome (Table 6.1) of the grazing cultures by these criteria thus consists of 24 putatively identified metabolites, primarily composed of short peptides,

lipids and indole derivatives. Lactones, purine and polyaromatic hydrocarbons was also found to be elevated in grazing cultures as compared to controls. All putatively identified metabolites were significantly elevated in 36 h samples where the maximum rate of predator ingestion was 8.47 x 10^{14} prey cells predator^{-1} d^{-1}. By 36 h, prey cells were reduced by 50 % with an exponential predator growth rate of 0.74 d^{-1}.

Table 6.1 List of top 24 signature metabolic features elevated from 4 h onwards over the course of active grazing of *D. tertiolecta* by *O. marina*.

Putative metabolite ID	Score	Retention time (min)	Mass	Class
His-Leu	5	8.02	268.15	short peptide
Ile-Met-Thr-Ser	5	7.13	450.21	short peptide
Arg-Phe-Asp-Gln	7	14.11	586.24	short peptide
Ile-Lys	7	12.03	259.18	short-peptide
Trp-Ala-Cys	7	13.54	400.11	short peptide
Asp-Phe-Cys-Cys	7	9.06	486.12	short peptide
Phe-Arg	7	11.04	321.18	short peptide
L-Tyrosyl-L-arginine	7	13.72	337.17	di-peptide
Glu-Glu-His	7	19.87	413.15	short-peptide
Ile-Cys-His	7	9.95	371.16	short-peptide
5-Hydroxy-N-formylkynurenine	8	10.24	274.05	free amino acid intermediate of tryptophan biosynthesis
PA(O-38:0)*	6	3.39	718.58	Phosphophatidic acid/ phospholipids
PA(O-36:1)*	6	3.37	688.54	phospholipids
Docosanediol-1,14-disulfate	7	4.37	519.28	sulfolipid / lipid

Putative metabolite ID	Score	Retention time (min)	Mass	Class
1-(14-methyl-pentadecanoyl)-2-(8-[3]-ladderane-octanyl)-sn-glycerol	5	3.40	602.52	glycerolipid
[PC acetyl(3:0)] 1-propionyl-2-acetyl-sn-glycero-3-phosphocholine	8	12.28	355.13	glycerophospholipid
Pregnenolone acetate	7	3.97	358.25	glucocorticosteroids/ sterol
2-Octenedioic acid	7	13.86	194.05	aliphatic di carboxylic acid UFA
3-hydroxy-2-oxindole-3-acetyl-asp	5	8.17	322.08	indole derivative
2-(5,6-dihydroxy-1H-indol-2-yl)-1H-indole-5,6-diol	7	7.60	342.08	indole derivative
6-hydroxy-indole-3-acetyl-valine	5	7.20	290.12	alkaloids/ indole derivative
Pyrene	7	4.55	202.07	polyaromatic hydrocarbon
Hypoxanthine	7	7.34	136.03	purine N-source
acinetobactin	7	9.56	332.14	sidospore
Scorpioidin	7	8.69	312.11	sesquiterpene lactone

*similar metabolite feature with different chain length and branching point

Ten putatively identified short peptide sequences represent a large proportion of elevated (based on fold change) exo-metabolites. Asp-Phe-Cys-Cys is the only short peptide sequences that was detected (Figure 6.3a) as early as 4 h post *O. marina* inoculation and sequentially increased ($R^2 = 0.5348$) over the course of grazing. The abundance of di-peptide sequences, Phe-Arg (Figure 6.3b) and L-Tyrosyl-L-arginine (Figure 6.3c) peaked by 8626- and 4484-folds, respectively, in 36 h grazing cultures. Ile-Lys (Figure 6.3d) showed a variable response at two time-points. Overall, 484- and 1323-fold increased levels of Ile-Lys were observed at 8and 36 h, respectively, in grazing samples compared to control. A sharp drop was

observed in relative abundance of the di-peptide sequences around 48 h where prey cells were depleted by 80 %.

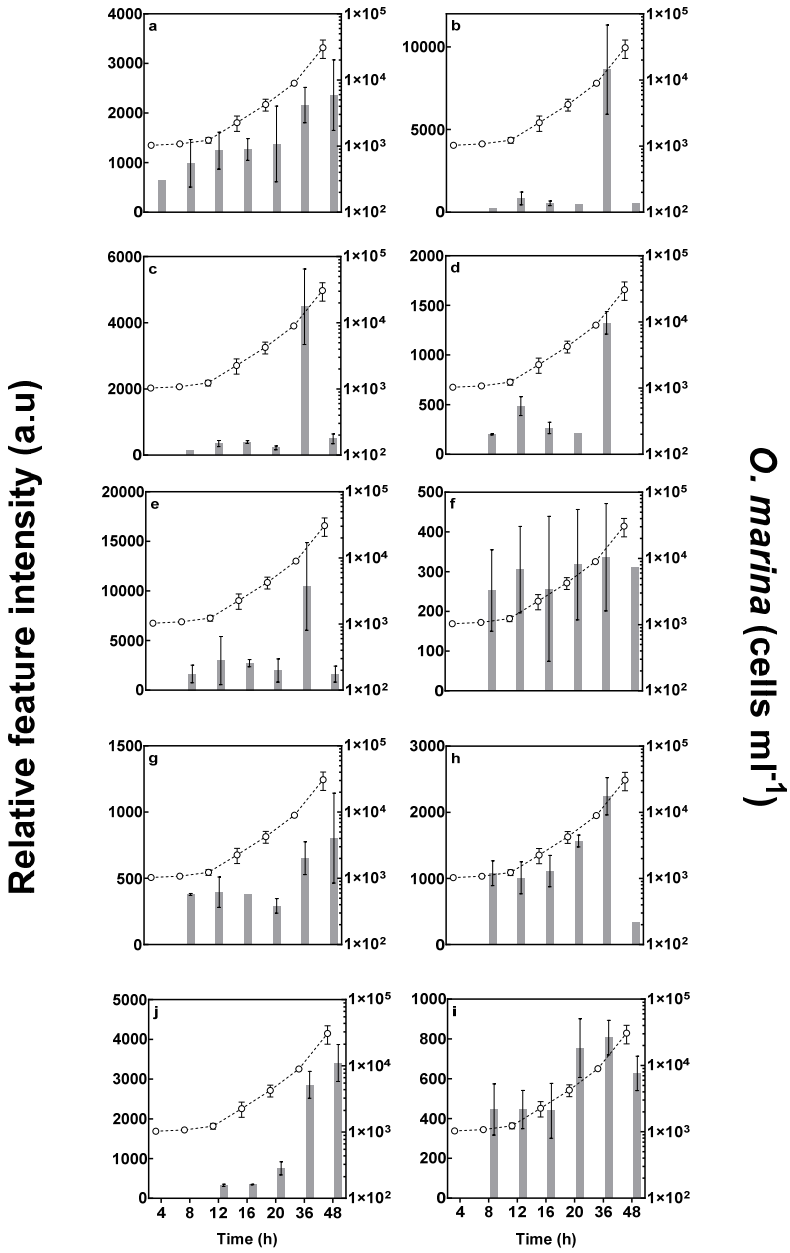

Figure 6.3 Relative abundance of putatively identified extracellular short-peptide sequences estimated as a fold change between feature intensity detected in the presence of active *O. marina* grazing (4–48 h) normalised to control samples. Solid grey bar represents average abundance (based on fold change) of the peptides a) Asp-Phe-Cys-Cys, b) Phe-Arg, c) L-Tyrosyl-L-arginine, d) Ile-Lys, e) His-Leu, f) Arg-Phe-Asp-Glu, g) Glu-Glu-His, h) Ile-Met-Thr-Ser, i) Trp-Ala-Cys, j) Ile-Cys-His, and dashed line indicates cell concentration of the predator as a function of time. n = 5

A similar trend was observed in the case of the His-Leu (Figure 6.3e) di-peptide sequence. All di-peptides were detected in significant amounts from 8 h onwards wherein minimal grazing activity, 1.3 x 10^{-3} prey cells ml^{-1}, was observed. The relative abundance of Arg-Phe-Asp-Gln (Figure 6.3f) was found to be consistently elevated in grazing samples from 8 h onwards. Similarly, Glu-Glu-His (Figure 6.3g) was increased at 8–20 h and further increased at 36 and 48 h. Around 1000-fold increased levels of Ile-Met-Thr-Ser (Figure 6.3h) peptide was observed in the first 16 hours and further increased by 40 % and 100 % subsequently at 20 and 36 h, respectively (R^2 = 0.7183). The tri-peptide, Trp-Ala-Cys (Figure 6.3i) showed a similar trend wherein a 400-fold increase was observed until 16 h and levels were further increased by 71 % at 16 h and by 84 % at 36 h. In contrast, the extracellular concentration of Ile-Cys-His (Figure 6.3j) was linearly elevated after 12 h and its relative abundance positively correlated (R^2= 0.9474) with the ingestion rate of the predator. In addition, the free non-proteogenic alpha-amino acid, 5-hydroxy-N-formylkynurenin which is an intermediate of tryptophan biosynthesis was absent at the initial time-point and gradually increased (R^2 = 0.7379) after 8 h over the course of grazing (Figure 6.4).

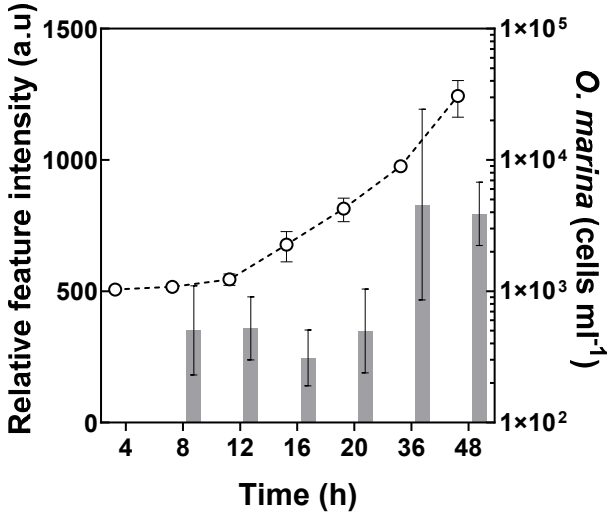

Figure 6.4 Relative abundance of a putatively identified extracellular free amino-acid intermediate, 5-hydroxy-N-formylkynurenine, estimated as a fold change between feature intensity detected in the presence of active *O. marina* grazing (4–48 h) and control samples. Solid grey bar represents average abundance (based on fold change) of the metabolite and dashed line indicates cell concentration of the predator as a function of time. n = 5

Various classes of lipids such as sulfolipids, sterols, phospholipids, glycerolipids and unsaturated fatty acids were detected in the exo-metabolic pool of grazing cultures. A dicarboxylic unsaturated fatty acid, 2-Octendioic acid (Figure 6.5a), was detected to be 766-fold higher at 12 h and levels, despite fluctuating, remained significantly elevated compared to the controls.

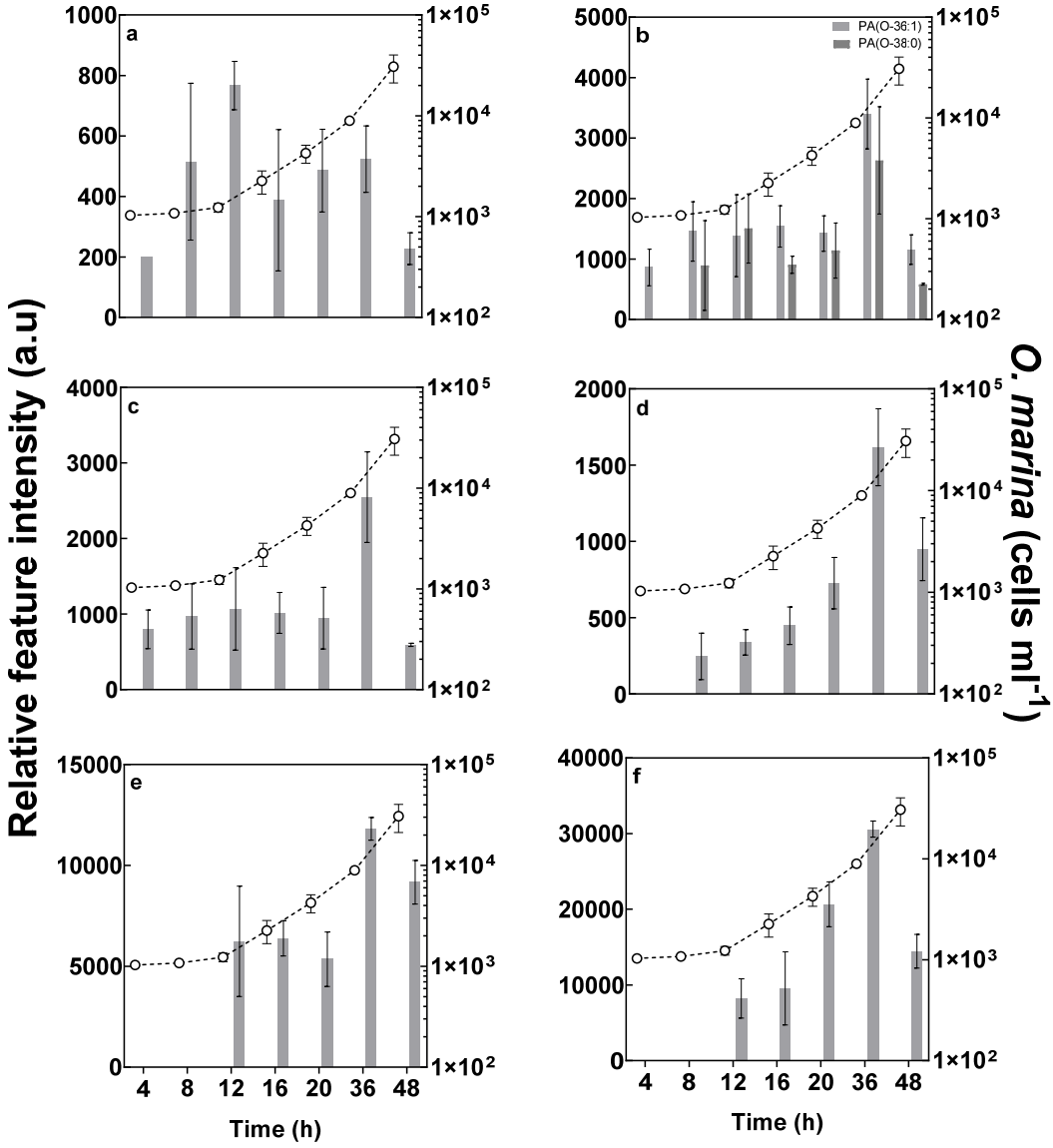

Figure 6.5 Relative abundance of putatively identified extracellular lipids estimated as a fold change between feature intensity detected in the presence of active *O. marina* grazing (4–48 h) and control samples. Solid grey bar represents average abundance (based on fold change) of the a) 2-octenedioic acid, b) phosphatidic acids (PA 36:1 and 38:0), c) 1-(14-methyl-pentadecanoyl)-2-(8-[3]-ladderance-octanyl)-sn-glycerol, d) 1-propionyl-2-acetyl-sn-glycero-3-phosphocholine, e) pregnenolone acetate, f) docosanediol-1,14-disulfate and dashed line indicates cell concentration of the predator as a function of time. n = 5

The levels of two structurally related phospholipids, phosphatidic acid – PA (O-36:1) and (O-38:0), were consistently elevated (1000–1500-fold) for the first 20 h, peaked at 36 h, and subsequently dropped (Figure 6.5b). A similar trend was observed in the case of glycerolipids in which the relative abundance of 1-(14-methyl-pentadecanoyl)-2-(8-[3]-ladderane-octanyl)-sn-glycerol increased by 2454-fold at 36 h in grazer-infested samples as compared to the controls (Figure 6.5c). Early time-points (4–20 h) also showed significantly elevated levels (750–1000-fold) of this glycerolipid. The relative abundance of glycerol containing phospholipid, [PC acetyl (3:0)] 1-propionyl-2-acetyl-sn-glycero-3-phosphocholin, linearly increased from 8–36 h but were offset by -41 % at 48 h (Figure 6.5d). Unlike the majority of the compounds detected, levels of a sterol derivative, pregnenolone acetate, were elevated from 12 h onwards (6234-fold) and further accumulated in grazing cultures by up to 11810-fold at 36 h (Figure 6.5e). The levels only marginally dropped (by 22 %) at 48 h. Accumulation of the metabolite around 12 h corresponds with the 99 % increase in rate of predator ingestion. Similarly, a sulfur containing lipid molecule, docosanediol-1,14-disufate, were increasingly accumulated from 12 h until 36 h ($R^2 = 0.8955$) though the levels dropped by 53 % by 48 h (Figure 6.5f).

The exo-metabolome of *D. tertiolecta* infestation also contained elevated levels of three indole-derivatives. 6-hydroxy-indole-3-acetyl-valine levels were consistently elevated from 4–20 h and further increased by 110 % by 36 h and showed a moderate decrease thereafter (Figure 6.6a). A similar trend was observed in the case of 2-(5,6-dihydroxy-1H-indole-2-yl)-1H-indole-5,6-diol, wherein maximum relative abundance (1136-fold) was observed at 36 h but reduced by 60 % at the end of 48 h (Figure 6.6b). In contrast, 3-hydroxy-2-oxindole-3-acetyl-asp steadily increased from 8–20 h and further plateaued around ~1100-fold at subsequent time-points (Figure 6.6c).

Other putatively identified metabolic features such as pyrene (Figure 6.7a) and hypoxanthine (Figure 6.7b) were accumulated from 8 h. Thereafter levels peaked and levelled off at 36 and 48 h, respectively. In contrast, a sesquiterpene lactone-like compound, scorpioidin, were exclusively detected 20th h onwards (Figure 6.7c). At 36 h the levels were 3243-fold higher in grazing cultures as compared to controls but dropped by 53 % at 28 h. A peptide-based toxin like structure, acinetobactin, accumulated over the course of grazing wherein its levels at 36 h peaked by 9619-fold in *D. tertiolecta* cultures infested with *O. marina* (Figure 6.7d). Overall, 9 out of 24 metabolites showed a moderately linear accumulation in first 20 hours of the grazing experiment. Ammonium chloride (10 mM) exposure for 4 h

resulted in >100-fold accumulation of 8 metabolites (Table 6.2) that were also found to be elevated over the course of *O. marina* grazing in mixed cultures.

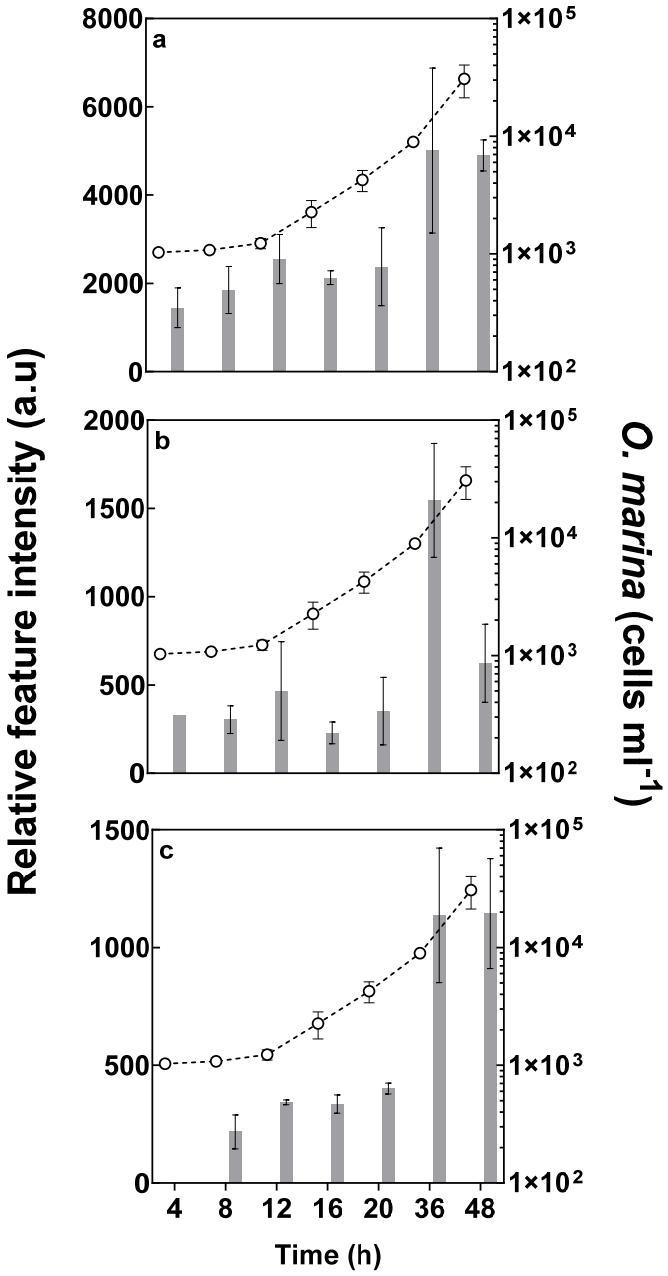

Figure 6.6 Relative abundance of putatively identified extracellular indole derivatives estimated as a fold change between feature intensity detected in the presence of active *O. marina* grazing (4–48 h) and control samples. Solid grey bar represents average abundance (based on fold change) of a) 6-hydroxy-indole-3-acetyl-valine, b) 2-(5,6-dihydroxy-1H-indol-2-yl)-1H-indole-5,6-diol, c) 3-hydroxy-2-oxindole-3-acetyl-asp, and dashed line indicates cell concentration of the predator as a function of time. n = 5

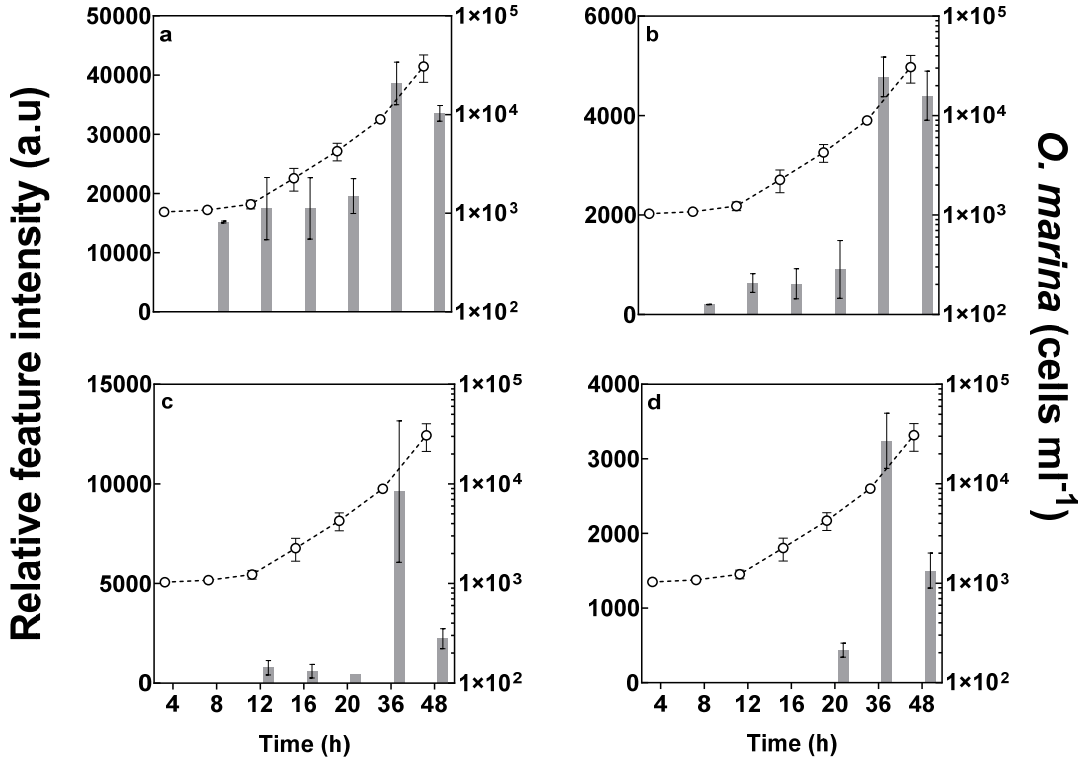

Figure 6.7 Relative abundance of putatively identified extracellular metabolites estimated as a fold change between feature intensity detected in the presence of active *O. marina* grazing (4–48 h) and control samples. Solid grey bar represents average abundance (based on fold change) of a) pyrene, b) hypoxanthine, c) acinetobactin, d) scorpioidin, and dashed line indicates cell concentration of the predator as a function of time. n = 5

Table 6.2 Average relative abundance (based on fold change) of feature intensities of the grazing-specific signature metabolites detected after 4 h exposure of a *D. tertiolecta* culture to ammonium chloride.

Putative metabolite ID	**Ammonium chloride (fold change±SD)**	**Grazing (fold change±SD)**
Pyrene	65694±58310	9686±200
6-hydroxy-indole-3-acetyl-valine	10075±2933	1446±447
Asp-Phe-Cys-Cys	2063±569	646±0
2-Octenedioic acid	324±89	200±0
Hypoxanthine	5076±2889	absent

Putative metabolite ID	Ammonium chloride (fold change±SD)	Grazing (fold change±SD)
[PC acetyl(3:0)] 1-propionyl-2-acetyl-sn-glycero-3-phosphocholine	613±270	absent
3-hydroxy-2-oxindole-3-acetyl-asp	3543±277	absent
Trp-Ala-Cys	1679±1249	absent

6.4 Discussion

The untargeted profiling revealed 24 unique features (Table 6.1) as a metabolic footprint over the course of *D. tertiolecta* grazing-mediated by *O. marina*. Increased accumulation of the signature metabolites in initial time-points (until 16 h) without significant loss of the prey cell concentration indicates that such signals are mainly contributed from grazing activity of *O. marina*. In addition to the grazing-mediated perturbations, alteration of the exo-metabolome composition is reported to be associated with growth; however, *D. tertiolecta* and *O. marina* cell concentrations were relatively unaltered in first 20 h of incubation (Figure 6.2). Thus, the observed linear increase in the relative abundance of at least 41 % of the signature metabolites can be exclusively attributed to increased encounters of prey and predator. Poulson-Ellestad et al. (2016) reported a similar trend wherein increased *O. marina* grazing on *Emiliania huxleyi* positively impacted accumulation of 9 metabolites out of which one (with a m/z = 400) with potentially similar features, Trp-Ala-Cys, was also detected in the current study. Grazing of *E. huxleyi* by *O. marina* also decreased accumulation of features associated with m/z values of 337 and 413 Poulson-Ellestad et al. (2016). Similar features are putatively identified as L-Tyrosyl L-arginine and Glu-Glu-His, respectively, and were detected at elevated levels in the current study (Figure 6.3c and 6.4g). Further characterization and validation of these features are required to access the extent of their similarity. In theory, reduced abundance of a feature can serve as a biomarker of grazing; however, for practical relevance, especially for outdoor cultures, estimation of elevated levels of metabolites is a more straightforward approach.

Elevated levels of VOC compounds as result of a carotenoid oxidation is reported as a potential biomarker of *M. salina* grazing. The carotenoid oxidation products, trans-β-ionone and β-cyclocitral, accumulated up to 2–3-fold after 24 h of rotifer addition in *M. salina* culture though no obvious linear increases in the level of oxidation products were seen (Reese et al.

2019). The apparent lack of correlation with rotifer concentration suggests that the elevated levels of metabolites is an indirect outcome of grazing activity. Production of VOCs due to carotenoid oxidation is an inevitable outcome under a variety of stress conditions such as high heat, light, sonication, etc. and is, therefore, viewed as essentially a damage release type of signal. Emission of VOCs from live cells are sparsely reported (Reese et al. 2019) thus, detection of the oxidation products suggests underlying stress conditions. This can result in a false alarm, especially in open cultures, with respective to the predator outbreak. In contrast, the current study attempts to profile the disturbance and prey recognition signals in order to exclusively leverage the extracellular response of live *D. tertiolecta* cells in the presence of a predator.

The exo-metabolome of the current study is largely represented by short peptides that are detected over 100–1000-fold range and are often absent in time-matched control samples. One of the signature peptides, Asp-Phe-Cys-Cys, accumulated as early as 4 h post predator infestation (Figure 6.3a). A linear increase in the peptide abundance with increased predator concentration suggests its role as a conspecific, i.e. within the same species, disturbance signal emitted either by the prey or predator. A constitutive expression of conspecific signals often carries an ecological cost of attracting predators in marine environments. However, the linear trend in this case suggests that the peptide is mostly emitted in presence of *O. marina* as its abundance was negligible in prey-only control cultures and was completely absent in grazer-only controls. This is further supported by incremental accumulation of Asp-Phe-Cys-Cys until 48 h, unlike the abundance of other metabolites. Banin et al. (2001) reported that a peptide rich in the cyclic amino acid, Proline, facilitates uptake of ammonia by zooxanthellae. The signature peptide also contains a cyclic amino acid, Phenyalanine, which may assist in the uptake of grazing-mediated ammonia-nitrogen (see chapter 4); however, further empirical validation is required. A moderately linearly increased accumulation of the free amino-acid intermediate, 5-Hydroxy-N-formylkynurenine, post 8 h (Figure 6.4) of infestation suggests its possible role as a conspecific disturbance signal. A similar catabolic product of tryptophan is reported to act as an indicator of high light stress on the photosynthetic machinery (Dreaden et al. 2011). N-formylkyurenine moiety is also found to be a part of a antimicrobial toxin, Brunsvicamides C, released by cyanobacteria associated with sponges (Müller et al. 2006).

Metabolites that were elevated in grazing cultures as early as 4 h are of particular importance to monitoring of grazing. Higher abundance of metabolites in grazing culture early in the infestation process suggests their probable role as a chemical cue involved in prey

predator interactions as opposed the metabolites distinctly observed at 36 h. Six out of 24 exo-metabolites were elevated in first 4 h of predator infestation with a marginally consistent response until 20 h. This suggest their probably role as a signalling molecule in the *D. tertiolecta* and *O. marina* interaction Other than one short peptide, signature metabolites exclusive to 4 h post infection were mainly lipid, fatty acid and indole derivatives. *O. marina* accumulates lipid and sterols, which are also reported as biomarkers in other studies (see chapter 5). The polyunsaturated fatty acid, 2-octenedioic acid, is also one of the markers detected early on, at 4 h, as a function of grazing (Figure 6.5.a). The role of free fatty acids as an extracellular signal is not clearly defined in microalgae though its secretion as an outcome of lipid remodelling in *Ochromonas danica* is reported by Banin et al. (2001). The levels of 2-octenedioic acid was neither consecutive nor increased linearly, hence its substantial role in grazing interactions cannot be supported. In contrast, a constitutive accumulation of the glycerolipid was observed from 4 to 20 h. Glycerolipids are esters of fatty acids and glycerol that are occasionally found in microalgal secretions (Kind et al. 2012a) however, their role as signalling molecules is unclear. Phosphatidic acid elevated ~1000-fold (Figure 6.5b) in current study, are constituents of membrane lipids and hypothesised to serve a role as messenger molecules in plants mainly during wounding and pathogen attack (Wang et al. 2006). In contrast, concentrations of 6-hydroxy-indole-3-acetyl-valine, commonly referred to as indole 3-acetic acid (IAA), were elevated up to 2000-fold in grazing cultures within the first 4 h (Figure 6.6a). IAA levels were not linearly correlated with predator concentrations, which suggests a stimulatory effect as opposed to a signalling role. The extracellular presence of IAA has been reported in cultures of *Chlorella*, *Scenedesmus* sp. and *E. Huxleyi* (Mazur et al. 2001). Growth-promoting potential is the most widely documented function of IAA in plants, whereas an increasing number of reports are now describing its alternative role in mediating physiological changes in microalgae. In *Desmodesmus* sp. IAA brought about a change in phenotype, causing inhibition of colony formation, in the presence of competing microbes (Labeeuw et al. 2016). In *E. huxleyi*, tryptophan-mediated IAA serves as the conspecific signal and is further hypothesised to act as a interspecies-specific signal (Labeeuw et al. 2016). Similar to the current study, Sue et al. (2011) reported the potential of metabolic profiles for detection of *Pseudomonas* sp. contamination within the first 3 h of the onset of fermentative metabolism by the microalga *Nitzschia laevis*.

In chapter 4, the time-dependent grazing-mediated excretion of ammonia nitrogen was suggested as a marker of the presence of *O. marina*. Untargeted profiling of the grazing culture

revealed an additional excretory product, hypoxanthine, as a potential marker (Figure 6.7b). Antia et al. (1980) reported a marine ciliate as a source of purine compounds, including hypoxanthine, and described its uptake by *D. tertiolecta*. *O. marina*-mediated excretion of hypoxanthine is not reported to-date and requires further investigation about its cause and effect with respect to microalgal grazing. The presence of extracellular ammonia and its uptake as a nitrogen source alters the physiology and photosynthesis of *Dunaliella* sp. (Fabregas et al. 1989*)*. In previous chapters 3 and 4, recycled ammonia-nitrogen is described as a potential source of photosynthetic alterations in the prey cells. Predator-free exudate also brought about similar changes in *D. tertiolecta* cells therefore, ammonia was hypothesised to play a role in mediating the chemical interactions. Exposure to ammonia of predator-free *D. tertiolecta* culture resulted in increased levels of 8 metabolites. Ammonia-specific metabolites that are also part of the signature exo-metabolome detected in grazing cultures of *O. marina* (Table 6.2). Only 4 of the ammonia-specific metabolites (hypoxanthine, PC acetyl (3:0), 3-hydroxy-2-oxindole-3-acetyl-asp and Trp-Ala-Cys) were not elevated by 4 h in grazing cultures, but showed linearly increasing accumulation until 36 h. Lack of the ammonia-specific metabolic feature may be due to reduced grazer ammonia-nitrogen early on in infection, but which increasingly accumulates in subsequent time-points. Overall, the overlap in the putatively identified metabolites between ammonia-treated and grazing cultures suggests a possible role of ammonia-nitrogen as an indirect mediator of the chemical response between the prey and predator. Other metabolites such as pyrene, scorpioidin and acinetobactin (Figure 6.7) were significantly elevated in grazing cultures, however its release by microalgal species is not documented. Therefore, their role as a marker of signalling cue must be carefully addressed.

The signature metabolites that are positively correlated with increased predator concentration are likely to serve as a marker of grazing irrespective of its possible role as the chemical cue. However, further experiments aimed at targeted MS detection of candidate metabolites are required to ensure reproducibility and reliability of the markers. Untargeted metabolic profiling offers in-depth view of low molecular weight compounds that are exclusively associated with microalgal grazing and are otherwise undetected through traditional wet-chemistry methods. Further a targeted and sensitive chemistry-based detection method can be developed for estimation of the candidate signature metabolites that can be implemented in-line with cultures. In outdoor cultures exo-metabolic chemistries are likely to be more complex than in closed cultures. Therefore, one particular metabolite cannot be pinpointed as a diagnostic marker. Instead a time-resolved dynamics of a pool of metabolites,

preferably belonging to a same metabolic pathway as described by (Reese et al. 2019), could serve as a reliable marker.

6.5 Conclusion

The current chapter suggests 24 potential exo-metabolic markers found in the presence of *O. marina* in *D. tertiolecta* culture. Six distinctive signature metabolites found at early time-points after infection are a unique feature of this study and to our knowledge this is the first report of grazer detection within the first 4 h. The early indicators can largely help in implementation of intervention measures to avoid algal biomass loss. High coverage and detection of small changes by MS offers a great advantage over other traditional techniques which are relatively less sensitive. However, the uncontrolled and ambient conditions of open ponds may introduce noise and as result may mask the signal of interest. MS-based identification of biomarkers can help in development of analyte-specific detection chemistry on microfluidic or on-chip devices, or alternatively sensors. Such setups can be easily integrated online for real-time and non-invasive measurement of the culture crash. Importantly, online deployments can greatly reduce the overall cost and sample preparation efforts involved with MS. Overall, in-depth understanding of extracellular metabolic interactions with respective ecological aspects of microalgal prey and predator is required for identification of fairly universal biomarker.

References

Achyuthan KE, JC Harper, RP Manginell, and MW Moorman. 2017. "Volatile metabolites emission by in vivo microalgae—an overlooked opportunity?" *Metabolites* 7 (3):39-85.

Adolf J, D Krupatkina, T Bachvaroff, and AR. Place. 2007. "Karlotoxin mediates grazing by *Oxyrrhis marina* on strains of *Karlodinium veneficum*." *Harmful Algae* 6 (3):400-412. doi: https://doi.org/10.1016/j.hal.2006.12.003.

Antia NJ, BR Berland, and DJ Bonin. 1980. "Proposal for an abridged nitrogen turnover cycle in certain marine planktonic systems involving hypoxanthine-guanine excretion by ciliates and their reutilization by phytoplankton." *Marine Ecology Progress Series* 2 (2):97-103.

Banin E, SK Khare, F Naider, and E Rosenberg. 2001. "Proline-Rich Peptide from the Coral Pathogen *Vibrio shiloi* That Inhibits Photosynthesis of Zooxanthellae." *Applied Environmental Microbiology* 67 (4):1536-1541.

Caldwell GS. 2009. "The influence of bioactive oxylipins from marine diatoms on invertebrate reproduction and development." *Marine Drugs* 7 (3):367-400.

Creek DJ, A Jankevics, KE Burgess, R Breitling, and MP Barrett. 2012. "IDEOM: an Excel interface for analysis of LC–MS-based metabolomics data." *Bioinformatics* 28 (7):1048-1049.

Dreaden TM, J Chen, S Rexroth, and BA Barry. 2011. "N-formylkynurenine as a marker of high light stress in photosynthesis." *Journal of Biological Chemistry* 286 (25):22632-22641.

Fabregas J, J Abalde, and C Herrero. 1989. "Biochemical composition and growth of the marine microalga *Dunaliella tertiolecta* (Butcher) with different ammonium nitrogen concentrations as chloride, sulphate, nitrate and carbonate." *Aquaculture* 83 (3):289-304. doi: https://doi.org/10.1016/0044-8486(89)90041-0.

Flynn KJ, and J Fielder. 1989. "Changes in intracellular and extracellular amino acids during the predation of the chlorophyte *Dunaliella primolecta* by the heterotrophic dinoflagellate *Oxyrrhis marina* and the use of the glutamine/glutamate ratio as an indicator of nutrient status in mixed populations." *Marine Ecology Progress Series. Oldendorf* 53 (2):117-127.

Hartz Aaron J, Barry F Sherr, and Evelyn B Sherr. 2008. "Using inhibitors to investigate the involvement of cell signaling in predation by marine phagotrophic protists." *Journal of Eukaryotic Microbiology* 55 (1):18-21.

He D, J Liu, Q Hao, L Ran, B Zhou, and X Tang. 2016. "Interspecific competition and allelopathic interaction between *Karenia mikimotoi* and *Dunaliella salina* in laboratory culture." *Chinese Journal of Oceanology and Limnology* 34 (2):301-313.

John U, U Tillmann, and LK Medlin. 2002. "A comparative approach to study inhibition of grazing and lipid composition of a toxic and non-toxic clone of *Chrysochromulina polylepis* (Prymnesiophyceae)." *Harmful Algae* 1 (1):45-57.

Kearns KD, and MD Hunter. 2001. "Toxin-producing Anabaena flos-aquae induces settling of *Chlamydomonas reinhardtii*, a competing motile alga." *Microbial ecology* 42 (1):80-86.

Kind T, JK. Meissen, D Yang, F Nocito, A Vaniya, Y Cheng, JS. VanderGheynst, and O Fiehn. 2012. "Qualitative analysis of algal secretions with multiple mass spectrometric platforms." *Journal of Chromatography A* 1244:139-147. doi: https://doi.org/10.1016/j.chroma.2012.04.074.

Labeeuw L, J Khey, AR Bramucci, H Atwal, AP de la Mata, J Harynuk, and RJ Case. 2016. "Indole-3-acetic acid is produced by *Emiliania huxleyi* coccolith-bearing cells and triggers a physiological response in bald cells." *Frontiers in Microbiology* 7:828-844.

Lürling MFLLW. 2003. "Phenotypic plasticity in the green algae *Desmodesmus* and *Scenedesmus* with special reference to the induction of defensive morphology." *Journal of Limnology* 39 (2):85-101.

Martel CM. 2006. "Prey location, recognition and ingestion by the phagotrophic marine dinoflagellate *Oxyrrhis marina*." *Journal of Experimental Marine Biology and Ecology* 335 (2):210-220. doi: https://doi.org/10.1016/j.jembe.2006.03.006.

Mazur H, A Konop, and R Synak. 2001. "Indole-3-acetic acid in the culture medium of two axenic green microalgae." *Journal of Applied Phycology* 13 (1):35-42.

Mendes LB, and AB Vermelho. 2013. "Allelopathy as a potential strategy to improve microalgae cultivation." *Biotechnology for Biofuels* 6 (1):152.

Müller D, Krick A, Kehraus S, Mehner C, Hart M, Küpper FC, Saxena K, Prinz H, Schwalbe H, and Janning P. 2006. "Brunsvicamides A− C: Sponge-Related Cyanobacterial Peptides with Mycobacterium tuberculosis Protein Tyrosine Phosphatase Inhibitory Activity." *Journal of Medicinal Chemistry* 49 (16):4871-4878.

Poulson-Ellestad KL, ElL Harvey, MD Johnson, and TJ Mincer. 2016. "Evidence for strain-specific exometabolomic responses of the coccolithophore Emiliania huxleyi to grazing by the dinoflagellate *Oxyrrhis marina*." *Frontiers in Marine Science* 3:1-13. doi: https://www.frontiersin.org/article/10.3389/fmars.2016.00001

Reese KL, CL Fisher, PD Lane, JD Jaryenneh, MW Moorman, AD Jones, M Frank, and TW Lane. 2019. "Chemical profiling of volatile organic compounds in the headspace of algal cultures as early biomarkers of algal pond crashes." *Scientific Reports* 9 (1):1-10.

Roberts EC, EC Wootton, K Davidson, HJ Jeong, CD Lowe, and DJ Montagnes. 2010. "Feeding in the dinoflagellate *Oxyrrhis marina*: linking behaviour with mechanisms." *Journal of Plankton Research* 33 (4):603-614.

Stoessel D, CJ Nowell, AJ Jones, L Ferrins, KM Ellis, J Riley, R Rahmani, KD Read, MJ McConville, and VM Avery. 2016. "Metabolomics and lipidomics reveal perturbation of sphingolipid metabolism by a novel anti-trypanosomal 3-(oxazolo [4, 5-b] pyridine-2-yl) anilide." *Metabolomics* 12 (7):126.

Sue T, V Obolonkin, H Griffiths, and SG Villas-Bôas. 2011. "An exometabolomics approach to monitoring microbial contamination in microalgal fermentation processes by using metabolic footprint analysis." *Applied Environmental Microbiology* 77 (21):7605-7610.

Tambiev AH, NN Shelyastina, and NN Kirikova. 1989. "Exometabolites of lipid nature from two species of marine microalgae." *Functional Ecology* 3 (2):245-247.

Tillmann U. 2003. "Kill and eat your predator: a winning strategy of the planktonic flagellate Prymnesium parvum." *Aquatic Microbial Ecology* 32 (1):73-84.

Volk RB, U Girreser, M Al-Refai, and H Laatsch. 2009. "Bromoanaindolone, a novel antimicrobial exometabolite from the cyanobacterium *Anabaena constricta*." *Natural Product Research* 23 (7):607-612.

Wang X, SP Devaiah, W Zhang, and R Welti. 2006. "Signaling functions of phosphatidic acid." *Progress in Lipid Research* 45 (3):250-278.

Wolfe GV, EB Sherr, and BF Sherr. 1994. "Release and consumption of DMSP from *Emiliania huxleyi* during grazing by *Oxyrrhis marina*." *Marine Ecology Progress Series* 111:111-119.

Zhang T, DJ Creek, MP Barrett, G Blackburn, and DG Watson. 2012. "Evaluation of coupling reversed phase, aqueous normal phase, and hydrophilic interaction liquid chromatography with Orbitrap mass spectrometry for metabolomic studies of human urine." *Analytical Chemistry* 84 (4):1994-2001.

Chapter 7

Conclusion and future work

Pond crash caused by grazer infestation is one of the major bottlenecks in successful outdoor microalgal cultivation. Although grazer mitigation efforts are at the forefront of pond management, little is known about the early signs of microalgal predation. Currently practised grazer monitoring methods such as microscopy and oligonucleotide-based markers pose several challenges in on-line culture monitoring. A quick, online and non-invasive grazer monitoring tools are required for effective microalgal pond management. This study demonstrates the effectiveness of various prey and predator specific features such as NPQ, TAN and 1363 cm^{-1} wavenumber for *O. marina* monitoring. This study recommends detection of NPQ and ammonia in tandem to overcome challenges associated with respective method. Minimal levels of NPQ can be particularly misleading under the dark phase of a diurnal day-night cycle, whereas, TAN builds up under darkness and is taken up in the presence of light. Therefore, NPQ monitoring in the light and TAN detection in the dark phase will be beneficial to provide accurate estimates of predator load. FTIR-based screening in principle is relatively straight-forward however, in-depth method development and prior calibration is required to detect a variety of predators. The reported markers, from this study, are an indirect indication of the predator load which can be immediately implemented for on-site grazer monitoring. Nonetheless traditional detection of grazers using microscopy and oligonucleotide-based markers are vital for the taxonomic identification of grazers.

Development of effective grazer monitoring measures is a two-fold challenge. First, in depth knowledge about predators of microalgal cultures is very limited. A lack of basic information regarding the proliferative, reproductive and infection mechanisms employed by predators limits the scope of designing novel detection tools and intervention measures. Our work demonstrates that understanding the changes associated with a unique microalgal prey predator process can enable development of novel grazer-detection methods. The processes involved in predation that are largely the same across a range of microalgae and zooplankton, such as ammonia excretion, are of particular importance as they can be developed as a universal marker of grazing. More work is required to identify, characterise and validate the crash-predative potential of intrinsic processes associated with microalgal prey predator interactions.

In addition, use of mathematical models can help to improve the understanding of prey-predator dynamics at pond level.

Further, a technological advancement is required to translate the applicability of the intrinsic process for real-time detection of invaders. A continuous effort, in parallel to improved understanding of basic processes, is required in order to integrate suitable sensors to mass culture approaches. Ideally, in-line implementation with microalgal cultures using such sensor-based detection platform is desirable for real-time estimation of predator load. Online sensor integration would facilitate multiple measurements, unlike currently practised offline methods, in a short span of time thereby increasing the likelihood of predator detection. Currently, several hand-held devices are available that can be implemented immediately to measure suggested markers, NPQ, TAN and absorbance at the 1363 cm^{-1} waveband, as a means of detection of *O. marina* infection on site. However, applicability of these markers for different microalgal prey and predator species needs to evaluated. Use of spectral information such as FTIR and hyperspectral images as means of fault detection are of particularly importance. The detection of spectral markers can be easily up-scaled for large scale cultivation, using currently available imaging tools such as RGB (Red Blue Green) cameras and remote sensing techniques for microalgal health monitoring purposes, including grazing. However, the relevance of high-throughput spectral data with the underlaying biological information would require in depth knowledge of microalgal prey-predator interactions. In addition, profiling and in detail characterisation of extracellular cues, such as the stress responses of the prey against predator, involved in microalgal predation can help to devise a quick point-of-care diagnostic test. Operational cost of portable devices (spectrophotometer) and sensor-based technologies can prove to be a relatively economical as compared to chemistry-based detection such as oligonucleotide-based markers. Development of quick and 'on-chip' grazer monitoring methods can help small-to-medium budget microalgal cultivation projects, whereas, relatively big projects can contribute in identification of potential predators (using sequencing technologies) in collaboration with smaller cultivation setups.

Overall, an integrated grazer detection approach is required wherein currently employed methods are implemented in combination with markers suggested in this work. The relative success of agents, physical or chemical, used for grazer elimination would largely depend on the early warning potential of available monitoring tools. A collaborative research effort for quality control (QC) and quality assurance (QA) method development of microalgal pond diagnostics is urgently required for timely implementation of grazer mitigation strategies.